

The use of ionic liquids as a platform for the sustainable development of high value materials from chitin waste

By

Catherine A. King

Department of Chemistry

McGill University

Montreal, Quebec, Canada

September 2017

A thesis submitted to McGill University in partial fulfillment of the requirements of the degree of Master of Science

Abstract

As petrochemical based polymers have become prevalent, so too has the environmental pollution which results from their widespread use. In recent years, increasing societal concern for environmental issues has led to a growing focus on the use of more sustainable materials. Chitin is the second most abundant biopolymer, can be obtained from “waste” generated in fisheries and shrimp farms, and possess many high value properties such as biocompatibility, biodegradability, and bioactivity. Although its use has traditionally been hindered due to its insolubility in common solvent systems, ionic liquids (ILs) have recently emerged as a solvent. ILs allow for the extraction, regeneration, and solution processing of chitin for the preparation of new materials.

In this thesis, the IL processing platform was utilized for the preparation of new functional materials from chitin. The thesis begins with a new method for the determination of purity of chitin samples. In biomass, chitin is mixed with proteins and minerals, but it is important for the quality of the resulting materials that the purity of the isolated biopolymer to be known. Here (Chapter 3), solid-state ^{13}C multiCP NMR was used to determine chitin content in a chitinous sample accurately, quickly, and non-destructively. From here, with knowledge of the chitin purity in mind, materials were prepared. In Chapter 4, the preparation of chitin films *via* IL processing was optimized, and the properties of the resulting films studied. It was found that preparation parameters such as the loading of chitin in the IL, the chitin source, and the casting method influenced the ability to cast a film. Caffeine was loaded and released from supercritically CO_2 dried films, demonstrating a potential application as a drug releasing membrane. The next chapter (Chapter 5) focused on using the platform for the preparation of functional composite chitin films, as the IL method allows for the incorporation of additives into the chitin/IL solution. Here, following the theme of using chitin for more sustainable polymeric materials, chitin/graphene

composite films were prepared and used in the assembly of a functioning supercapacitor. Dispersion of graphene into the chitin/IL solution was studied, and composite films of up to 80 wt% graphene were cast. The graphene/chitin composite films (used as electrodes), along with neat chitin films (used as separators) were assembled into a working chitin-based supercapacitor. The work done in this thesis aims to pave the way for the development of high-value, sustainable advanced materials from IL-processed biopolymers for a more sustainable world.

Resume

Avec l'utilisation de plus en plus répandue de polymères basés sur les composés pétrochimiques la pollution environnementale s'est accrue. L'inquiétude sociétale pour les problèmes environnementaux de ces dernières années a entraîné un intérêt grandissant pour développer l'utilisation de matériaux durables. La chitine est le deuxième bio polymère le plus abondant dans la nature, et elle peut être récoltée parmi les « déchets » des zones de pêche et des fermes d'élevage de crevettes, elle possède également de nombreuses propriétés à forte valeur ajoutée telles que la biocompatibilité, la biodégradabilité et la bio activité. Bien que son utilisation fût historiquement entravée par son insolubilité dans les systèmes de solvant traditionnels, les liquides ioniques (LI) sont récemment apparus comme de nouveaux solvants. Les LI permettent l'extraction, la régénération et le traitement de la chitine pour la préparation de nouveaux matériaux.

Dans cette thèse, les LI furent employés comme moyens de traitement de la chitine pour préparer de nouveaux matériaux. La thèse débute avec une nouvelle méthode de détermination de la pureté des échantillons de chitine. La chitine est mélangée avec des protéines et des minéraux dans la biomasse, mais il est important de connaître la pureté des bio polymères isolés pour la qualité des matériaux futurs. Ici (chapitre 3) la RMN du ^{13}C à polarisation croisée multiple (multi-CP) du solide fût utilisée pour déterminer précisément, rapidement et de manière non destructive la teneur en chitine d'un échantillon chitineux. Les matériaux préparés pour cette thèse furent ensuite préparés en toute connaissance de la pureté de la chitine. Dans le chapitre 4, la préparation de films de chitine *via* traitement par LI fut optimisée, et les propriétés de ces films furent étudiés. Il a été constaté que les paramètres de préparation tels que le chargement de chitine dans le LI, la source de chitine ou la méthode de coulage ont un effet sur la performance du coulage de film. Pour démontrer une application potentielle en tant que membrane libérant des médicaments, de la

caféine fut chargée puis relâchée depuis des films séchés par CO₂ supercritique. Le chapitre suivant (Chapitre 5) est axé sur l'utilisation de la plate-forme de préparation de films de chitine composites fonctionnels, la méthode utilisant les LI permettant l'incorporation d'additifs dans la solution chitine/IL. En poursuivant sur le thème de l'utilisation de la chitine en tant que matériau polymérique plus durable, des films composites de chitine/graphène furent préparés et utilisés pour la construction d'un super condensateur fonctionnel. La dispersion du graphène dans la chitine fut étudiée, et des films composites ayant jusqu'à 80% en poids de graphène furent coulés. Les films composites de graphène/chitine (utilisés en tant qu'électrodes), ainsi que les films de chitine purs (utilisés en tant que séparateurs) furent assemblés en un super condensateur fonctionnel basé sur la chitine. Le travail effectué dans cette thèse vise à jeter les bases du développement de matériaux avancés, durables et à forte valeur ajoutée obtenus par le traitement de bio polymères par LI pour un monde ayant une meilleure durabilité.

Acknowledgements

First and foremost, I would like to express my sincere gratitude to my supervisor, Prof. Robin D. Rogers, for his support, advice, and patience throughout my studies and research, and for introducing me to green chemistry and giving me the opportunity to do work that I enjoy.

I would like to thank all of the members of the group I have worked with both past and present, including Julia, Gabi, Paula, Steven, Hatem, Max, Tom, Giampiero, Shagha, Hemant, Manish, Kai, Prof. Tian, Sowmiah, Thomas and Nick. Thanks to all of you for your support, encouragement, your guidance and scientific insights, for the coffee breaks, and for being such great colleagues and friends. I want to specially thank Julia for all of the guidance she has given me from the first day I stepped into a chemistry lab.

I would like to thank the Canada Excellence Research Chairs Program for the funding provided which allowed me to carry out my research, and the Department of Chemistry. I would like to thank everyone in the Department who helped me through my studies here, and especially to Dr. Robin Stein for all of the assistance she has given to me. I would also like to extend a special thanks to Prof. Mark P. Andrews for acting as my co-supervisor.

Lastly, I would like to thank my family and friends for their support over the last two years. To all of the friends that I have made in Montreal and at McGill for making my time here wonderful and giving me countless memories. To my family, especially my parents, for their unyielding support, and to my boyfriend who has endlessly encouraged me throughout my time here. It would not have been the same without you all.

Thesis overview and contribution of authors

This thesis comprises three manuscripts which were authored primarily by the author of the thesis, and co-authored by Robin D. Rogers who acted as the research supervisor. The citation for each chapter is given below, along with an explanation of the author's contribution.

Chapter 1. Introduction

This chapter was written by the author of the thesis.

Chapter 2. Experimental

This chapter was written by the author of the thesis, and parts were taken from the manuscripts of the following chapters.

Chapter 3. Measuring the purity of chitin with a clean, quantitative solid-state NMR method

This chapter was adapted from the manuscript, reprinted with permission from: Catherine King, Robin S. Stein, Julia L. Shamshina, and Robin D. Rogers. Measuring the Purity of Chitin with a Clean, Quantitative Solid-State NMR Method. *ACS Sustainable Chem. Eng.* **2017**, *5*, 8011-8016.

The author wrote the manuscript and collected the data. Robin S. Stein designed NMR experiments and wrote sections of the chapter. Julia L. Shamshina helped in the design of the experiments and edited the manuscript. Robin D. Rogers directed and edited the manuscript.

Chapter 4: Platform for the preparation of chitin films from an ionic liquid process

This chapter was adapted from the manuscript, reproduced by permission of The Royal Society of Chemistry: Catherine King, Julia L. Shamshina, Gabriela Gurau, Paula Berton, Nur Farahnadiah

Abdul Faruk Khan, and Robin D. Rogers. A platform for more sustainable chitin films from an ionic liquid process. *Green Chem.* **2017**, *19*, 117-126.

The author collected all the data and wrote the manuscript. Julia L. Shamshina helped in collection of data, design of experiments, and editing the manuscript. Gabriela Gurau helped in the discussion of results and review of the manuscript. Paula Berton edited the manuscript and discussed results. Nur Farahnadiah Abdul Faruk Khan collected data on shrinkage of chitin films and release of caffeine from chitin films. Robin D. Rogers directed the design of the project and edited the manuscript.

Chapter 5. Graphene/chitin composite films for the assembly of a more sustainable supercapacitor

This chapter was adapted from a manuscript which is currently in preparation: Catherine King, Max E. Easton, and Robin D. Rogers. Graphene/chitin composite films for the assembly of a more sustainable supercapacitor. Manuscript in preparation.

The author collected and compiled the data and wrote the manuscript. Max E. Easton designed the cyclic voltammetry experiments, collected the electrochemical data, and wrote electrochemical data discussion. Robin D. Rogers directed the design of and edited the manuscript.

Table of contents

Abstract.....	i
Resume.....	iii
Acknowledgements.....	v
Thesis overview and contribution of authors.....	vi
List of abbreviations.....	xi
List of tables.....	xii
List of figures.....	xiii
Chapter 1. Introduction.....	1
1.1 Plastic waste and the role of green chemistry.....	1
1.2 Biopolymers for the replacement of petrochemical based polymers.....	3
1.3 Chitin and the production of high value materials.....	5
1.3.1 Chitin structure, sources, and production.....	6
1.3.2. Utilization of chitin for high value materials.....	8
1.4 Ionic liquid manipulation of chitin.....	10
1.4.1 Dissolution of biopolymers in ionic liquids.....	10
1.4.2 Manipulation of chitin using ionic liquids for the preparation of functional materials.....	11
1.5 Overview of chapters.....	13
1.6 References.....	15
Chapter 2. Experimental.....	18
2.1 Chemicals.....	18
2.2 Instrumental methods.....	19
2.2.1 Viscosity testing.....	19
2.2.2 Fourier transform infrared spectroscopy (FTIR).....	19
2.2.3 Solid-state nuclear magnetic resonance (SSNMR).....	20
2.2.3.1 Solid-state ¹³ C cross polarization/magic angle spinning NMR (SS CP/MAS NMR).....	20
2.2.3.2 Solid-state ¹³ C direct polarization NMR (DP NMR).....	20
2.2.3.3 Solid-state ¹³ C multiple CP NMR (multiCP NMR).....	20
2.2.4 Thermogravimetric analysis (TGA).....	21
2.2.5 Mechanical testing.....	21
2.2.6 Optical microscopy.....	22

2.2.7 Scanning electron microscopy (SEM).....	22
2.2.8 Cyclic voltammetry (CV).....	22
2.3 Chitin content characterization techniques	23
2.3.1 Chitin content determination by Black and Schwartz pulping.....	23
2.3.2 Construction of calibration curve for chitin content determination using multiCP NMR	24
2.4 Ionic liquid extraction of chitin.....	24
2.5 Material preparation	25
2.5.1 Film preparation from COOP chitin.....	25
2.5.1.1 Film casting.....	25
2.5.1.2 Film drying.....	26
2.5.2 Film preparation from BT chitin	27
2.5.2.1 Neat film casting.....	27
2.5.2.2 Composite film casting	28
2.6 Material characterization.....	29
2.6.1 Chitin film shrinkage	29
2.6.2 Chitin film water content.....	29
2.6.3 Loading and release of caffeine from COOP chitin film.....	30
2.6.4 Swelling of neat BT chitin and graphene/BT chitin composite films	31
2.6.5 Assembly of electrochemical cell from BT chitin films.....	31
2.7 References	32
Chapter 3. Measuring the purity of chitin with a clean, quantitative solid-state NMR method ...	33
3.1 Introduction	33
3.2 Results and discussion.....	36
3.2.1 CP buildup curves of deproteinized and untreated chitin.....	36
3.2.2 Application of multiCP method and comparison with CP and DP NMR	38
3.2.3 Construction of a calibration curve from PG chitin	39
3.2.4 Chitin content measurements using multiCP with calibration curve	42
3.3 Conclusions	44
3.4 References	45
Chapter 4. A platform for more sustainable chitin films from an ionic liquid process	47
4.1 Introduction	47
4.2 Results and discussion.....	48

4.2.1 Film preparation	49
4.2.2 Drying of films	53
4.2.3 Purity of dry films.....	55
4.2.4 Film thickness.....	56
4.2.5 Film morphology	57
4.2.6 Tensile strength.....	60
4.2.7 Water content.....	61
4.2.8 Film swelling	61
4.2.9 Drug loading and release	62
4.3 Conclusions	66
4.4 References	67
Chapter 5. Graphene/chitin composite films for the assembly of a more sustainable supercapacitor	68
5.1 Introduction	68
5.2 Results and Discussion.....	70
5.2.1 Preparation of films	70
5.2.2 Film thickness.....	72
5.2.3 Film morphology	73
5.2.4 Physical properties of films	73
5.2.5 Swelling of films in aqueous electrolyte	76
5.2.6 Assembly of supercapacitor and electrochemical testing.....	76
5.3 Conclusions.....	80
5.4 References	81
Chapter 6. Conclusions and Future Directions	83
6.1 Conclusions, contributions to knowledge, and future directions	83
6.2 References	89

List of abbreviations

API	Active pharmaceutical ingredient
ATR	Attenuated total reflection
BSA	Bovine serum albumin
BT chitin	Chitin from black tiger shrimp shells
BT SS	Black tiger shrimp shells
[Amim][Br]	1-allyl-3-methylimidazolium bromide
[C ₂ mim][Cl]	1-ethyl-3-methylimidazolium chloride
[C ₂ mim][OAc]	1-ethyl-3-methylimidazolium acetate
[C ₂ mim][OPr]	1-ethyl-3-methylimidazolium propionate
[C ₄ mim][Cl]	1-butyl-3-methylimidazolium chloride
[C ₄ mim][OAc]	1-butyl-3-methylimidazolium acetate
COOP chitin	Chitin from COOP shrimp shells
COOP SS	Shrimp shells from the Gulf Coast Agricultural and Seafood Cooperative
CP	Cross polarization
CPMAS	Cross polarization magnetic angle spinning
CV	Cyclic voltammetry
DI	Deionized
DMAc/LiCl	<i>N,N</i> -dimethylacetamide/ lithium chloride
DP	Direct polarization
ERETIC	Electronic reference to access in vivo concentrations
FTIR	Fourier transform infrared spectroscopy
IL	Ionic liquid
multiCP	Multiple cross polarization
NA chitin	Chitin from NA SS
NA SS	North Atlantic shrimp shells
NMP	<i>N</i> -methylpyrrolidone
NMR	Nuclear magnetic resonance
PBS	Phosphate buffered saline
PTFE	Polytetrafluoroethylene
PVDF	Polyvinylidene fluoride
PG chitin	Practical grade chitin
PULCON	Pulse length based concentration determination
PXRD	Powder X-ray diffraction
Sc-CO ₂	Supercritical CO ₂
SEM	Scanning electron microscopy
SSNMR	Solid-state nuclear magnetic resonance
TCA	Trichloroacetic acid
TGA	Thermogravimetric analysis
USP	United States Pharmacopeia
YM	Young's Modulus

List of tables

Table 3.1 T_{CP} and T_{1pH} values for chitin ring carbons of untreated and deproteinized chitin extract.....	37
Table 3.2 Chitin content of different sources as determine from multiCP and from Black and Schwartz (B & S) methods.	44
Table 4.1 Critical parameters for chitin film preparation.	49
Table 4.2 Weight percent loading of chitin and resulting solution and film.	51
Table 4.3 Effect of rolling rod on the film thickness of press and sc-CO ₂ dried films.....	57
Table 4.4 Tensile strength of RDS 100, RDS 135, and RDS 150 for press and sc-CO ₂ dried films.	60
Table 4.5 Rehydration percentage of dry films.	62
Table 5.1 Observations and properties of neat chitin film and 80 wt% graphene/chitin composite films.	72
Table 5.2 Capacitance values normalized to the mass of the electrode films.....	79

List of figures

Figure 1.1 Structures for (a) cellulose, (b) chitin, and (c) chitosan (deacetylated derivative of chitin), and (d) a representative structure of lignin.	4
Figure 1.2 Exoskeleton structure of the shell of the <i>Homarus americanus</i> lobster, adapted from ref [36]. Chitin chains are encased in proteins, which make up bundles, and form a helical structure. The spacing between the fibers is filled with CaCO ₃ minerals.	7
Figure 1.3 1-ethyl-3-methylimidazolium acetate ([C ₂ mim][OAc]).	11
Figure 3.1 Structure of chitin, ring carbon atoms labeled.	35
Figure 3.2 Buildup curves for each chitin peak for both untreated (left) and deproteinized (right) NA chitin. Note differences in the scales.	37
Figure 3.3 Comparison of CP-standard (2 h 20 min), CP-long (2 h 20 min), DP (using a recycle delay of 1440 s, 62 h) and multiCP (1 h 40 min) spectra of NA chitin.	38
Figure 3.4 Contour plots showing peak intensity of the (a) C3 peak in a 1:4 chitin:BSA mixture, (b) C5 peak in a 1:4 chitin:BSA mixture, (c) C3 peak in NA chitin, and (d) C5 peak in NA chitin in multiCP spectra as a function of CP contact time per period and number of CP periods.	40
Figure 3.5 MultiCP spectra of chitin:BSA mixtures by mass. Signals arising from the BSA protein are circled on the 25% PG chitin spectra. The region of the spectrum used for integration is 77.99-70.70 ppm (C3 and C5 chitin peaks).	41
Figure 3.6 Chitin content calibration curve from C3 and C5 peaks. Peak integrals are scaled such that the integral of the sample containing only PG chitin is 100. The best fit curve (straight line) is described by Eq. 3.2.	42
Figure 3.7 PXRD diffractograms for BT chitin, NA chitin, and CaCO ₃	43
Figure 4.1 Preparation chart for chitin films.	50
Figure 4.2 Viscosity of chitin/IL solutions from 40 to 80 °C.	52
Figure 4.3 Chitin films dried by different methods.	54
Figure 4.4 FTIR spectra of chitin film (red), and [C ₂ mim][OAc] (black).	55
Figure 4.5 TGA data for press dried chitin film.	56
Figure 4.6 Press dried (left) and sc-CO ₂ dried (right) films.	58
Figure 4.7 Press dried (left) and sc-CO ₂ dried (right) films at 100X magnification.	58
Figure 4.8 (a) press dried film (5.4(3) μm thick), (b) sc-CO ₂ dried film. (6.7(8) μm thick), (c) sc-CO ₂ film (14.2(8) μm thick), (d) its backside. Image magnifications: 150X-250X. (The magnifications are not the same, as magnification was gradually increased while taking the SEM and the best pictures were selected).	59
Figure 4.9 Representative tensile strength curves for RDS 100, 135, and 150 press dried films (left), and RDS 135 sc-CO ₂ dried film (right).	61
Figure 4.10 Optical microscopy at 40X of caffeine crystals on the surface of a press dried film.	63
Figure 4.11 ¹ H NMR (500 MHz, DMSO-d ₆) for caffeine (top), and ¹ H NMR (500 MHz, DMSO-d ₆) for the solution of the washed film (bottom).	63
Figure 4.12 Optical microscopy image of sc-CO ₂ film embedded with caffeine (no visible crystals).	65
Figure 4.13 Percentage of caffeine released (left) and mg of caffeine released (right).	66

Figure 5.1 SEM images at 2000X magnification for neat chitin film (left) and 80 wt% graphene/chitin composite film (right).	73
Figure 5.2 TGA of neat chitin and graphene chitin composite films (with the mass of the composite film normalized to mass of chitin) (left), and full TGA for neat chitin film, 80 wt% chitin/graphene composite film, chitin powder, and graphene powder (right).	74
Figure 5.3 Stress/strain curves of neat chitin and 80 wt% graphene/chitin composite film.	75
Figure 5.4 (a) Dry films, (b) wetted film assembly, (c) assembled supercapacitor test cell, and (d) schematic showing arrangement of components in test cell.	78
Figure 5.5 Cyclic voltammograms showing current densities (left) and capacitance (right) for the chitin thin film supercapacitor, performed between 0 and 1 V at scan rates ranging from 5-50 mV/s.	79

Chapter 1. Introduction

1.1 Plastic waste and the role of green chemistry

Since the early 1990s, the practice of Green Chemistry has grown exponentially as it has been called upon to solve many of the environmental issues facing society today. In 1998, the 12 Principles of Green Chemistry were presented as guidelines to be used in the design and use of more environmentally benign products and chemical processes. As a broad concept, the principles of green chemistry can be applied to many of today's global problems, from food waste to climate change to pollution.¹

One of the major challenges facing society today is that of environmental pollution, especially of plastics based on synthetic, petrochemical-based polymers. The “plastic age” arguably began in 1907 with the invention of the Bakelite, and although they were first seen as novelties, synthetic plastics quickly became ubiquitous in everyday life, with about 311 million tons of synthetic plastics produced worldwide in 2014.^{2,3} Major commercial development of plastics occurred between the 1920s and the 1950s, with the invention of synthetic polymers such as polyethylene, polystyrene, and polypropylene, which are used in textiles, packaging, and transportation.⁴ At the time of their introduction, plastics were lauded for their potential societal benefits; in their 1941 book “Plastics,” Yarsley and Couzens make bold claims about the world to come, a “...*much brighter and cleaner a world... than that which preceded the plastics age.*”⁵ However, as time went on, an unanticipated consequence of the widespread use of plastics became apparent in the form of environmental pollution.

Today, the prevalence of synthetic plastics in the environment has become a major societal issue, with increasing concern on their effects on both land and marine environments, wildlife, and human health.^{6,7} Problems arise from petrochemical based plastics (both microplastics and

macroplastics) which persist in the environment rather than degrade, and can last for centuries.⁶ Especially concerning is the increasing amount of plastic waste which enters the marine environment; a study in 2015 estimated that even with recycling and landfilling of waste, 4.8-12.7 million metric tons of mismanaged plastic waste entered the ocean in 2010 alone.⁸ Large fragments of plastic debris can cause problems such as the entanglement and ingestion by marine organisms and can spread non-native species to different environments, as well as break down into fragments of microplastics.⁶ Microplastics (which have been defined by different size ranges, though always less than 10 mm) are perhaps an even greater threat, as aside from problems previously mentioned, they also have been observed to leach additives and to carry chemical pollutants due to their large surface area to volume ratio.⁹

Though there have been attempts to mitigate the effects of plastics on the environment, such as the direct removal of plastic waste, it is often more effective to prevent their release in the first place.¹⁰ Legislative action has been taken over the past 50 years to accomplish the reduction of plastic pollution. Initial strategies sought to deter the dumping of plastic waste into the environment, such as MARPOL 73/78 in 1973, which banned the disposal of plastics at sea. More recently, there has been a growing focus on reducing the use of plastics in the first place, with many countries or regions enacting bans on or fees for the use of plastic bags or microplastic beads.^{11,12}

The principles of green chemistry can work as a guide towards the mitigation of many of the environmental problems caused by plastics, principles such as “it is better to prevent waste than to treat or clean up waste after it has been created,” and “A raw material or feedstock should be renewable rather than depleting whenever technically and economically practicable.”¹³ Synthetic plastics, which are derived from non-renewable petrochemical sources are fundamentally

inconsistent with these two principles of green chemistry. To avoid this problem, there is a solution in the use of materials from renewable resources, such as biopolymers.

Here, I have worked to use these principles in order to design more sustainable materials as potential replacements for unsustainable petrochemical-based plastics, using biopolymers. Biopolymers (biodegradable polymers obtained from natural sources)¹⁴ in particular have the potential for performing many of the functions of petrochemical-based materials in common use today. In this thesis, I show how biopolymers (obtained from renewable feedstocks rather than depleting ones), can be designed and utilized into functional materials for use in applications which have been traditionally dominated by petrochemical based materials.

1.2 Biopolymers for the replacement of petrochemical based polymers

As societal concern for environmental issues such as climate change and a shift toward more renewable energy sources have increased, so too has the focus grown on the use of materials obtained from renewable feedstocks. Thus, the scientific community has become more and more interested in utilizing biopolymers and bio-based polymers (which are obtained directly from renewable sources and prepared from bio-based monomers, respectively)¹⁵ towards many of the functions currently performed by petrochemical-based polymers.¹⁴ Nature has made these complex structural polymers, and by extracting them, they can be harnessed for use in advanced materials. Though biomaterials have been used for centuries (such as the use of wood in construction), recently there has been greater appreciation for the potential of their biopolymer components such as starch, lignin, cellulose, chitin, and chitosan.¹⁶ Cellulose, obtained from lignocellulosic biomass, and chitin, obtained from arthropod exoskeletons and fungi, are the two most abundant biopolymers on earth, and due to their biodegradability, the renewable feedstocks from which they

are obtained, and the native properties which they possess, these natural polymers (**Figure 1.1**) have seen use in packaging, medical applications, and cosmetics.^{17,18}

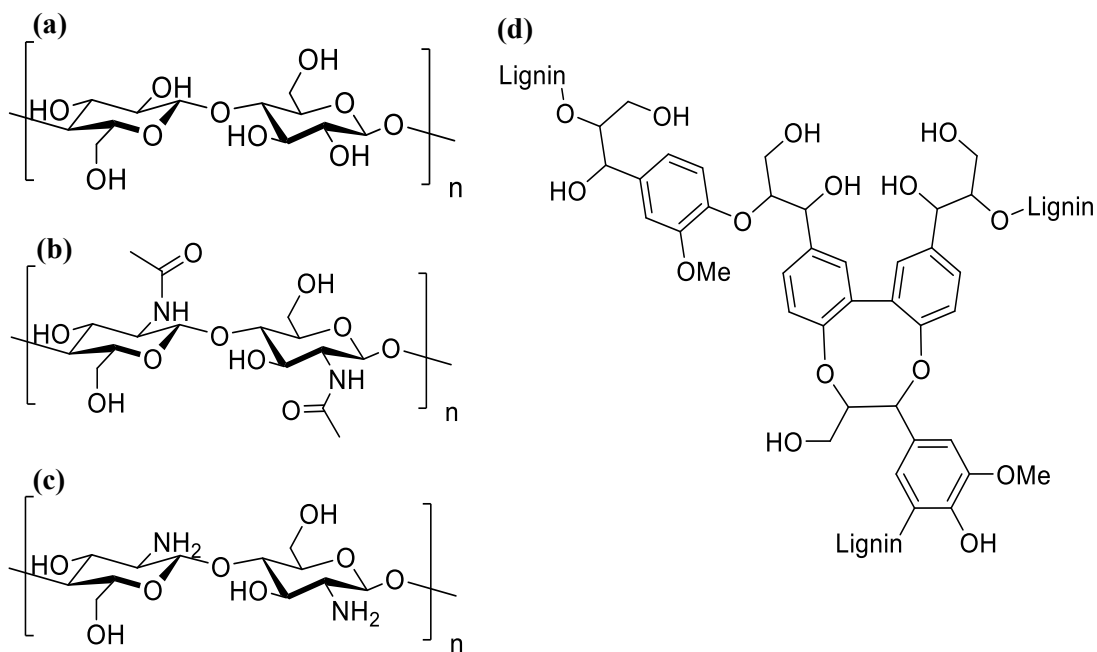


Figure 1.1 Structures for (a) cellulose, (b) chitin, and (c) chitosan (deacetylated derivative of chitin), and (d) a representative structure of lignin.

However, widespread use of these biopolymers in advanced materials applications has been limited due to difficulties in their separation and their insolubility in common solvent systems. Although it is estimated that about 70 billion tons of polysaccharides are produced *via* photosynthesis in nature each year, only 3% of that available is utilized annually.¹⁹ Cellulose, for example, has seen limited use in its native form, and is often chemically modified to allow for ease of processing of the polymer. Such methods include the viscose method (which involves treatment of the polymer with CS_2), and the Lyocell process (which utilizes an amine oxide solvent), both of which are not without hazard due to the toxicity of the chemicals involved.^{20,21} Furthermore, though cellulose can be separated from cellulosic biomass *via* the Kraft chemical pulping process,

the process is intensive and the use of the resulting material is often limited to the preparation of low-value products such as paper products and textiles.

Nature has shown that biopolymers have great potential for the formation of complex materials with advanced properties, exemplified with the extreme strength of limpet teeth or the structural iridescence of butterfly wings.^{22,23} Although traditional uses of biopolymers have been rather low-value, recently the preparation of new, more advanced material applications have emerged. For example, microcellulose and nanocellulose (cellulose fibrils of micro or nano size) were first used additives in the preparation of composite materials, but more recently they have been used for higher-end materials applications for which petrochemical based polymers have traditionally been used, such as optically transparent films, self-assembled composites, and aerogels.^{24,25} Lignins (which along with cellulose and hemicellulose help to give structure to plants) have traditionally been treated as a waste material,²⁶ but have recently seen use as additives for the preparation of polymer composites, as stabilizing agents, and due to their antioxidant properties, more high value applications such as biodegradable packaging.²⁷⁻²⁹

1.3 Chitin and the production of high value materials

Chitin is the second most abundant polysaccharide on Earth after cellulose, and has potential for use in functional materials due to its high value properties such as biocompatibility, biodegradability, and bioactivity.³⁰ Chitin is ubiquitous in nature, produced from organisms including shellfish, squid, and fungi; production from marine ecosystems alone is predicted to be about 1300 million tons per year.³¹ And although about 30 million tons of shellfish (which can have 2-12% chitin by body mass of the organism) are harvested per year,³⁰ chitin has largely remained an untapped resource.

1.3.1 Chitin structure, sources, and production

Chitin, poly(β -(1 \rightarrow 4)-*N*-acetyl-D-glucosamine), is a linear polysaccharide which makes up the main structural component of shells, exoskeletons, or other structural architectures within organisms including crustaceans, insects, and fungi.³² Chitin occurs in three different polymorphs in nature, depending on the source from which the chitin is obtained; these are: α -chitin, β -chitin, and γ -chitin. The most abundant form is α -chitin, occurring in crustacean shells and insect cuticles, while β -chitin is found most commonly in squid pens; γ -chitin is much less common and is a variant of α -chitin, found in the cocoons of some insects.^{33,34} α -chitin is formed by alternately antiparallel chitin chains, and β -chitin is formed by parallel chitin chains, giving them different hydrogen bonding characteristics and therefore making them distinguishable by FTIR, solid-state NMR, and X-ray diffraction.³⁵ In both forms, strong networks of inter and intramolecular hydrogen bonding occur within the chitin chains which form densely packed sheets and make it insoluble in common solvents.

In crustacean shells (perhaps the most accessible source, as they are a large agricultural by-product of the harvest of shellfish), α -chitin fibrils exist in a matrix along with proteins and minerals. Chitin fibrils are encased in protein matrices, which form bundles and organize into helicoidal structures. In the example of the lobster cuticle, below, the mineral CaCO_3 fills the spacing between the chitin/protein fibrils. This model also applies to other crustacean species and arthropods (**Figure 1.2**).³⁶

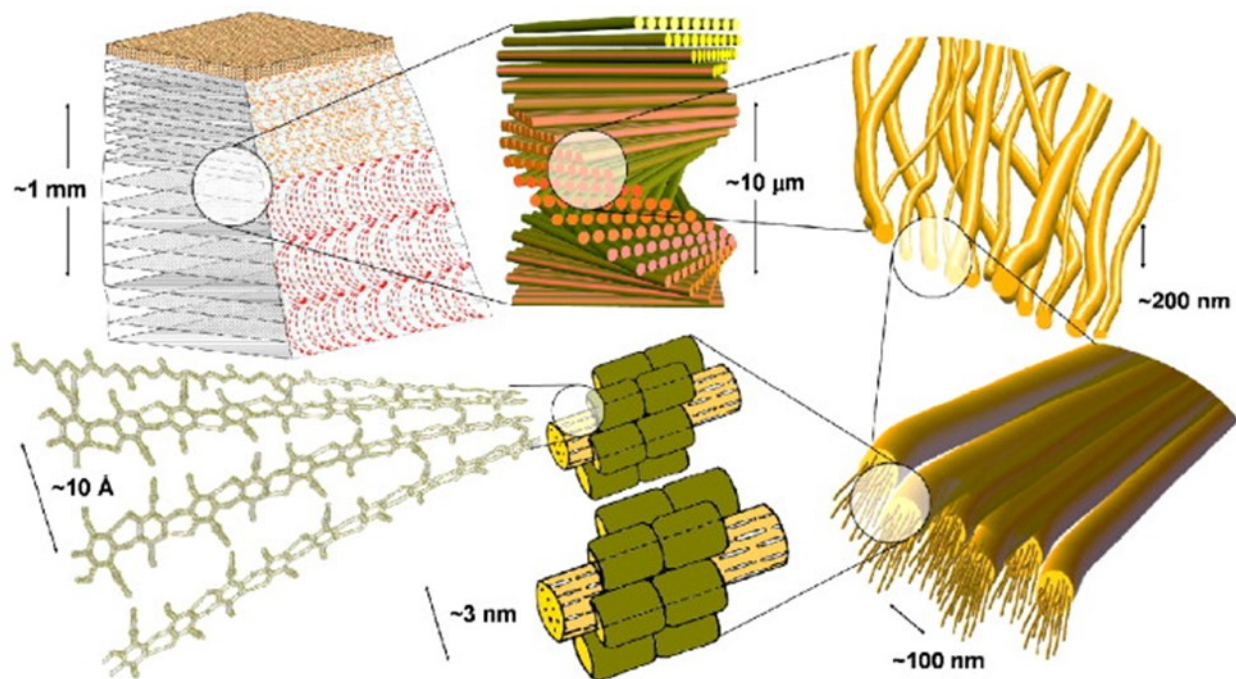


Figure 1.2 Exoskeleton structure of the shell of the *Homarus americanus* lobster, adapted from ref [36]. Chitin chains are encased in proteins, which make up bundles, and form a helical structure. The spacing between the fibers is filled with CaCO_3 minerals.

This dense composite structure, and the hydrogen bonding between the chitin chains themselves, makes the separation of chitin from biomass sources difficult, necessitating harsh conditions to isolate chitin.³⁷ The industrial production of chitin involves a chemical pulping method, whereby the minerals and proteins are removed by harsh chemical processing. Generally, this is done by first demineralizing the chitin with HCl and then by deproteinizing it using NaOH. The combined process tends to reduce the molecular weight and to deacetylate the chitin, and is far from environmentally friendly.^{34,38} This method is also used for the production of chitosan, another important biopolymer, and the deacetylated derivative of chitin. Aside from the chemical pulping of chitin, there have also been studies on the use of enzymatic deproteinization, though

the efficiency of these methods is lower than that of the traditional chemical pulping, leaving residual protein behind.³⁷

1.3.2. Utilization of chitin for high value materials

Both chitin and its derivative, chitosan, are of high interest for use in a wide range of applications due to their multitude of high-valuable properties such as non-toxicity, biodegradability, biocompatibility, bactericidal and fungicidal activities, hemostatic activity, wound healing properties, chelation properties, film and gel forming properties, and functionalizability.^{30,39,40} Accordingly, interest in the use of chitin for biomedical applications has been increasing since it was identified as a “potent pure chemical wound-healing accelerator” in a 1970 study.⁴¹ Since then, study of the biopolymer has shown that these properties arise from the presence of the *N*-acetyl and amine moieties in chitin and chitosan respectively, which enhance interaction between the polymer and its environment. The acetyl and amino groups present on the C-2 position of chitin and chitosan respectively, along with the hydroxyl groups present allow for a variety of interactions to take place such as the chelation of metal ions and the formation of complexes with different compounds such as other polysaccharides, proteins, and dyes, to name a few.⁴²

Many of the bioactive properties result from the interaction of the biopolymer with the biological system in question. Chitinous materials have been shown to stimulate the formation of fibroblasts and cytokines, allow for cell migration, and promote collagen synthesis for wound healing. In biological systems, this results either from the interaction of cells with the polymer itself, or with oligochitins which result from the chemical or enzymatic degradation of the polymer in the system. Chitin and chitosan degrade into *N*-acetyl glucosamine and glucosamine, respectively, which can both be further utilized biologically for the production of glycoproteins.⁴³

Thus, the use of chitin in biomedical research has seen enormous growth, with chitin and chitosan being used in the preparation of new materials for applications such as drug delivery, tissue engineering, and wound care.⁴⁴⁻⁴⁷

Aside from biomedical uses, the bioactive and physiochemical properties which chitin possess make it suitable for other high value applications. Due to its antifungal, antibacterial, and antioxidant activities, it lends itself to use in materials which have direct contact with humans, such as in the food industry where chitin can act as a preservative as well as a dietary fiber and thickening agent;⁴⁸ in cosmetics applications, where it has been used in hair and skin products,^{48,49} or as functional textiles.⁵⁰ Due to its chelation and absorption capacities, chitin materials have been used in wastewater treatment for the removal of toxic metal ions and other pollutants.⁵¹ Additionally, the biocompatibility and affinity for proteins of chitin and chitosan have spurred interest in their use as supports for enzyme immobilization and biosensing.⁵²

In addition to the use of native chitin or chitosan, the amine moiety on chitin can be functionalized by acetylation, amine quaternization, or reactions with aldehydes and ketones to form Schiff's bases.⁵³ Other functional groups can be incorporated for the further derivatization of the polymer or for grafting to prepare co-polymers for the incorporation of specific functionalities.⁵⁰

However, despite this collection of high value properties, the widespread use of chitin in materials applications has been hindered due to its previously mentioned insolubility in common solvent systems which results from the dense hydrogen bonding network of the polymer. A few solvent systems in which chitin can be dissolved and processed have been found, including *N,N*-dimethylacetamide (DMAc)/lithium chloride (LiCl),⁵⁴ aqueous NaOH/urea,⁵⁵ trichloroacetic acid (TCA) and a chlorinated hydrocarbon, and some fluorinated solvents,⁵³ but all of these solvent

systems are so harsh that they degrade the polymer or are difficult to remove from the final material.

1.4 Ionic liquid manipulation of chitin

1.4.1 Dissolution of biopolymers in ionic liquids

Over the past 15 years, ionic liquids (ILs) have emerged as a platform for the dissolution and manipulation of biopolymers, first realized with the complete dissolution of cellulose in the IL 1-butyl-3-methylimidazolium chloride ([C₄mim][Cl]) in 2002.⁵⁶ ILs are defined as salts with a melting point below 100 °C, and are often liquids at room temperature.⁵⁷ They have unique properties such as high thermal stability, negligible vapor pressure, and a wide liquid range, and, due to the fact that ions can be selected for desired properties, ILs have been called “designer solvents.”⁵⁸ In the case of many traditionally insoluble biopolymers, ILs with small, basic anions have been shown to solvate the polymer chains by disrupting the strong network of inter- and intramolecular hydrogen bonding which has traditionally hindered dissolution attempts.⁵⁹ Since the first use of [C₄mim][Cl] for cellulose dissolution, ILs have been shown to dissolve numerous biopolymers such as lignin,⁶⁰ starch,⁶¹ silk,⁶² and chitin.⁶³

Various ILs have been found to dissolve commercially available chitin, including [C₄mim][Cl],⁶³ 1-butyl-3-methylimidazolium acetate ([C₄mim][OAc]),⁶⁴ 1-allyl-3-methylimidazolium bromide ([Amim][Br]),⁶⁵ and 1-ethyl-3-methylimidazolium acetate ([C₂mim][OAc]). Studies have suggested that anion basicity plays an extremely important role in the dissolution of chitin in a given IL; in a 2008 study by Wu et al.,⁶² it was found that while chitin was completely soluble in [C₄mim][OAc] up to 6 wt%, it was only partially soluble in [C₄mim][Cl]. In 2010, a study by Wang et al. further elucidated this phenomenon, demonstrating that chitin dissolves more readily in ILs with more basic anions, as anions with greater basicity

more easily disrupt the hydrogen bonding network by interacting with the hydroxyl groups of the chitin structure and allowing for solvation of the polymer.⁶⁶ It was also found that the dissolution of chitin depends on factors relating to the polymer such as the degree of acetylation, molecular weight, and crystallinity. This finding that ILs with anions which are strong hydrogen bond acceptors more readily dissolve chitin is a phenomenon similar to that observed in the dissolution of cellulose in IL, where the solubility of cellulose in various ILs was also found to increase with the hydrogen bond accepting ability of the anions.⁶⁷

Aside from the dissolution of pure chitin, ILs can be used for the direct extraction of the polymer from biomass sources. In 2010, the IL [C₂mim][OAc] (**Figure 1.3**) was used to extract and regenerate chitin from a biomass waste source (shrimp shells) without pretreatment or derivatization.⁶⁸ Chitin dissolved in the IL can be regenerated by coagulation in an antisolvent (such as water), in which the IL is soluble and the chitin is not. This method allows for the production of high molecular weight chitin for the preparation of functional materials. The extracted chitin can either be directly processed into materials from the shrimp shell solution, or regenerated *via* coagulation for further processing.

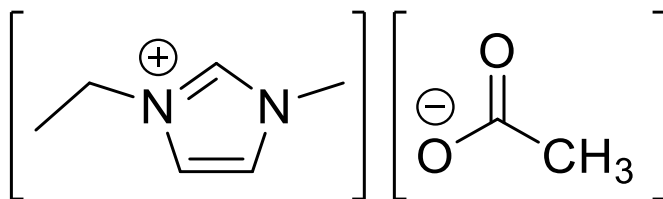


Figure 1.3 1-ethyl-3-methylimidazolium acetate ([C₂mim][OAc]).

1.4.2 Manipulation of chitin using ionic liquids for the preparation of functional materials

The IL [C₂mim][OAc] has been used both for the direct preparation of materials from the shrimp shell extract and for the regeneration of high molecular weight chitin which can be further

processed using the IL for material preparation. The chitin extraction procedure involves the microwave-assisted dissolution of shrimp shells in the IL and the regeneration of chitin in water as an antisolvent. The mineral CaCO_3 is insoluble in the IL, and is therefore separated as the chitin is dissolved, removing the need for harsh acid treatments which can hydrolyze the polymer. In addition, most of the protein is removed from the chitin during the extraction. This chitin extraction and processing procedure can be used for the extraction of chitin from renewable feedstocks for the production of sustainable, high value chitinous materials with unique functionalities which can be used for the replacement of less sustainable petrochemical based materials.

The IL process can be used for the solution processing of the biopolymer from shrimp shell sources for the direct and quick preparation of functional material architectures or composites. The processing has been used for the preparation of materials such as fibers,⁶⁸⁻⁷⁰ and nanomats,⁷¹⁻⁷³ and IL-extracted chitin used for the preparation of hydrogels.⁷⁴ The control of the different architectures allows for preparation of materials which are suitable for different applications: hydrogels (with their high porosity) are suitable for the loading and release of molecular compounds, and nanomats for example, (with their high surface area) are suitable for applications such as implementation in filtration systems. Pure chitin materials can be used for the loading and release of active pharmaceutical ingredients or can be modified for further use. For example, once prepared into a desired architecture, pure materials can be functionalized for particular applications, such as the preparation of chitin fibers surface functionalized with amidoxime for the absorption of uranium.⁷⁰ Composite materials can be simply prepared by IL processing, whereby another polymer or material is incorporated into the solution prior to the casting of the material from solution. In this way, chitin/nanotube composites have been made.⁷⁵ Also, material blends of different polymers can be prepared, such as composite chitin/alginate fibers for wound care, which

showed 95-99% wound closure after only 10 days using a single patch in rat studies.⁶⁹ However, other architectures of chitin have yet to be explored from the IL processing of chitin *via* this method, including films.

1.5 Overview of chapters

The thesis presented here will consist of five chapters in addition to the introduction. Chapter 2 is an overview of the chemicals, materials, instrumentation, and methods used. Chapter 3, Chapter 4, and Chapter 5 discuss work done on determining the purity of chitin, the preparation of chitin films, and the use of chitin films in an advanced material application, respectively.

Chapter 3 is adapted from a recently published manuscript, whereby a method for the determination of chitin content was determined using a solid-state ^{13}C NMR.⁷⁶ As it is obtained from living organisms, chitin obtained from any source will have impurities in the form of proteins and minerals. The relative amounts of chitin, proteins, and minerals in a crustacean shell depends on a number of factors such as the organism from which the chitin is obtained, biological aspects relating to the organism, the environment of the organism, and the processing and peeling conditions.³⁰ For those materials which are to be used in highly sensitive applications (such as those medical in nature), for example, medical devices must meet certain specifications such as those of the US FDA (which involves, for example, the biocompatibility, cytotoxicity, and sensitivity), before they can be used.⁷⁷ It is therefore necessary to be able to both determine the purity of the chitin quantitatively as well as purify chitin containing impurities.

With this in mind, a new method for the quantification of chitin content in chitinous samples has been developed using solid-state ^{13}C NMR. The chitin content in a material has traditionally been determined by the pulping method of Black and Schwartz,⁷⁸ which is intrinsically a destructive and inaccurate method as it utilizes harsh acid and base washes to purify chitin, and is

highly operator dependent. Thus, in Chapter 3, a non-destructive, accurate method for the quantification of chitin purity is presented. This method can be used for the determination of chitin purity in order that the chitin can be used for the preparation of new materials.

Once the purity of chitin could be determined, different materials were prepared. Chapter 4 is adapted from a published article, where the preparation of chitin films from an IL process was optimized.⁷⁹ Biopolymer based films and chitin based films are of great interest due to their diversity of application. The film form is often used in packaging materials and medical devices, and is therefore of interest for the preparation of new biodegradable materials.⁸⁰ Because of chitin's functional properties, it is well suited to such applications in the film architecture. In Chapter 4, the preparation of pure chitin films is discussed, whereby the procedure was optimized to design a platform for the tunable and scalable preparation of neat chitin films which can be suited toward the desired application. The film preparation method was based on chitin loading in the IL, casting thickness of the films, and drying method. The films were characterized, and load and release of caffeine as a model drug compound was studied as a potential application.

In Chapter 5, the method for the IL processing of chitin into films is used for the preparation of composite film materials. As the IL solution processing method allows for the incorporation of additives to the chitin solution, conductive graphene was added for the preparation of chitin/graphene composite films. These films were used as electrodes for a proof-of-concept supercapacitor. Though the green energy economy strives to use more sustainable energy sources *via* energy storage devices, the materials used in the construction of such devices are often unsustainable. Here, biomass-derived chitin was used to prepare both the conductive composite electrodes and non-conductive separators through the IL processing of the biopolymer, to act as a sustainable polymer replacement to the more commonly used petrochemical based polymers. The

morphology and physical properties of the films were studied, and the films were used for the assembly and testing of an electrochemical cell, demonstrating the ability to assemble a proof-of-concept sustainable supercapacitor, and showed entry level performance.

Through the work shown here, the principles of green chemistry have been implemented in order to progress towards the use of renewable materials rather than environmentally harmful, persistent polymers. The abundance of chitin and the numerous high value properties it possesses make it suitable for applications across different fields in which petrochemical based polymers are now ubiquitous. The technology of IL processing of chitin has allowed for the use of chitin for which the preparation had been a challenge in the past. Through the use of IL processing, chitin from waste has here been used for the preparation of new materials and forms, which can be implemented into new technologies for a more sustainable world.

1.6 References

- ¹ Anastas, P. T.; Kirchoff, M. M. *Acc. Chem. Res.* **2002**, *35*, 686-694.
- ² Crespy, D.; Bozonnet, M.; Meier, M. *Angew. Chem. Int. Ed.* **2008**, *47*, 3322-3328.
- ³ *Plastics – the facts 2015*. Plastics Europe; Brussels, Belgium, 2015.
- ⁴ Andrady, A. L.; Neal, M. A. *Philos. Trans. R. Soc. Lond. B. Bio. Sci.* **2009**, *364*, 1977-1984.
- ⁵ Yarsley, V. E.; Couzens, E. G. *Plastics*, Penguin Books Limited: Middlesex, 1941.
- ⁶ Derraik, J. G. B.; *Mar. Pol. Bull.* **2002**, *44*, 842-852.
- ⁷ Thompson, R. C.; Moore, C. J.; vom Saal, F. S.; Swan, S. H. *Phil. Trans. R. Soc. B.* **2009**, *364*, 2153-2166.
- ⁸ Jambeck, J. R.; Geyer, R.; Wilcox, C.; Siegler, T. R.; Perryman, M.; Andrady, A.; Narayan, R.; Law, K. L. *Science*, **2015**, *347*, 768-771.
- ⁹ Cole, M.; Lindeque, P.; Halsband, C.; Galloway, T. S. *Mar. Pol. Bull.* **2011**, *62*, 2588-2597.
- ¹⁰ Ryan, P. G.; Moore, C. J.; van Franeker, J. A.; Moloney, C. L. *Phil. Trans. R. Soc. B.* **2009**, *364*, 1999-2012.
- ¹¹ Xanthos, D.; Walker, T. R. *Mar. Pol. Bull.* **2017**, *118*, 17-26.
- ¹² United States Congress, 2015, H. R. 1321 – Microbead-Free Waters Act of 2015.
- ¹³ Anastas, P. T.; Warner, J. C. *The Twelve Principles of Green Chemistry, Green Chemistry Theory and Practice*, Oxford University Press: New York, 1998; p. 30.
- ¹⁴ Mohanty, A. K.; Misra, M.; Drzal, L. T. *J. Polym. Environ.* **2002**, *10*, 19-26.
- ¹⁵ Mulhaupt, R. *Macromol. Chem. Phys.* **2012**, *214*, 159-174.
- ¹⁶ Babu, R. P.; O'Connor, K.; Seeram, R. *Prog. Biomater.* **2013**, *2*, 8-16.
- ¹⁷ Rhim, J. W.; Ng, P. K. W. *Crit. Rev. Food Sci. Nutr.* **2007**, *47*, 411-433.
- ¹⁸ Van Vlierberghe, S.; Dubrue, P.; Schacht, E. *Biomacromolecules*, **2011**, *12*, 1387-1408.
- ¹⁹ Gilbert, R. D.; Kadla, J. F. Polysaccharides – Cellulose. In *Biopolymers from Renewable Resources*; Kaplan, D. L. Ed.; Springer: Berlin, 1998; pp. 47-95.
- ²⁰ Klemm, D.; Heublein, B.; Fink, H.P.; Bohn, A. *Angew. Chem. Int. Ed.* **2005**, *44*, 3358-3393.
- ²¹ Rosenau, T.; Potthast, A.; Sixta, H.; Kosma, P. *Prog. Polym. Sci.* **2001**, *26*, 1763-1837.
- ²² Barber, A. H.; Lu, D.; Pugno, N. M. *J. R. Soc. Interface*, **2015**, *12*, 20141326.

- 23 Kinoshita, S.; Yoshioka, S.; Kawagoe, K. *Proc. R. Soc. Lond. B.* **2002**, *269*, 1417-1421.
- 24 Moon, R. J.; Martini, A.; Nairn, J.; Simonsen, J.; Youngblood, J. *Chem. Soc. Rev.* **2011**, *40*, 3941-3994.
- 25 Eichhorn, S. J.; Dufresne, A.; Aranguren, M.; Marcovich, N. E.; Capadona, J. R.; Rowan, S. J.; Weder, C.; Thielemans, W.; Roman, M.; Renneckar, S.; Gindl, W.; Veigel, S.; Keckes, J.; Yano, H.; Abe, K. *J. Mater. Sci.* **2010**, *45*:1.
- 26 Stewart, D. *Ind. Crops and Prod.* **2008**, *27*, 202-207.
- 27 Calvo-Flores, F. G.; Dobado, J. A. *ChemSusChem.* **2010**, *3*, 1227-1235.
- 28 Thakur, V. K.; Thakur, M. K.; Raghavan, P.; Kessler, M. R. *ACS Sustainable Chem. Eng.* **2014**, *2*, 1072-1092.
- 29 Domenek, S.; Louaifi, A.; Guinault, A.; Baumberger, S. *J. Polym. Environ.* **2013**, *21*, 692-701.
- 30 Synowiecki, J.; Al-Khateeb, N. A. *Crit. Rev. Food Sci. Nutr.* **2003**, *43*, 145-171.
- 31 Chauchie, H. M. *Hydrobiologia*, **2002**, *470*, 63-96.
- 32 Smith, C.; Hudson, S. M. Polysaccharides: Chitin and Chitosan: Chemistry and Technology of Their Use As Structural Materials. In *Biopolymers from Renewable Resources*; Ed.: D. L. Caplan; Springer: Berlin, 1998; pp 96-118.
- 33 Rudall, K. M.; Kenchington, W. *Biol. Rev.* **1973**, *49*, 597-636.
- 34 Rinaudo, M. *Prog. Polym. Sci.* **2006**, *31*, 603-632.
- 35 Jang, M.-K.; Kong, B.-G.; Jeong, Y.-I.; Lee, C.-H.; Nah, J.-W. *J. Polym. Sci. A Polym. Chem.* **2004**, *42*, 3423-3432.
- 36 Raabe, D.; Romano, P.; Sachs, C.; Al-Sawalmih, A.; Brokmeier, H.-G.; Yi, S.-B.; Servos, G.; Hartwig, H. G. *J. Cryst. Growth.* **2005**, *283*, 1-7.
- 37 Younes, I.; Rinaudo, M. *Mar. Drugs*, **2015**, *13*, 1133-1174.
- 38 Barber, P. S.; Shamshina, J. S.; Rogers, R. D. *Pure Appl. Chem.* **2013**, *85*, 1693-1701.
- 39 Muzzarelli, R. A. A. *Carbohydr. Polym.* **2009**, *76*, 167-182.
- 40 Muzzarelli, R. A. A. Chitin. In *Natural chelating polymers: alginic acid, chitin and chitosan*, 1st ed.; Pergamon Press: New York, 1973; pp. 83-143.
- 41 Prudden, J. F.; Migel, P.; Hanson, P.; Friedrich, L.; Balassa, L. *Am. J. Surg.* **1970**, *119*, 560-564.
- 42 Kardas I.; Struszczyk, M. H.; Kucharska, M.; van den Broek, L. A.; van Dam, J. E.; Ciecchanska, D. Chitin and chitosan as functional biopolymers for industrial applications. In *The European Polysaccharide Network of Excellence (EPNOE)*; Springer: Vienna, 2012; pp. 329-373.
- 43 Prashanth, K. H.; Tharanathan, R. N. *Trends Food Sci. Technol.* **2007**, *18*, 117-131.
- 44 Jayakumar, R.; Menon, D.; Manzoor, K.; Nair, S. V.; Tamura, H. *Carbohydr. Polym.* **2010**, *82*, 227-232.
- 45 Jayakumar, R.; Prabakaran, M.; Sudheesh Kumar, P. T.; Nair, S. V.; Tamura, H. *Biotechnol. Adv.* **2011**, *29*, 322-337.
- 46 Khor, E.; Lim, L. Y. *Biomaterials*, **2003**, *24*, 2339-2349.
- 47 Azuma, K.; Izumi, R.; Osaki, T.; Ifuku, S.; Morimoto, M.; Saimoto, H.; Minami, S.; Okamoto, Y. *J. Funct. Biomater.* **2015**, *6*, 104-142.
- 48 Shahidi, F.; Arachchi, J. K. V.; Jeon, Y.-J. *Trends Food Sci. Technol.* **1999**, *10*, 37-51.
- 49 Dutta, P. K.; Dutta, J.; Tripathi, V. S. *J. Sci. Ind. Res.* **2004**, *63*, 20-31.
- 50 Pillai, C. K. S.; Paul, W.; Sharma, C. P. *Prog. Polym. Sci.* **2009**, *34*, 641-678.
- 51 Bhatnagar, A.; Sillanpaa, M. *Adv. Colloid Interface Sci.* **2009**, *152*, 26-38.
- 52 Krajewska, B. *Enzyme Microb. Technol.* **2004**, *35*, 126-139.
- 53 Kumar, M. N. R. V. *React. Funct. Polym.* **2000**, *46*, 1-27.
- 54 Poirier, M.; Charlet, G. *Carbohydr. Polym.* **2002**, *50*, 363-370.
- 55 Hu, X.; Du, Y.; Tang, Y.; Wang, Q.; Feng, T.; Yang, J.; Kennedy, J. F. *Carbohydr. Polym.* **2007**, *70*, 451-458.
- 56 Swatloski, R. P.; Spear, S. K.; Holbrey, J. D.; Rogers, R. D. *J. Am. Chem. Soc.* **2002**, *124*, 4974-4975.
- 57 *Ionic Liquids. Industrial Applications for Green Chemistry*, Ed. Rogers, R. D.; Seddon, K. R. ACS Symposium Series 818, American Chemical Society, Washington, DC, 2002.
- 58 Freemantle, M. *Chem. Eng. News*, **1998**, *76*, 32-37.
- 59 Wang, H.; Gurau, G.; Rogers, R. D. Dissolution of Biopolymers in Ionic Liquid. In *Structures and Interactions of Ionic Liquids*; Springer: Berlin Heidelberg, 2014; pp. 79-105.
- 60 Pu, Y.; Jiang, N.; Ragauskas, A. J. *J. Wood Chem. Technol.* **2007**, *27*, 23-33.
- 61 Biswas, A.; Shogren, R. L.; Stevenson, D. G.; Willett, J. L.; Bhowmik, P. K. *Carbohydr. Polym.* **2006**, *66*, 546-550.
- 62 Phillips, D. M.; Drummy, L. F.; Conrady, D. G.; Fox, D. M.; Naik, R. R.; Stone, M. O.; Trulove, P. C.; De Long, H. C.; Mantz, R. A. *J. Am. Chem. Soc.* **2004**, *126*, 14350-14351.
- 63 Xie, H.; Zhang, S.; Li, S. *Green Chem.* **2006**, *8*, 630-633.

-
- 64 Wu, Y.; Sasaki, T.; Irie, S.; Sakurai, K. *Polymer*, **2008**, *49*, 2321-2337.
- 65 Prasad, K. Murakami, M.; Kaneko, Y.; Takada, A.; Nakamura, Y.; Kadokawa, J. *Int. J. Biol. Macromol.* **2009**, *45*, 221-225.
- 66 Wang, W. T.; Zhu, J.; Wang, X. L.; Huang, Y.; Wang, Y. Z. *J. Macromol. Sci. Part B Phys.* **2010**, *49*, 528-541.
- 67 Xu, A.; Wang, J.; Wang, H. *Green Chem.* **2010**, *12*, 268-275.
- 68 Qin, Y.; Lu, X.; Sun, N.; Rogers, R. D. *Green Chem.* **2010**, *12*, 968-971.
- 69 Shamshina, J. L.; Gurau, G.; Block, L. E.; Hanson, L. K.; Dingee, C.; Walters, A.; Rogers, R. D. *J. Mat. Chem. B.* **2014**, *2*, 3924-3936.
- 70 Barber, P. S.; Kelley, S. P.; Griggs, C. S.; Wallace, S.; Rogers, R. D. *Green Chem.* **2014**, *16*, 1828-1836.
- 71 Barber, P. S.; Griggs, C. S.; Bonner, J. R.; Rogers, R. D. *Green Chem.* **2013**, *15*, 601-607.
- 72 Shamshina, J.L.; Zavgorodnya, O.; Bonner, J. R.; Gurau, G.; Di Nardo, T.; Rogers, R. D. *Chem. Sus. Chem.* **2016**, *10*, 106-111.
- 73 Zavgorodnya, O.; Shamshina, J. L.; Bonner, J. R.; Rogers, R. D. *ACS Sustainable Chem. Eng.* **2017**, *5*, 5512-5519.
- 74 Shen, X.; Shamshina, J. L.; Berton, P.; Bandomir, J.; Wang, H.; Gurau, G.; Rogers, R. D. *ACS Sustainable Chem. Eng.* **2016**, *4*, 471-480.
- 75 Singh, N.; Koziol, K. K. K.; Chen, J.; Patil, A. J.; Gilman, J. W.; Trulove, P. C.; Kafienah, W.; Rahatekar, S. S. *Green Chem.* **2013**, *15*, 1192-1202.
- 76 King, C.; Stein, R. S.; Shamshina, J. L.; Rogers, R. D. *ACS Sustainable Chem. Eng.* **2017**, *5*, 8011-8016.
- 77 Food and Drug Administration. Use of International Standard ISO 10993-1, "Biological evaluation of medical devices – Part 1: Evaluation and testing within a risk management process."
<https://www.fda.gov/downloads/medicaldevices/deviceregulationandguidance/guidancedocuments/ucm348890.pdf>. (Accessed May 1, 2017).
- 78 Black, M. M.; Schwartz, H. M. *Analyst*, **1950**, *75*, 185-189.
- 79 King, C.; Shamshina, J. L.; Gurau, G.; Berton, P.; Khan, N. F. A. F.; Rogers, R. D. *Green Chem.* **2017**, *19*, 117-126.
- 80 Tharanathan, R. N. *Trends Food Sci. Technol.* **2003**, *14*, 71-78.

Chapter 2. Experimental

2.1 Chemicals

All materials were used as supplied unless otherwise noted. The IL 1-ethyl-3-methylimidazolium acetate ([C₂mim][OAc], purity >95%, water content below 0.5%) was purchased from IoLiTec, Inc. (Tuscaloosa, AL, USA). Acetone, phosphate buffered saline (PBS), 'practical grade' chitin (PG chitin), bovine serum albumin (BSA) lyophilized powder, and ammonium sulfate (purity >99%) were purchased from Sigma-Aldrich Co. LLC (St. Louis, MO, USA). NaOH pellets were purchased from ACP (Montreal, QC, CA). Anhydrous 200 proof pure ethanol was obtained from KOPTEC DLI, (King of Prussia, PA, USA). Anhydrous caffeine was obtained from Spectrum Chemical (Gardena, CA, USA). Graphene nanopowder, grade AO3 (specific surface area 80 m²/g, average particle size 4500 nm), was purchased from Graphene Supermarket (Calverton, NY, USA). Deionized (DI) water was obtained from a commercial deionizer (Culligan, Northbrook, IL, USA) with a specific resistivity of 16.82 MΩ•cm at 25 °C.

Chitin was obtained from three different shrimp shell sources, referred to as COOP, NA, and BT. Dried COOP shrimp shells (COOP SS), for laboratory use, were received from the Gulf Coast Agricultural and Seafood Cooperative in Bayou La Batre, AL, USA, where they were dried by screw press to eliminate the majority of the water, heated to 160 °C in a fluidized bed dryer until the material had a final moisture content of less than 5 wt%, then pulverized with a hammer mill to particles 0.635 cm diameter and smaller. This material was used for chitin extraction.

NA shrimp shells (NA SS), for laboratory use, were obtained from La Crevette du Nord Atlantique Inc. (Gaspé, QC, CA). *Pandalus borealis* shrimp were caught in the Canadian North Atlantic Ocean, then thermally pre-treated followed by peeling and drying of the shells. The shrimp were steam-cooked by the producer (150-160 °C) for 50-70 s, followed by mechanical

peeling. The peeling process did not guarantee the complete removal of the meat from the shell. Once peeled, shells were simultaneously mechanically pulverized and dried by pressing in an oven at 175 °C for 30 s. The final powder was sieved to a particle size of 105 µm or less. This material was used for chitin extraction.

BT shrimp shells (BT SS) were obtained from a local restaurant in Montreal, QC, Canada. Frozen headless black tiger shrimp (*Panaeus monodon*, product of Vietnam) were peeled at the restaurant and kept frozen until they were transported to the laboratory. There they were placed into DI water to thaw and to remove any excess meat which may have remained on the shell. Once thawed, the legs and tails were removed from the shells. Shells were then placed on parchment paper to dry in air. Dry shells were ground using a Bel-Art micromill with stainless steel chamber (Bel-Art Products, Wayne, NJ, USA), and sieved using Cole-Parmer sieves (Cole-Parmer Canada Company, Montreal, QC, CA) to a particle size of 125 µm particle size.

2.2 Instrumental methods

2.2.1 Viscosity testing

The viscosity of chitin/IL solutions from different chitin sources or different chitin loadings were determined using a VISCOLab 3000 viscometer (Medford, MA, USA). Approximately 2 mL of each chitin/IL solution was placed into the viscometer chamber and a piston of appropriate range selected (500-10,000 cP or 100-2000 cP, depending on the solution). Measurements were obtained for different polymer solutions from 40 to 80 °C, with 5 °C intervals.

2.2.2 Fourier transform infrared spectroscopy (FTIR)

FTIR spectra of all chitin materials were recorded on extracted chitin or whole films using a Bruker Alpha FTIR instrument, (Bruker Optics Inc., Billerica, MA, USA) featuring an attenuated

total reflection (ATR) sampler equipped with a diamond crystal. Spectra were obtained in the range of 400-4000 cm^{-1} .

2.2.3 Solid-state nuclear magnetic resonance (SSNMR)

All solid-state NMR spectra of shrimp shell or chitin samples in Chapter 3 were acquired on a 400 MHz Varian VNMRs spectrometer using a 4 mm double-resonance Varian Chemagnetics T3 probe (now Agilent, Santa Clara, CA, USA). Approximately 35 mg of sample were center-packed into rotors, and spun at 8 kHz.

2.2.3.1 Solid-state ^{13}C cross polarization/magic angle spinning NMR (SS CP/MAS NMR)

Basic CP parameters used in Chapter 3 were based on those suggested by Marchessault *et al.*,¹ with a recycle delay of 3 s and a contact time (the time during which the proton and carbon are spin locked to allow for cross polarization to occur) of 1000 μs using a spin-lock field of approximately 60 kHz (referred to as CP-standard). CP spectra were also acquired with a contact time of 8000 μs (referred to as CP-long). A total of 2872 scans were acquired for each sample, with an acquisition time of 2 h 24 min. SPINAL-64 decoupling at an rf field of 90 kHz was applied during acquisition. Furthermore, CP build-up curves were acquired with the contact time varying from 30 μs to 8 ms and 512 scans were acquired per point. When measuring CP build-up curves, the contact time was varied from 1 to 8 ms and 512 scans were acquired for each contact time.

2.2.3.2 Solid-state ^{13}C direct polarization NMR (DP NMR)

For direct polarization spectrum, 156 scans were acquired over a time of 62 hours with a recycle delay of 1440 s. Spectra were referenced to the C=O resonance of α -glycine at 175.7 ppm.

2.2.3.3 Solid-state ^{13}C multiple CP NMR (multiCP NMR)

MultiCP parameters were examined by varying the various pulse sequence parameters. The best parameters, adopted as standard, were 8 periods of 1 ms CP at about 60 kHz rf field alternated

with delay periods of 1.4 s. The recycle delay was 3 s. An echo was performed at the end of the multiCP experiment with echo time of one rotor period (125 μ s). 200 scans were acquired for each sample in the calibration curve and 500 scans (105 min) were acquired for all other experiments; the integrals of the peaks were scaled according to the number of transients acquired. ^1H 90° pulses were 2.4 μ s long and ^{13}C pulses were 3.7 μ s long.

2.2.4 Thermogravimetric analysis (TGA)

TGA analyses for Chapter 4 were performed on a Mettler-Toledo TGA/DSC (Columbus, OH, USA). The instrument's internal temperature was calibrated by observing the melting point of Au, Zn, and In standards (melting points 1064 °C, 419.5 °C, and 155.6 °C, respectively). The samples were analyzed in 70 mL alumina pans using dried air as a purge gas. Samples between 2–5 mg were heated from room temperature to 700 °C and measured in the dynamic heating regime, using a constant heating ramp of 5 °C/min with a 30 min isotherm at 75 °C. Decomposition temperatures are reported as 5 wt% mass loss ($T_{5\% \text{ dec}}$) and 50 wt% mass loss ($T_{50\% \text{ dec}}$), respectively.

TGA analyses for Chapter 5 was performed on a TA Instruments Q500 TGA instrument (New Castle, DE, USA). Samples of 2-5 mg were analyzed in 70 μ L alumina pans using dried air as a purge gas. Samples between 2-5 mg were heated from room temperature to 700 °C and measured in the dynamic heating regime, using a constant heating ramp of 5 °C/min with a 30 min isotherm at 75 °C. Decomposition temperatures is reported at 5 wt% mass loss ($T_{5\% \text{ dec}}$).

2.2.5 Mechanical testing

Tensile testing of chitin or composite films was conducted using a TestResources 220Q Universal Test Machine (Shakopee, MN, USA). Mechanical testing was done on chitin films for measuring tensile properties such as tensile strength and Young's Modulus (YM). For each type of film, tensile testing was conducted in triplicate. Large films were cast in order to cut strips of

sufficient size. Films with uniform thickness and no obvious flaws were selected and used for testing. The films were cut into strips 2.54 cm wide and 5.08 to 15.24 cm long. Tensile strength (MPa) was calculated by dividing the load at break (Newton) by the original cross cut area. YM (MPa) was calculated by dividing stress (MPa) by strain (mm/mm).

2.2.6 Optical microscopy

Optical images in Chapter 4 were obtained using a Motic BA 200 Microscope (Carlsbad, CA, USA) equipped with an XLI 2.0 camera (XL Imaging, Houston, TX, USA) at magnifications of 40X and 100X. The images were analyzed with XLI-Cap image analysis software that was used to measure the thickness.

2.2.7 Scanning electron microscopy (SEM)

SEM images for Chapter 4 were taken using a LYRA3 TESCAN (Brno, Czech Republic). Films were mounted onto carbon tape and run in a low vacuum environment to prevent charging. All films were scanned using 15 kV electron beam, with a working distance of 10 to 12 mm. SEM images for Chapter 5 were taken using a Delong America LVEM5 5 kV benchtop electron microscope (Montreal, QC, CA). Scans were taken using a 5 kV electron beam.

2.2.8 Cyclic voltammetry (CV)

Cyclic voltammetry was performed on a Stanford Research Systems EC301 Potentiostat/Galvanostat (Sunnyvale, CA, USA) in a two-electrode set-up. The cell was first pre-conditioned with 20 CV cycles at a scan rate of 50 mV/s between 0 and 1 V prior to immediate measurement at 50, 40, 30, 20, and 10 mV/s (selected to accurately reflect the charge/discharge times expected of supercapacitor devices).² CVs were normalized to the mass of the whole electrode film (9.4 mg) in order to calculate specific capacitance (C_s). C_s was calculated using Eq 2.1, below:

$$C_s = \frac{j}{vd\Delta} \quad \text{Eq. 2.1}$$

Where j is current density, v is scan rate, and $d\Delta$ is the voltage difference.

2.3 Chitin content characterization techniques

2.3.1 Chitin content determination by Black and Schwartz pulping

Chitin content of shrimp shell or extracted chitin samples was determined using the Black and Schwartz pulping method,³ where minerals and proteins were removed with 1 M HCl and then with 1.25 M NaOH, respectively. For each sample, 6 mL of 1 M HCl was added to 0.25 g of sample in a 20 mL vial (loosely capped) along with a stir bar, and the suspension stirred with heating at 90 °C in an oil bath for 1 h. The vial was removed from the heat, the solid was centrifuged, and the supernatant discarded. The solid was repeatedly washed with DI water through addition of fresh DI water (*ca.* 20 mL), centrifugation, removal of supernatant, until the supernatant pH reached 7. At this point the NaOH wash was carried out.

6 mL of 1.25 M NaOH solution was then added to the solid in the same 20 mL vial. The vial was equipped with a stir bar, the top was closed (not tightly), and the suspension was heated with stirring in a 90 °C oil bath for 1 h. The vial was removed from the heat, and the washing was conducted in the same manner as described above (removal of supernatant, washing with fresh DI water, and centrifugation repeated until the pH reached 7). The supernatant was then pipetted out. The remaining chitin was oven dried overnight (80 °C) and then weighed to determine the chitin content. For extracted chitin (which contains no minerals, but could have contained proteins), deproteinization was achieved by the same method, but without the acidic treatment. The process was repeated in triplicate for each chitin sample.

2.3.2 Construction of calibration curve for chitin content determination using multiCP NMR

A mass-based calibration curve was constructed from mixtures of PG chitin and BSA protein in Chapter 3. Six mixtures of 50 mg each were prepared as 1:0, 3:1, 1:1, 1:3, and 0:1 chitin: BSA mixtures by mass. A spectrum of each mixture was acquired using multiCP. The C3 and C5 chitin peaks (77.99-70.70 ppm) from the multiCP spectra were integrated, and this used for the construction of a calibration curve. The limit of quantification was determined using a mixture of 1 part chitin to 9 parts BSA protein.

To measure variation between experiments, eight separate multiCP spectra (64 scans) were acquired of a single chitin sample (BT chitin). The variation in the integrals was converted to percent chitin.

2.4 Ionic liquid extraction of chitin

IL extraction of chitin was done from dry, ground shrimp shells based on a procedure modified from the reference.⁴ The procedure for a single batch is given, though dissolution time was modified based on the chitin source (COOP, NA, or BT SS). For each source, extraction was done on 2 wt% shrimp shell/IL solutions. 1.00 g of shrimp shell was added to a 250 mL Erlenmeyer flask along with 49 g of the IL [C₂mim][OAc]. The shrimp shell was dissolved *via* microwave assisted dissolution (Danby Products, Ltd., Guelph, ON, CA) over a total time of 4 min for COOP and BT SS, and 12 min for NA SS. Heating was done over 2-4 s pulses, while the solution was manually stirred between each pulse using a glass rod to avoid overheating. Dissolution was monitored visually, and was finished when the solution became honey-like in viscosity. The solution was then transferred into a 50 mL centrifuge tube, and centrifuged for 7 min at 3000 rpm (Thermo Fischer Scientific Sorval Legend XF centrifuge series, Waltham, MA, USA), followed by coagulation into a 500 mL beaker containing 200 mL of water to remove the IL. The chitin was

strained, the IL/water solution discarded, and the beaker filled completely with water. The water was replaced 5 times to ensure complete removal of the IL, then the chitin strained and air dried on parchment paper. Extracted chitin was ground to a particle size of at least $<125\ \mu\text{m}$ for use or characterization. Chitin from COOP, NA, or BT SS is referred to as COOP chitin, NA chitin, and BT chitin, respectively.

2.5 Material preparation

2.5.1 Film preparation from COOP chitin

2.5.1.1 Film casting

All films in Chapter 4 were made using COOP chitin. Neat chitin films were cast from solutions of COOP chitin. For film casting, a 2.5 wt% chitin/IL solution was prepared by dissolving 0.258 g of $<90\ \mu\text{m}$ particle size COOP chitin in 10 mL $[\text{C}_2\text{mim}][\text{OAc}]$. The chitin and IL along with a magnetic stir bar were placed into a 20 mL vial (loosely capped), and placed into an oil bath. The mixture was heated at $90\ ^\circ\text{C}$ with stirring (760 rpm) for 3 h until full dissolution of chitin was achieved. Dissolution was considered complete when the solution became homogeneous, honey-like in viscosity, and turned an amber color. The vial was then taken out of the bath, the stir bar removed, and the solution centrifuged (Dynac Becton Dickinson Centrifuge model 42010, Sparks, MD, USA) for 10 min at 3000 rpm to separate any undissolved residue. The vial was then placed into an oven ($70\ ^\circ\text{C}$), so that the solution would become free flowing.

The hot solution was then poured over a glass plate and cast using a gapped stainless steel rolling rod (R&D Specialties, Webster, NY, USA) of RDS 100, 135, or 150 (which had wire diameters of 0.26 mm, 0.41 mm, and 0.50 mm, respectively). The steel rolling rods (made of a stainless steel cylindrical bar wrapped with a wire of a certain diameter) evenly distributed the solution, passing it through the grooves between the wires, and forming a layer with a thickness

proportional to the wire diameter. Once the solution had settled to uniform thickness (a few seconds), the glass plate was submerged into a DI water bath (29.52 x 10.79 x 29.52 cm, length x width x height) to allow film coagulation. After about 5 min, the film detached from the glass plate and rose to the surface. The glass plate was carefully removed, and the DI water was replaced about 4 times ensure complete removal of the IL. The IL was considered washed out after four washes; after two to three washes the IL was no longer visible in the bath, then two additional washes were done to be sure that the IL was not detected visually. The film was removed from the solution by sliding a piece of wax paper underneath and gently lifting the paper from the water, with the film mounted onto the wax paper. At this point the film was transferred to non-stick parchment paper for drying. To do this, the wax paper with the film mounted on it was carefully placed onto a piece of parchment paper with the film side face down. The wax paper was then carefully peeled away, leaving the wet film mounted on parchment paper. The films were then dried and characterized.

2.5.1.2 Film drying

Drying of films in Chapter 4 was carried out by five different methods: air, oven, acetone, press, and supercritical CO₂ (sc-CO₂) drying. For air drying, the wet chitin film was placed onto a piece of parchment paper, and left on the bench top to dry in air for 24 h, or until dry to the touch. For oven drying, the wet chitin film was placed onto a piece of parchment paper, and then put into the oven (90 °C) for 24 h, or until dry to the touch. Acetone drying was done by placing the wet film into a small bath of acetone, then removing the film from the bath and placing onto a piece of parchment paper on the benchtop until dry to the touch. Press drying and sc-CO₂ drying yielded viable films and are therefore described in more detail.

For press drying, the wet film was placed between two pieces of parchment paper. This was then placed under a flat weight of 2 kg. The film was left under the weight for approximately 24 h, or until the film was dry to the touch, and then carefully removed.

For sc-CO₂ drying, the wet film was placed into a bath of anhydrous ethanol, replacing the bath with fresh ethanol 5 times over a period of 24 h, followed by supercritical drying for 3 h. Drying was done in a DCP-1 Critical Point Drying Apparatus (Denton Vacuum, Moorestown, NJ, USA) equipped with an 11 x 3.5 cm (height x diameter) drying chamber. The wet film was placed between two pieces of porous Teflon coated mesh (100 Mesh T304 Stainless 0.0045" Wire Dia. Green PTFE, Part # 100X100S0045W36_PTFE, TVP Inc., Berkeley, CA, USA), and the encased film was placed into the sealed chamber, which was immersed in room temperature water. The chamber was closed, and liquid CO₂ was allowed to flow into the chamber for 7 min, then the chamber was vented for another 7 min. These 7 min/7 min cycles were repeated up to 12 times. At the final cycle, the chamber was sealed and the CO₂ flow stopped. The room temperature water bath was then replaced with a 60 °C water bath. As the bath heated the chamber, the pressure in the chamber rose to about 1750 psi. Once this pressure was reached, the chamber was slowly vented at a rate of about 100 psi/min. When the pressure inside the chamber had reached atmospheric pressure, the chamber was opened and the dry film removed.

2.5.2 Film preparation from BT chitin

2.5.2.1 Neat film casting

All films in Chapter 5 are made using BT chitin. For neat chitin films, 1.25 wt% chitin IL solutions were prepared for film preparation in the same way as above, with minor modifications to the casting method. Briefly, 1.25 wt% chitin/IL solutions were prepared by dissolution of the BT chitin in IL at 90 °C in an oil bath overnight. Films were cast on a glass plate using a double

blade micrometer film applicator (MTI Corporation, Richmond, CA, USA) at a casting height of 75 μm . It should be mentioned that the casting height of the film applicator will not produce films of that thickness, as the solution tends to spread slowly on the glass. The glass plate with the chitin solution mounted was submerged into a DI water bath for coagulation. The water was replaced 4-5 times, with about 20 min in between, to remove all of the IL, then the film was mounted onto parchment paper and press dried under a flat weight (*ca.* 2 kg).

2.5.2.2 Composite film casting

For the preparation of conductive electrode materials in Chapter 5, commercially sourced graphene was chosen as the conductive material, using BT chitin as a binder for the preparation of graphene/chitin composite films. Different ratios of graphene were incorporated in the chitin-IL solution for dispersion and composite film preparation. A 1.25 wt% solution was prepared by dissolving 0.0632 g chitin in 4.99 g IL, and a 1.5 wt% solution was prepared by dissolving 0.0632 g chitin in 4.15 g IL. A stir bar was added to each, and they were placed in an oil bath at 90 °C to dissolve for 18 and 24 h for the 1.25 and 1.5 wt% solutions, respectively. Different dissolution times were required for different solutions loadings (higher chitin loading requires a longer time for full dissolution). Once chitin had dissolved (monitored visually), AO3 graphene powder was added. For the preparation of graphene slurries in 1.25 wt% chitin/IL solutions (containing 0.0632 g chitin), 0.0948 g, 0.1474 g, 0.2528 g, and 0.5677 g graphene was added to prepare mixtures of 60:40, 70:30, 80:20, and 90:10 graphene: chitin, respectively.

The powder tended to form aggregates when first added to the solutions, and had to be dispersed by stirring using a magnetic stir bar, which was done over 4 h at 90 °C. During the dispersion period, the 1.5 wt% chitin solution formed a paste due to the high solution viscosity and large amount of graphene added, leading to nonhomogeneous mixtures which could not be cast

into films. The 1.25 wt% chitin/IL/graphene solution, however, allowed for the complete dispersion of graphene at all graphene loadings, and each remained a free-flowing liquid. Once the graphene was well dispersed in 1.25 wt% chitin solutions (monitored visually), the films were cast from the solutions as described above, according to the reference with a minor modification in the casting method.⁵ Briefly, solutions of graphene dispersed into chitin/IL solution were placed into an oven at 90 °C until warm and free-flowing. Films were cast on a glass plate using a double blade micrometer film applicator (MTI Corporation, Richmond, CA, USA) at a casting height of 75 µm. It should be mentioned that the casting height of the film applicator will not produce films of that thickness, as the solution tends to spread slowly on the glass. The glass plate with the chitin solution mounted was submerged into a DI water bath for coagulation. The water was replaced 4-5 times, with about 20 min in between, to remove all of the IL, then the film was mounted onto parchment paper and press dried under a flat weight (*ca.* 2 kg).

2.6 Material characterization

2.6.1 Chitin film shrinkage

The shrinkage of films in Chapter 4 was determined by measuring the initial and final lengths and widths of each film before and after drying. The areas before and after were calculated and the percent shrinkage was obtained using the following **Eq. 2.2**:

$$\text{Percent change} = (\text{initial area} - \text{final area}) / (\text{initial area}) * 100\% \quad \text{Eq. 2.2}$$

2.6.2 Chitin film water content

Water content of sc-CO₂ dried films and press dried films was determined in Chapter 4. Films were placed into separate 20 mL glass vials and were covered with aluminium foil with pin holes. These were weighed, placed in an oven at 80 °C overnight, and then reweighed the next day. The water content in the films was determined based on the percentage difference in weight.

2.6.3 Loading and release of caffeine from COOP chitin film

To load press dried films with caffeine, a saturated caffeine solution was first prepared by adding 16 g of caffeine to 1 L of DI water. A petri dish was filled with approximately 15 mL of this caffeine solution, and a freshly prepared wet chitin film was immersed into the bath, covered, and allowed to soak for *ca.* 24 h; the solution was replaced once. The film was then removed and press dried by the method described above. The remaining stock solution was kept in a bottle for further use.

In order to load sc-CO₂ dried films with caffeine, they were cast, coagulated and washed described above. Prior to drying by sc-CO₂, a film was placed in super-saturated ethanolic caffeine solution (prepared by dissolving 6.50 g of caffeine into 500 mL of anhydrous ethanol). The ethanolic solution was placed in a 1 L bottle and capped until used. Approximately 15 mL of caffeine solution was added to a Petri dish, and the film was placed in and covered. The caffeine solutions were replaced once within 72 h. After the loading period, the films were dried by the supercritical drying procedure outlined above.

For the release, a small piece of sc-CO₂ dried film was weighed (2.0(1) mg) and then placed into a 3.5 mL spectrophotometer quartz cuvette (VWR, Radnor, PA, USA) along with 3.7 mL PBS solution. The PBS solution was prepared by dissolving one tablet in 200 mL DI water. The film was hooked to a syringe needle to prevent it from dropping to the bottom of the cuvette and to ensure the UV light would pass through the PBS solution without being blocked by the film, once in the spectrophotometer. The cuvette along with the film and solution was then placed into a UV-vis spectrophotometer (UV-1800 Shimadzu Corporation, Canby, OR, USA). The scanned wavelength range was set from 200 to 400 nm as caffeine has a molar absorptivity of 273 nm. The

data was collected for approximately 24 h, with a 5, 10, 25, 35, 125 min, and finally around 14-16 h interval. The experiment was run in duplicate.

2.6.4 Swelling of neat BT chitin and graphene/BT chitin composite films

In Chapter 5, swelling of the both the neat chitin films and graphene/chitin composite films was measured in the aqueous 2 M $(\text{NH}_4)_2\text{SO}_4$ electrolyte. Small 1 x 1 cm (length x weight) sections of each of the films were cut out and pre-weighed. Films were then placed into individual vials and soaked in 2 mL of the electrolyte for 2 h. The films were removed, and the excess electrolyte removed for weighing, and the swelling measured as the mass gained per amount of chitin. The swelling ratio of both the neat chitin films and graphene/chitin composite films in aqueous $(\text{NH}_4)_2\text{SO}_4$ electrolyte was measured.

2.6.5 Assembly of electrochemical cell from BT chitin films

The dried BT chitin and graphene/ BT chitin composite films were prepared as separator and electrodes, respectively, by first cutting the films in circular discs using a precision disc cutter (MTI Corporation, Richmond, CA, USA) at diameters of 20 mm (separator) and 19 mm (electrode). The cut films were then stacked (in sequence: electrode, separator, electrode) in a stainless-steel test cell (MTI Corporation) with the aid of a 20 mm PTFE guide sleeve. The electrolyte (2 M $(\text{NH}_4)_2\text{SO}_4$ in DI water) was added by pipette to wet the electrode surface as each layer was stacked. The stainless-steel counter electrode plate was then placed on top of the stack, and the cell flooded with excess electrolyte prior to soaking for 2 h. The excess electrolyte was removed by pipette, and the cell tightened and sealed prior to settling for a further 2 h prior to cycling voltammetry measurements.

2.7 References

- ¹ Raymond, L., Morin, F.G., Marchessault, R.H., *Carbohydr. Res.* **1993**, *246*, 331-336.
- ² Stoller, M. D.; Ruoff, R. S. *Energy Environ. Sci.* **2010**, *3*, 1294-1301.
- ³ Black, M. M.; Schwartz, H. M. *Analyst*, **1950**, *75*, 185–189.
- ⁴ Qin, Y.; Lu, X.; Sun, N.; Rogers, R. D. *Green Chem.* **2010**, *12*, 968-971.
- ⁵ King, C.; Shamshina, J. L.; Gurau, G.; Berton, P; Khan, N. F. A. F.; Rogers, R. D. *Green Chem.* **2017**, *19*, 117-126.

Chapter 3. Measuring the purity of chitin with a clean, quantitative solid-state NMR method

3.1 Introduction

Chitin, the second most abundant biopolymer on earth,¹ is well suited for biomedical applications due to its biocompatibility, biodegradability and nontoxicity, and accordingly has seen growing interest in biomedical and pharmaceutical fields.²⁻⁴ As a source for bioactive materials (used in wound care, drug delivery, and tissue engineering^{5,6} for example), chitin must be obtained and purified to a certain specification for use on humans, meeting at least the requirements of USP (US Pharmacopeia) Class VI and ISO 10993.^{7,8}

As it is obtained from biomass sources (most frequently shellfish, where it exists in a matrix along with CaCO₃, proteins, and pigments⁹), the processed chitin can vary in purity, depending mainly on the biomass source itself and the processing conditions used.¹⁰ Chitin can be obtained through either pulping¹¹ or direct extraction from crustacean shells using the IL [C₂mim][OAc].¹² Independent of the isolation method used, proteinaceous tissue of the animal can remain on the shell during processing, leading to higher protein content in both the biomass source in the and extracted chitin. According to one study, crustaceans cause allergic reaction in up to 2% of people in the United States.¹³ Four allergens have been identified as the cause of such reactions, two of which are muscle proteins found in crustacean species.¹⁴ For chitin to be used in high value-added applications in medicine and cosmetics, the presence of any protein that might induce an allergic response is not acceptable.

Thus, it is necessary to determine the purity of the chitin and to quantify residual protein content. While the presence of traces of CaCO₃ can be determined by PXRD,¹² chitin content can be determined by the method of Black and Schwartz (which involves chemical pulping of

biomass),¹⁵ but the harsh chemical treatment used in this method causes deacetylation, lowers the molecular weight, and is highly operator-dependent (and hence of low precision).

We have therefore looked for a clean, quick, and non-destructive technique for the quantification of chitin content, and thereby purity. We hypothesized that NMR spectroscopy could be useful in this regard, as it is intrinsically a quantitative method where the intensity (or integral) of a given signal is directly proportional to the population of a chemical site. This property is commonly exploited in solution-state NMR where the pulse length based concentration determination (PULCON) technique¹⁶ is used to measure concentration referenced to an external standard, taking into account variations in sample quality and experimental conditions.¹⁷

As chitin is not normally soluble in common solvents, we used SSNMR spectroscopy. ¹³C SSNMR spectra of chitin samples display signals from each of the chitin carbon sites (shown in **Figure 3.1**) as well as from other carbon sites present in the sample.¹⁸ In ¹³C SSNMR, however, intensities are typically distorted due to the cross-polarization (CP) phenomenon, where the signal detected is enhanced by magnetization transfer from normally abundant proton (¹H) spins in an uneven, non-quantitative fashion.¹⁹ The apparent signal varies according to **Eq 3.1**:²⁰

$$M(t_c) = \frac{M_0}{1 - \frac{T_{CP}}{T_{1\rho H}}} (e^{-\frac{t_c}{T_{1\rho H}}} - e^{-\frac{t_c}{T_{CP}}}) \quad \text{Eq. 3.1}$$

where M_0 is the initial amplitude, $T_{1\rho H}$ is the longitudinal relaxation time constant for hydrogen in the rotating frame, T_{CP} is the cross-polarization relaxation time constant, and t_c is the cross-polarization contact time.

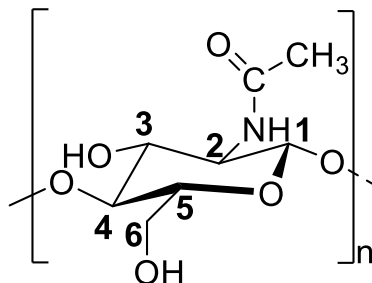


Figure 3.1 Structure of chitin, ring carbon atoms labeled.

Sometimes conditions can be found which permit CP spectra to reflect the actual populations of components in the sample. This technique has been used to calculate the deacetylation degree of chitin samples²¹ using ^{13}C CPMAS measurements validated against measurements made by other methods.²²⁻²⁴ However, few simple general methods have been reported for solid-state ^{13}C CPMAS spectra where integrals can be translated into absolute fractions of component present in a sample. Some of the techniques are reviewed in references.²⁵

One viable technique is Electronic REference To access In vivo Concentrations (ERETIC), where a synthetic signal which always has the same intensity is fed into the NMR probe and used to calibrate the spectroscopy signal intensities.²⁶ This technique permits the integral of a resonance from a compound in one spectrum to be compared with the integral of the same resonance in another spectrum, but requires hardware modifications. One main alternative is to use simulations which take into account the effect of different relaxation parameters for different sites or components.²⁷ The simplest approach is to use calibration curves to relate NMR signal intensity to the quantity of a given component in a sample,^{28,29} so we decided to construct a calibration curve from ^{13}C CPMAS SSNMR spectra for chitin-protein mixtures. This technique has already been applied to measuring the protein content in whole cells³⁰ and to measuring lignin content in lignocellulosic biomass.¹⁹

However, the problem of measuring the purity of chitin was further complicated as the presence of protein changes $T_{1\rho H}$ of the chitin signal, making it impossible to compare spectra of samples with widely different proportions of the two components directly using CP. Therefore, we used the recently introduced technique of cross polarization by multiple contact periods (multiCP)³¹ to obtain quantitative ^{13}C NMR spectra with good sensitivity and which are independent of $T_{1\rho H}$. This technique has already been applied with success to pharmaceuticals³² and wood materials.³³ It has also been used to measure the crystallinity index of cellulose in bagasse samples by using spectral editing to remove lignin signals.³⁴ In our hands, a calibration curve constructed using multiCP was applied to proteinaceous chitin sources to yield a clean, quantitative method for measuring the purity of a chitin sample.

3.2 Results and discussion

3.2.1 CP buildup curves of deproteinized and untreated chitin

The first attempt to develop a simple SSNMR method for quantitatively measuring the chitin content in a sample used CPMAS ^{13}C NMR. As the chitin content of extracted chitin samples was of primary interest, the first spectra were acquired of extracted NA chitin samples containing an unknown amount of proteins and of deproteinized NA chitin, in order to determine if the presence of proteins would affect the chitin signals. CP buildup curves were obtained for both chitin samples. CP buildup was measured with a contact time from 1 to 8 ms for each chitin peak, and the curves fitted to **Eq 3.1** using Bruker Dynamics Center.³⁵ CP buildup curves demonstrated that $T_{1\rho H}$ and T_{CP} values differed in chitin samples in the presence and absence of protein. Buildup curves are shown below in **Figure 3.2**, and values for $T_{1\rho H}$ and T_{CP} are shown below in **Table 3.1**.

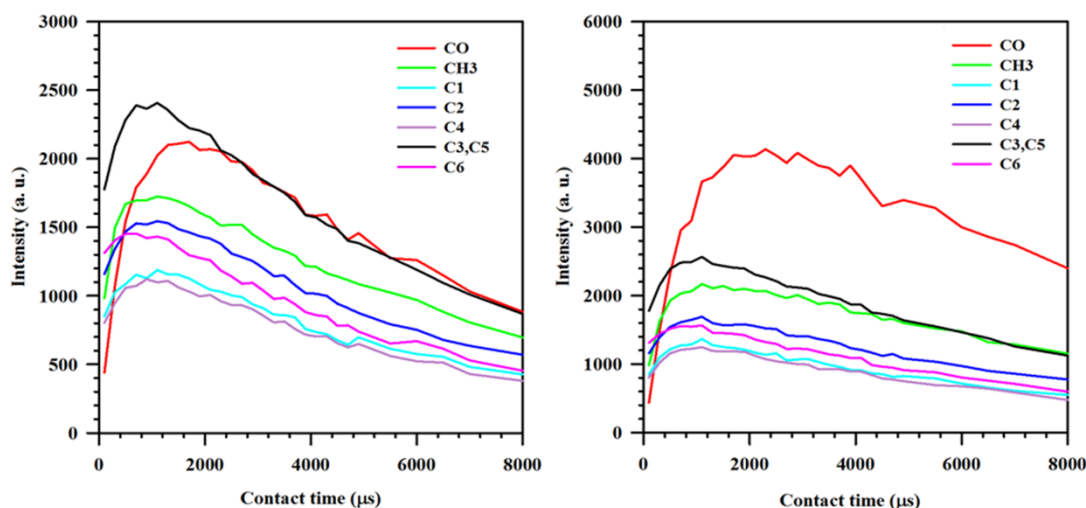
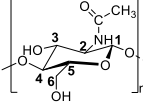


Figure 3.2 Buildup curves for each chitin peak for both untreated (left) and deproteinized (right) NA chitin. Note differences in the scales.

Table 3.1 T_{CP} and $T_{1\rho H}$ values for chitin ring carbons of untreated and deproteinized chitin extract.

(Structure provided for C-atom reference)	Peak	Untreated	Deproteinized	Difference [%]	Untreated	Deproteinized	Difference [%]
		T_{CP} [s] ($*10^{-4}$)	T_{CP} [s] ($*10^{-4}$)		$T_{1\rho H}$ [s] ($*10^{-3}$)	$T_{1\rho H}$ ($*10^{-3}$)	
	C1	0.82±0.09	1.17±0.08	29.6	8.65±0.4	10.2±0.4	15.2
	C2	0.92±0.01	1.22±0.1	24.3	8.64±0.6	11.7±0.5	26.1
	C3	1.15±0.06	1.16±0.05	0.862	8.17±0.3	10.7±0.3	23.6
	C4	0.79±0.07	1.27±0.05	37.5	8.15±0.3	9.61±0.3	15.2
	C5	0.92±0.06	1.05±0.07	12.2	8.20±0.3	10.4±0.4	21.1
	CH ₃	1.81±0.09	2.67±0.1	32.2	10.9±0.4	13.5±0.5	19.3

Differences between the buildup curves can be seen from **Figure 3.2**, but comparing the values obtained from the Bruker Dynamics Center curves fitting reveals the significant differences between the treated and untreated chitin samples. Values for T_{CP} and $T_{1\rho H}$ values differed by up to 40% between the deproteinized and untreated NA chitin, indicating that the presence of proteins has a pronounced effect on the $T_{1\rho H}$ of the chitin signal, and making it impossible to compare CP spectra of samples with different proportions of the two components. Because of this, CPMAS ^{13}C

NMR was found to not be a suitable method for the determination of chitin content in samples with different protein contents.

3.2.2 Application of multiCP method and comparison with CP and DP NMR

Thus, we employed a recently developed technique, multiCP,³¹ to quantify chitin. The technique utilizes multiple CP periods separated by delay periods which allow for the repolarization of ^1H during a net long CP contact time. The peaks from all carbon sites are, therefore, represented in the spectra proportionately to the population of the site. The different multiCP parameters were varied to maximize the similarity of the multiCP spectrum of NA chitin spectrum to the DP spectrum of NA chitin (**Figure 3.3**); the best were 8 periods of 1.0 ms CP time separated by 1.4 s delay periods.

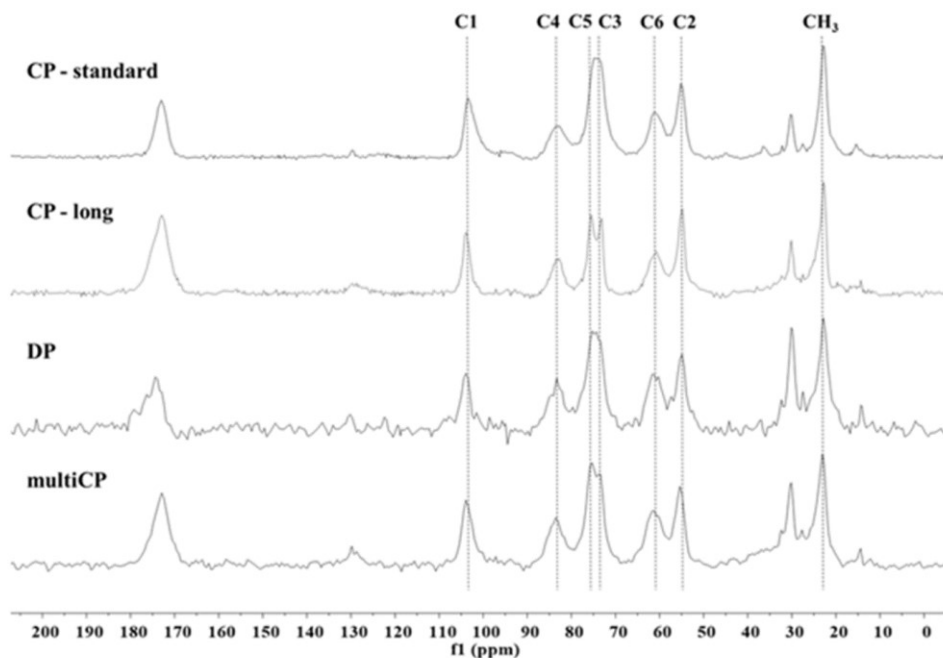


Figure 3.3 Comparison of CP-standard (2 h 20 min), CP-long (2 h 20 min), DP (using a recycle delay of 1440 s, 62 h) and multiCP (1 h 40 min) spectra of NA chitin.

As seen from the figure, multiCP was compared to both DP spectra and CP spectra (both long and standard). Standard CP refers to spectra taken using a 1000 μs contact time, and long CP was taken using an 8000 μs contact time. This was done to ensure that it was in fact the application of the multiple CP periods which allowed for quantitative spectra, rather than the long contact time, which was confirmed in the comparison of the two spectra. It can be seen from **Figure 3.3** that the intensities of the sharp chitin peaks, such as at 23 ppm, differ significantly between both the CP and the multiCP spectra, while those of the DP and multiCP spectra are in agreement (the DP spectrum is noisier, as expected). There are significant differences in the protein region between 30 and 40 ppm, even between DP and multiCP spectra, which we cannot explain and which we could not reduce regardless of recycle delay used in the DP spectrum nor the parameters used in multiCP. However, those regions can be excluded from our analysis.

3.2.3 Construction of a calibration curve from PG chitin

For the quantification of chitin content with multiCP, a calibration curve of chitin was constructed from mixtures of PG chitin with BSA protein. BSA was chosen as it is a standard protein which can simulate the chemical shift of the protein backbone and amino acid residues. PG chitin and BSA protein were physically mixed to prepare mass-based blends as standards to simulate the chitin-protein mixture found in the biomass source.

Although this physical mixture of chitin and BSA protein is not an ideal simulation of the interactions between chitin and proteins in a real sample, the use of multiCP minimizes the effect of the relaxation parameters of different carbon sites and instead leads to very nearly equal excitation of all sites. Because of this, the BSA/chitin mixture does not need to simulate the natural interactions between the protein and chitin in order to act as a suitable substitute for the construction of a calibration curve. In order to demonstrate this, the intensity of NA chitin and 20

wt% PG/BSA physical mixture were plotted as a function of both CP contact time per period and the number of CP periods, below in **Figure 3.4**.

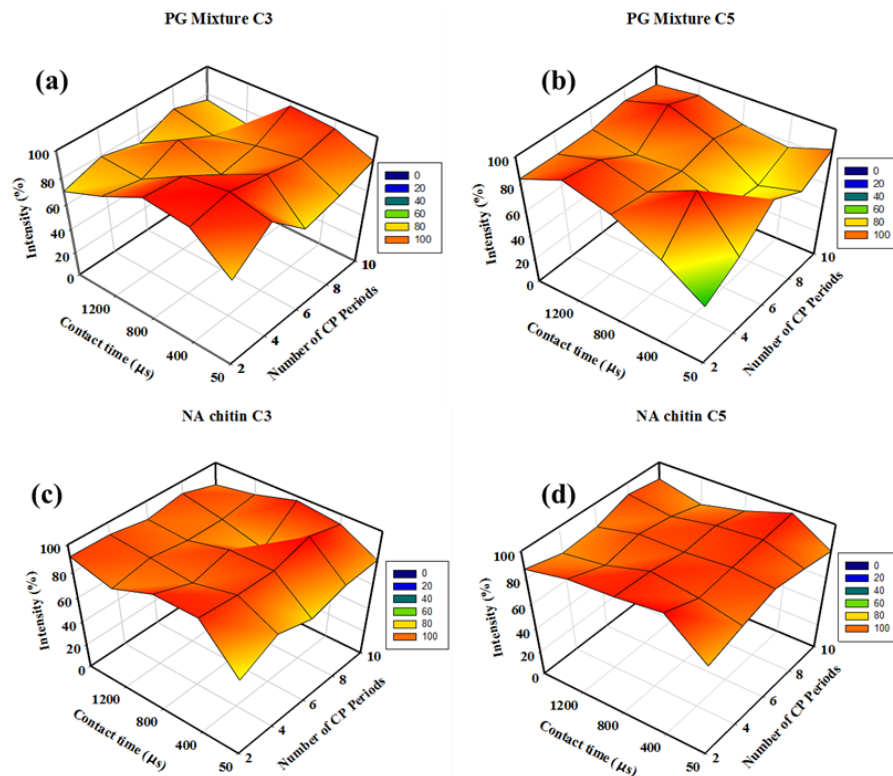


Figure 3.4 Contour plots showing peak intensity of the (a) C3 peak in a 1:4 chitin:BSA mixture, (b) C5 peak in a 1:4 chitin:BSA mixture, (c) C3 peak in NA chitin, and (d) C5 peak in NA chitin in multiCP spectra as a function of CP contact time per period and number of CP periods.

Contour plots were constructed by fixing the delay periods at 1.4 s, and sampling was done with contact time of 40, 400, 800, 1200, and 1600 μs with the number of CP periods varied from 2 to 10 in increments of 10. The plots show that generally, when the number of CP periods is greater than 6, and when the contact time is between 400 and 1000 μs , 90% or greater of the theoretical signal is obtained for the two sites, despite their different relaxation parameters. In this way, differential relaxation affecting standard CP is avoided, and physical chitin/ protein mixtures can be used construction of a calibration curve for quantification in real samples.

MultiCP spectra were taken on PG chitin/BSA protein physical mixtures of 1:0, 3:1, 1:1, and 1:3 chitin:BSA. Spectra exhibited signals corresponding to chitin and BSA (**Figure 3.5**).

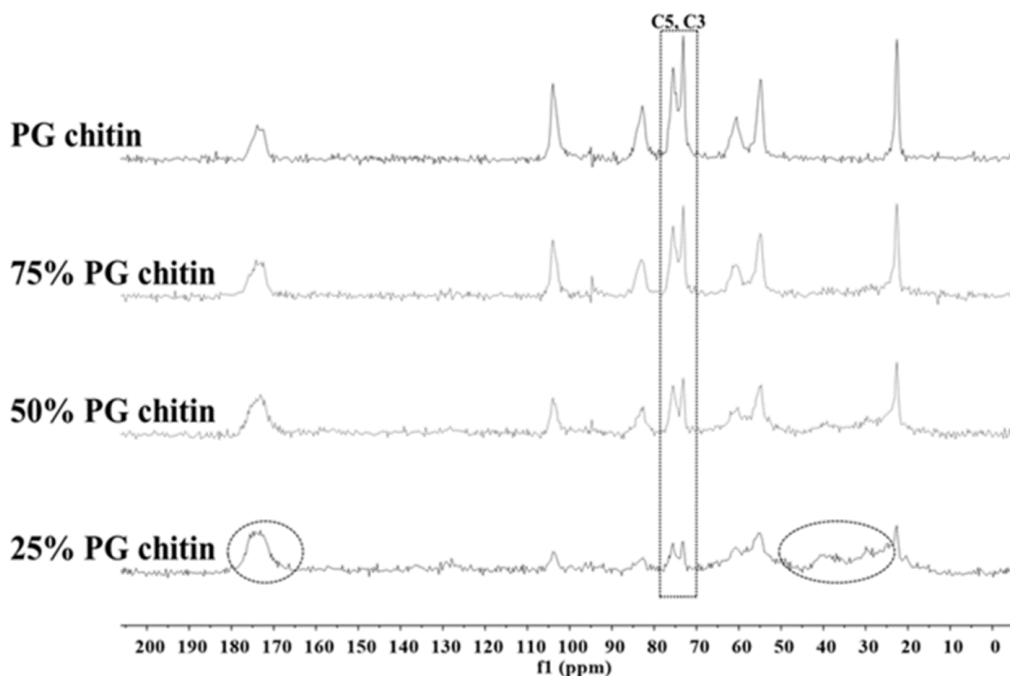


Figure 3.5 MultiCP spectra of chitin:BSA mixtures by mass. Signals arising from the BSA protein are circled on the 25% PG chitin spectra. The region of the spectrum used for integration is 77.99-70.70 ppm (C3 and C5 chitin peaks).

Signals from the C3 and C5 positions in the chitin appear in a spectral region free from amino acid signals. The integrals of this region (77.99-70.70 ppm) included the entirety of both peaks and were kept consistent for each spectrum in order to construct the calibration curve. As expected, chitin mass percentage y varies linearly as a function of the C3, C5 peak integral x according to

Eq 3.2:

$$y = (0.0101 \pm 0.0002)x + 0.0028 \pm (0.0122) \quad \text{Eq. 3.2}$$

The coefficient of determination indicates good fit with the data ($R^2 = 0.999$), with the standard error of the estimate of 0.016. The calibration curve, with linear fit, is shown in **Figure 3.6**.

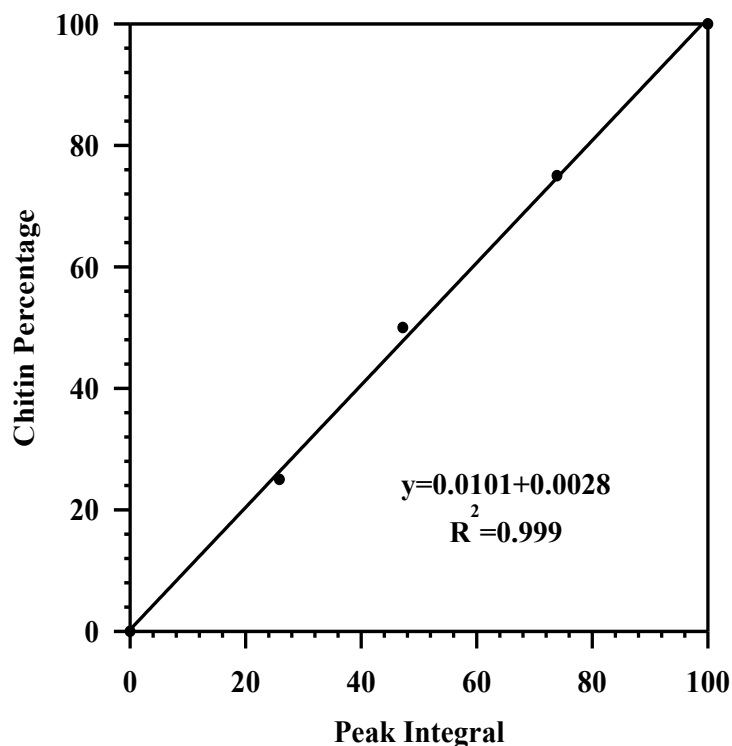


Figure 3.6 Chitin content calibration curve from C3 and C5 peaks. Peak integrals are scaled such that the integral of the sample containing only PG chitin is 100. The best fit curve (straight line) is described by Eq. 3.2.

The limit of quantification was determined using a mixture of 1 part chitin to 9 parts BSA protein. The signal to noise ratio of the C3 and C5 signals was 10(1):1 and 10% chitin by mass was therefore established to be the limit of quantification, using commonly accepted criteria.³⁶

3.2.4 Chitin content measurements using multiCP with calibration curve

To validate this NMR method for chitin quantification, the chitin content of four samples obtained from different sources and subjected to different treatment were measured both by NMR and the Black and Schwartz pulping method. Shrimp shell samples were fully treated by the Black and Schwartz methodology, applying both the acid and the base washes. The extracted chitin

samples, however, were treated only with base wash because IL extraction using a biomass load of less than 2 wt% removes all CaCO_3 .¹² The acid wash unnecessary for the removal of CaCO_3 , for which the absence was confirmed with PXRD (**Figure 3.7**).

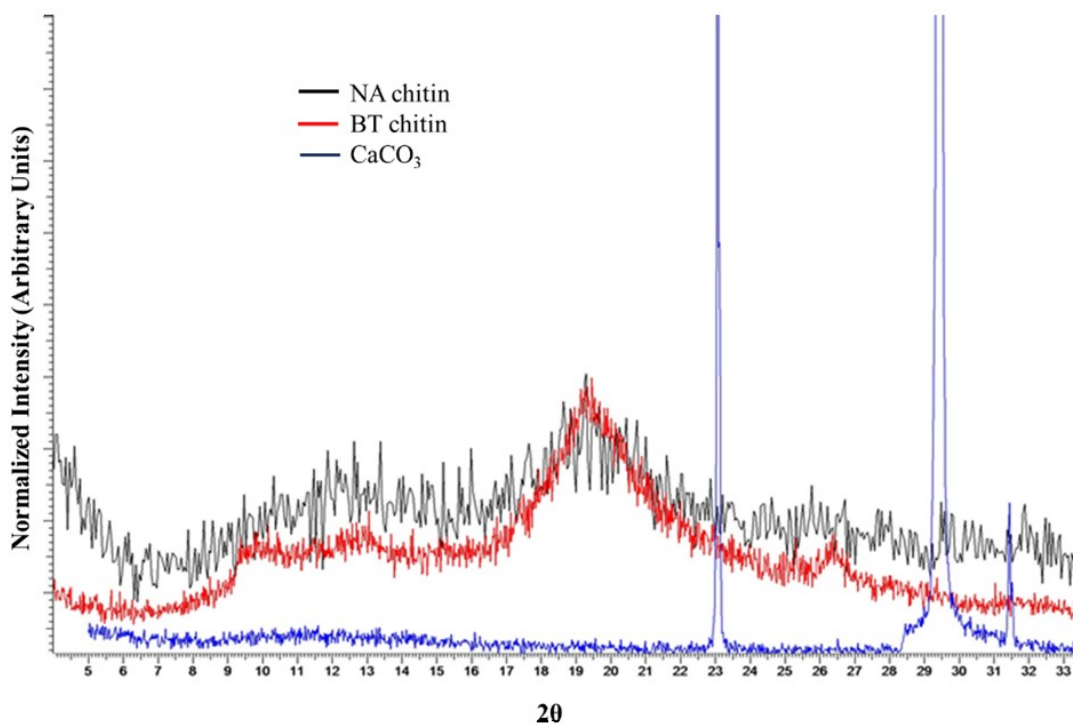


Figure 3.7 PXRD diffractograms for BT chitin, NA chitin, and CaCO_3 .

The chitin peaks in the PXRD are observed at $2\theta = 9.5^\circ$ (020), 12.3° (101), 19.4° (040) and (110), and 26.5° (013), characteristic of α -chitin,³⁷ while peaks resulting from CaCO_3 appear at $2\theta = 23.2^\circ$, 29.5° , and 31.6° . It should be noted that the NA chitin features of the powder pattern are much less sharp than that of BT chitin, but this is due to the excess of proteinaceous material in the sample. Because of the absence of CaCO_3 observed here, the acid wash was avoided in

extracted chitin samples, as it could serve to hydrolyze the chitin and give an overly low measurement of chitin content. Therefore, only the NaOH wash was used.

The results are shown in **Table 3.2** and generally indicate good agreement between the two methods. The nature of the Black and Schwartz method can lead to high error in the measurement, as the method involves multiple washing and sample transfer steps, which might lead to an artificially decreased chitin content. Furthermore, the authors themselves mention the difficulty in properly sampling a bulk chitin sample or making precise measurements of it.¹⁵ MultiCP measurements were repeated 8 times on a single chitin sample and showed a 4% variation between measurements.

Table 3.2 Chitin content of different sources as determined from multiCP and from Black and Schwartz (B & S) methods.

Chitin source	Sample Description	NMR Chitin Content [%]	B & S Chitin Content [%]
NA SS	Ground shrimp shells obtained from La Crevette du Nord Atlantique	16(1)	21(5)
BT SS	Ground shrimp shells from untreated <i>Panaeus monodon</i>	47(3)	44(1)
NA IL-extracted chitin	Chitin extracted from NA SS using IL	56(3)	55(5)
BT IL-extracted chitin	Chitin extracted from BT SS using IL	72(4)	66.0(0.4)

3.3 Conclusions

Chitin (and chitosan) are versatile biopolymers suitable for use in sensitive biomedical applications. However, due to the nature of the biomass from which the biopolymer is obtained, impurities such as proteins may remain in the chitinous samples. Knowing the purity of chitin is critical for materials science applications.

We have here developed a method for determining chitin content of chitinous biomass in a simple manner by applying the multiCP quantitative solid-state NMR method to chitinous biomass and extracted chitin. Using solid-state ^{13}C multiCP NMR, the chitin content, and therefore the purity of chitin samples was measured in a quick, clean, accurate, and non-destructive manner which avoids both harsh treatment of the chitin sample and technically difficult or lengthy NMR experiments. The multiCP method permitted us to avoid the interactions between protein and chitin that were apparent in $T_{1\rho\text{H}}$ changes between low-protein and high-protein chitin samples.

The multiCP method was combined with the use of a calibration curve constructed from mass based mixtures of PG chitin and BSA protein, allowing for accurate determination of chitin content in both chitinous biomass and in IL-extracted chitin. The chitin content measured using the NMR was in agreement with that determined by the method of Black and Schwartz, within the error of each of the methods. NMR determination of chitin content of NA SS and BT SS were found to be 16(1)% and 47(3)%, respectively (compared with 21(5)%, and 44(1)% from method of Black and Schwartz), and for NA and BT chitin, the chitin content was 56(3)% and 72(4)%, respectively (compared with 55(5)%, and 66(0.4)% from method of Black and Schwartz).

3.4 References

- ¹ Rinaudo, M. *Prog. Polym. Sci.* **2006**, *31*, 603-632.
- ² Kumar, M.N.V.R. *React. Funct. Polym.* **2000**, *46*, 1-27.
- ³ Jayakumar, R.; Menon, D.; Manzoor, K.; Nair, S. V.; Tamura, H. *Carbohydr. Polym.* **2010**, *82*, 227-232.
- ⁴ Younes, I.; Rinaudo, M. *Mar. Drugs*, **2015**, *13*, 1133-1174.
- ⁵ Kim, I. Y.; Seo, S. J.; Moon, H. S.; Yoo, M. K.; Park, I. Y.; Kim, B. C.; Cho, C. S. *Biotechnol. Adv.* **2008**, *26*, 1-21.
- ⁶ Jayakumar, R.; Prabakaran, M.; Sudheesh Kumar, P. T.; Nair, S. V.; Tamura, H. *Biotechnol. Adv.* **2011**, *29*, 322-337.
- ⁷ Medical Design Briefs. The Value of USP Class VI Testing for Medical Device Cable and Wire. <http://www.medicaldesignbriefs.com/component/content/article/mdb/features/20248>. (Accessed May 1, 2017).
- ⁸ Food and Drug Administration. Use of International Standard ISO 10993-1, "Biological evaluation of medical devices – Part 1: Evaluation and testing within a risk management process." <https://www.fda.gov/downloads/medicaldevices/deviceregulationandguidance/guidancedocuments/ucm348890.pdf>. (Accessed May 1, 2017).

-
- ⁹ Shamshina, J. L.; Barber, P. S.; Gurau, G.; Griggs, C. S.; Rogers, R. D. *ACS Sustainable Chem. Eng.* **2016**, *4*, 6072-6081.
- ¹⁰ Synowiecki, J.; Al-Khateen, N. A. *Crit. Rev. Food Sci. Nutr.* **2003**, *43*, 145-171.
- ¹¹ Barber, P. S.; Shamshina, J. S.; Rogers, R. D. *Pure Appl. Chem.* **2013**, *85*, 1693-1701.
- ¹² Qin, Y.; Lu, X.; Sun, N.; Rogers, R. D. *Green Chem.* **2010**, *12*, 968-971.
- ¹³ Sicherer, S. H.; Munoz-Furlong, A.; Sampson, H. A. *J. Allergy Clin. Immunol.* **2004**, *114*, 159-165.
- ¹⁴ Lopata, A. L.; O'Hehir, R. E.; Lehrer, S. B. *Clin. Exp. Allergy*, **2010**, *40*, 850-858.
- ¹⁵ Black, M. M.; Schwartz, H. M. *Analyst*, **1950**, *75*, 185-189.
- ¹⁶ Wider, G.; Dreier, L. *J. Am. Chem. Soc.* **2006**, *128*, 2571-2576.
- ¹⁷ Burton, I. W.; Quilliam, M. A.; Walter, J. A. *Anal. Chem.* **2005**, *77*, 3123-3131.
- ¹⁸ Baccile, N.; Falco, C.; Titirici, M.-M. *Green Chem.* **2014**, *16*, 4839-4869.
- ¹⁹ Straasø, L. A.; Qasim Saleem, Q.; Hansen, M. R. Chapter Six-A Toolbox of Solid-State NMR Experiments for the Characterization of Soft Organic Nanomaterials. In *Annual Reports on NMR Spectroscopy*; **2016**, *88*, 307-383.
- ²⁰ Kolodziejcki, W.; Klinowski, J. *Chem. Rev.* **2002**, *102*, 613-628.
- ²¹ Kasai, M. R. *Carbohydr. Polym.* **2010**, *79*, 801-810.
- ²² Raymond, L.; Morin, F.G.; Marchessault, R.H. *Carbohydr. Res.* **1993**, *246*, 331-336.
- ²³ Yu, G.; Morin, F.G.; Nobes, G.A.R.; Marchessault, R.H. *Macromolecules*, **1999**, *32*, 518-520.
- ²⁴ Heux, L.; Brugnerotto, J.; Desbrières, J.; Versali, M.-F.; Rinaudo, M. *Biomacromolecules*, **2000**, *1*, 746-751.
- ²⁵ Giraudeau, P.; Tea, I.; Remaud, G. S.; Akoka, S. *J. Pharm. Biomed. Anal.* **2014**, *9*, 3-16.
- ²⁶ Ziarella, F.; Caldarelli, S. *Solid-state Nucl. Magn. Res.* **2006**, *29*, 214-218.
- ²⁷ Rethwisch, D. G.; Jacintha, M. A.; Dybowski, C. R. *Anal. Chim. Acta.* **1993**, *283*, 1033-1043.
- ²⁸ Harris, R. K.; Hodgkinson, P.; Larsson, T.; Muruganatham, A. *J. Pharma. Biomed. Anal.* **2005**, *38*, 858-864.
- ²⁹ Fu, L.; McCallum, S. A.; Miao, J.; Hart, C.; Tudryn, G. J.; Zhang, F.; Linhardt, R. J. *Fuel*, **2015**, *141*, 39-45.
- ³⁰ Vogel, E. P.; Weliky, D. P. *Biochemistry*, **2013**, *52*, 4285-4287.
- ³¹ Johnson, R. L.; Schmidt-Rohr, K. *J. Magn. Reson.* **2014**, *239*, 44-49.
- ³² Zhang, R.; Chen, Y.; Rodriguez-Hornedo, N.; Ramamoorthy, A. *ChemPhysChem.* **2016**, *17*, 2962-2966.
- ³³ Tai, H.-C.; Li, G.-C.; Huang, S.-J.; Jhu, C.-R.; Chung, J.-H.; Wang, B. Y.; Hsu, C.-S.; Brandmair, B.; Chung, D.-T.; Chen, H. M.; Chan, J. C. C. *Proc. Nat. Acad. Sci.* **2017**, *114*, 27-32.
- ³⁴ Bernardinelli, O. D.; Lima, M. A.; Rezende, C. A.; Polikarpov, I.; deAzevedo, E. R. *Biotechnol. Biofuels*, **2015**, *8*, 110.
- ³⁵ Bruker Dynamics Center, Bruker Corp., 2016.
- ³⁶ Watson, S. A.; Edwards, A. J.; Parkinson, J. A. *Anal. Lett.* **2017**, *50*, 161-172.
- ³⁷ Cardenas, G.; Cabrera, G.; Taboada, E.; Miranda, S. P. *J. Appl. Polym. Sci.* **2004**, *93*, 1876-1885.

Chapter 4. A platform for more sustainable chitin films from an ionic liquid process

4.1 Introduction

In our society where environmental concern is increasing, there is heightened consumer demand for more sustainable alternatives to many petrochemical based synthetic polymers.^{1,2} Recycling of these materials is often impractical, but their disposal leads to accumulation in landfills and pollution of the environment.³ Due to their biodegradability, natural biopolymers can avoid many of these problems and are a promising alternative to petrochemical based materials. Biopolymer based materials, such as those made from cellulose, are available on the market today, but are often produced using non-sustainable processes. For example, the processing of cellulose into useful materials comprises the use of harsh or toxic solvent systems for chemical modification in order to obtain a more “soluble” form of the biopolymer.⁴ Cellophane, one such cellulose material, is a biodegradable packaging material made from cellulose, but the manufacturing process employs toxic chemicals such as carbon disulfide in order to modify the polymer into a form that is easy to manipulate.

Chitin, the second most abundant biopolymer in the world after cellulose, is biocompatible, biodegradable, biorenewable, and has long been known to possess regenerative properties.⁵ Despite its desirable properties, chitin has long been underutilized due to its insolubility in common solvent systems. In order to dissolve and manipulate chitin, harsh solvent systems are employed, such as *N,N*-dimethylacetamide (DMAc)/lithium chloride (LiCl),⁶ aqueous NaOH/urea,⁷ strong acids, and some fluorinated solvents.^{8,9}

In recent years, it has been found that by using ILs (defined as salts that melt below 100 °C),¹⁰ chitin can be dissolved and regenerated. Various imidazolium based ILs such as 1-butyl-3-methylimidazolium acetate ([C₄mim][OAc]) and 1-butyl-3-methylimidazolium chloride ([C₄mim][Cl]),¹¹ 1-allyl-3-methylimidazolium bromide ([Amim][Br]),¹² and 1-ethyl-3-

methylimidazolium propionate ([C₂mim][OPr])¹³ have been employed. Recently, IL systems other than those based on imidazolium cations have been investigated, such as tris(2-hydroxyethyl)methylammonium acetate with added ethylenediamine, which was shown to dissolve chitin without heating.¹⁴

In the last decade, our group has used the IL 1-ethyl-3-methylimidazolium acetate ([C₂mim][OAc]) as a tool for biopolymer dissolution.¹⁵⁻¹⁷ This IL has been used to manipulate high molecular weight chitin (regenerated from shrimp shells) into various architectures such as fibers,^{17,18} nanomats,¹⁹ and hydrogels.²⁰ Another important architecture to be explored using the IL system is films. Biopolymer films are desirable for applications^{1,21} ranging from high value medical devices²² (such as wound dressings,²³ drug delivery systems,²⁴ and pharmaceutical coatings²¹) to packaging applications.^{25,26} We hypothesized that the IL process could be used to produce chitin films with different properties depending on the method of preparation, which would lead to the ability to also tune the film applications. Here we demonstrate a versatile platform for the preparation of chitin films, without the use of harsh solvents or chemical modification of the polymer, which allows the tailoring of film properties and thereby their utility.

4.2 Results and discussion

To develop a platform for the preparation of biocompatible chitin films with tunable properties, the parameters that influence the final properties of the films must first be well understood. The most critical parameters to consider when preparing a chitin films are: chitin source, loading of chitin in IL, size of the rod used to cast the film, and the drying method (**Table 4.1**).

Table 4.1 Critical parameters for chitin film preparation.

Parameter	Effect
Chitin source	The molecular weight of the chitin (and entanglement of the polymer chains) determines the stability of the films once rolled and this depends on the chitin source
Loading of chitin in IL	The loading of the chitin in the IL solution determines the viscosity of the solution and thereby the ability to be cast
Rolling rod size	Rolling rods of different size determine the thickness of the dried film
Drying method	The drying method determines the flexibility, strength, porosity, and morphology of the film

4.2.1 Film preparation

The first step of chitin film preparation was to dissolve the selected chitin source in [C₂mim][OAc], to form a homogenous chitin solution. Film preparation was attempted using both commercially available PG chitin and IL-regenerated COOP chitin (COOP chitin). Solutions of each were prepared by the dissolution of the chitin source in the IL to obtain 2.5 wt% chitin solutions, based on the work we have done previously with fibers.¹⁷ The film cast from the PG-chitin solution yielded a very thin, web-like film which immediately broke apart after casting, likely due to its low molecular weight. This is a phenomenon that we have observed previously when preparing chitin/IL solutions from PG chitin. During coagulation, the low molecular weight chains come apart due to lower entanglement density, and the film breaks apart. The regenerated COOP chitin can be cast into a film and stays together as the IL leaches out due to the longer polymer chains, which yield more chain entanglements.²⁷ The film prepared from COOP chitin was stable during all steps of preparation, and yielded flexible films which could be handled with ease.

With the choice of chitin source made, the ideal loading of chitin in the IL had to be determined. The loading of the solution determined the ease with which a film could be rolled and the ability of the cast film to be handled. Five chitin/IL solutions ranging from 2 to 3 wt% COOP chitin, in increments of 0.25 wt%, were prepared by thermal dissolution of chitin in IL. Each solution was used to cast a film using the procedure schematically shown in **Figure 4.1**.

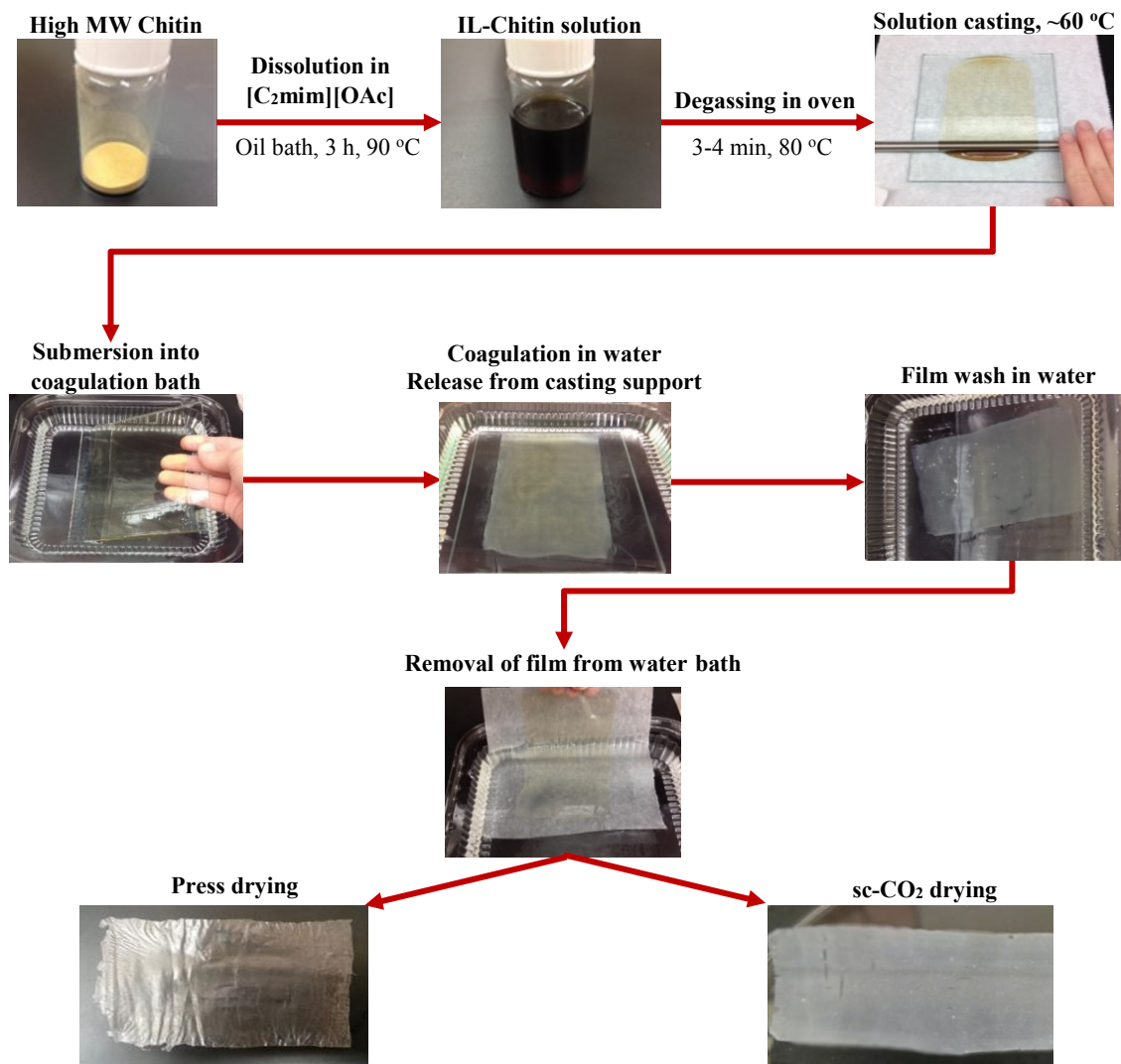


Figure 4.1 Preparation chart for chitin films.

For these initial steps, films were characterized only visually (appearance, thinness) and by resistance to manipulation (ability to handle the film). It was found that a chitin/IL solution of 2.5

wt% yielded films that appeared uniform, flexible, and could be easily handled. Chitin solutions with loading less than 2.5 wt% chitin gave free flowing solutions and yielded films that were excessively thin, weak, and that could not be removed from the water bath without breaking apart. Solutions with chitin loading of more than 2.75 wt% were too viscous, which caused difficulty in rolling and resulted in films of non-uniform thickness (**Table 4.2**). The 2.5 wt% chitin/IL solution was thus selected for all subsequent film casting.

Table 4.2 Weight percent loading of chitin and resulting solution and film.

% Chitin	Results
2.00	Very thin film, fell to pieces
2.25	Tougher than 2.0 wt% chitin film, but was too difficult to handle
2.50	Film was easy to manipulate and was easy to roll
2.75	Film was more tough than 2.5 wt% chitin film, but very difficult to roll
3.00	Yields film, but pouring and rolling were very difficult

After the solutions were tested for casting viability, small aliquots of the prepared solutions were used for viscosity measurements, which were conducted from 40–80 °C. This range was chosen because chitin-IL solutions are heated in an oven at 80 °C immediately prior to casting. Viscosity was important for the casting of solutions, though it was ultimately the ease of rolling of the solutions and the ability to handle the cast films that dictated the choice of chitin load. Viscosity curves for each of the solutions is shown in **Figure 4.2**. As seen in the curve, solutions over 2.5 wt% had viscosities over 1000 mPa·s at 40 °C, which made manipulation difficult. Solutions under 2.5 wt% had viscosities less than 500 mPa·s at 40 °C, which also led to difficulty of manipulation. The solutions cooled as they were cast, and because of this viscosity was not constant during the

casting process. However, as mentioned above, the viscosity value itself during the process is not crucial, but rather the ease with which the solution could be cast into a film.

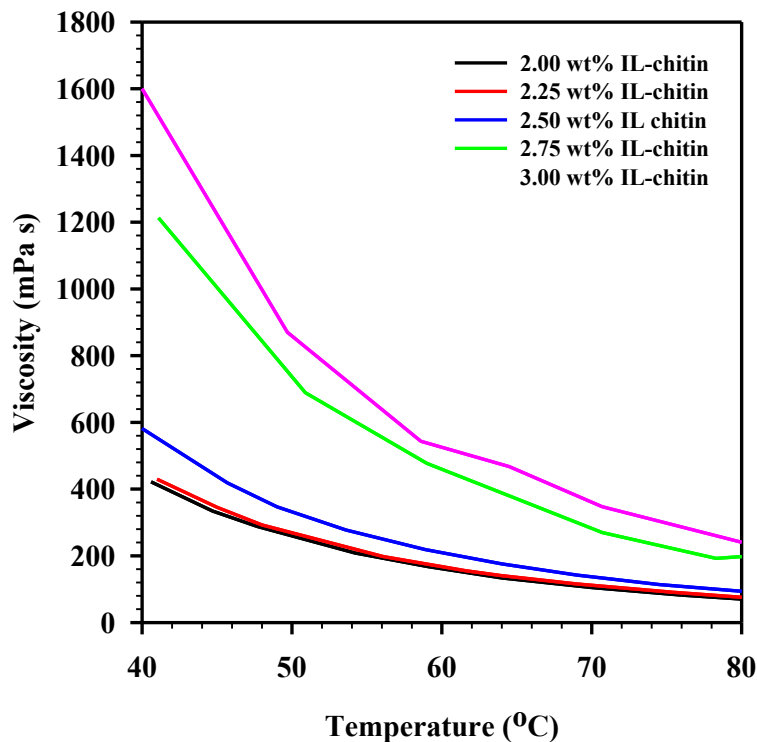


Figure 4.2 Viscosity of chitin/IL solutions from 40 to 80 °C.

As the rolling rod used determined the films thickness, seven rolling rods were tested for film viability, and three were selected to be used in film preparation. Rolling rods RDS 100 (wire diameter 0.26 mm), RDS 135 (wire diameter 0.41 mm), and RDS 150 (wire diameter 0.50 mm), yielded films that had visually uniform thickness and were strong enough to be submerged into a coagulation bath. Rods with wire diameters less than 0.26 mm yielded films that were too thin and difficult to manipulate, while rods with wire diameters larger than 0.50 mm resulted in films of non-uniform thickness (streaks from the rolling rods could be seen in the film, as the solution had not settled to a uniform thickness).

Once rolled onto the glass plate, the plate along with the mounted chitin solution was placed into a water bath in order to allow coagulation of the film as the IL leached into the water. The film slowly released from the glass casting support, becoming free floating and transparent. Films were removed from the water by sliding wax paper underneath the film to mount, and then carefully removing both. The film was then transferred to another surface (parchment paper) for drying because films dried on the wax paper would adhere and could not be removed. Air drying attempts were made on glass, wax paper, aluminum, and parchment paper. This was a critical step, since the film must be mounted on a material for drying, but adhesion must be avoided. This was an issue with chitin films on surfaces likely due to the hydrogen bonds that the film forms with the surface as it dries. Parchment paper was chosen as it allowed for easy removal of films, likely because parchment paper is coated with a non-stick, non-polar silicone coating. With the other drying surfaces (glass, wax paper, and aluminum foil) the chitin film stuck once dry and could not be removed.

4.2.2 Drying of films

Once a drying mount was selected, five drying methods were attempted on films cast from the RDS 135 rod (**Figure 4.3**). This rod was chosen because it was in the middle of the range of rods that produced uniform films. Drying of the film was crucial because the drying method determined the film's final properties, such as flexibility, uniformity, and porosity. Three of the tested drying methods, *i.e.* air drying, oven drying, and acetone drying, led to shriveled films that were deemed unusable. We speculate that conventional ambient drying techniques, such as air drying or oven drying, comprise the removal of the solvent (water or acetone, in the case of acetone drying) by evaporation. This quick evaporation of solvent resulted in strengthening of the intermolecular hydrogen bonding between the biopolymer chains, which led to a strong 3D network, collapse of

the pores, shriveling, and much lower surface areas. The percent shrinkage from wet to dry for oven, air, and acetone was 46%, 48%, and 50%, respectively.



Figure 4.3 Chitin films dried by different methods.

Press drying and sc-CO₂ drying yielded flexible films that could be easily handled and showed no visible signs of shriveling. For press drying, severe shriveling was prevented by placing *ca.* 2 kg of weight on the film as it dried. This prevented hydrogen bonding other than that in-plane for the most part, though some shrinkage could be seen under SEM microscopy. For sc-CO₂ dried films, structure collapse was prevented by means of highly pressurized supercritical fluid. It is a known phenomenon of supercritical fluid drying, where pore collapse is prevented by creating a mixture of the supercritical CO₂ with the solvent that has no surface tension inside the structure, and the fluid is removed.²⁸ Area of the dry films decreased compared to the wet film, although there was no shriveling observed. The change in area was found by comparing the area of the wet film to the area of the dry film. Films obtained after press drying decreased in area less so (20%) than corresponding sc-CO₂ dried film (28%), likely due to the heavy weight which prevented

shrinkage. Once it was determined that press drying and sc-CO₂ drying yielded flat and flexible films, these drying methods were used exclusively and subsequent films of different sizes were made.

4.2.3 Purity of dry films

Purity of the chitin films was studied by FTIR and TGA to ensure that there was no remaining IL or CaCO₃, respectively. FTIR was done on dry, ground press dried films (**Figure 4.4**). FTIR revealed no peaks related to the IL, indicating that the IL concentration was below the sensitivity of the technique (this has been observed in our previously published chitin materials).¹⁸

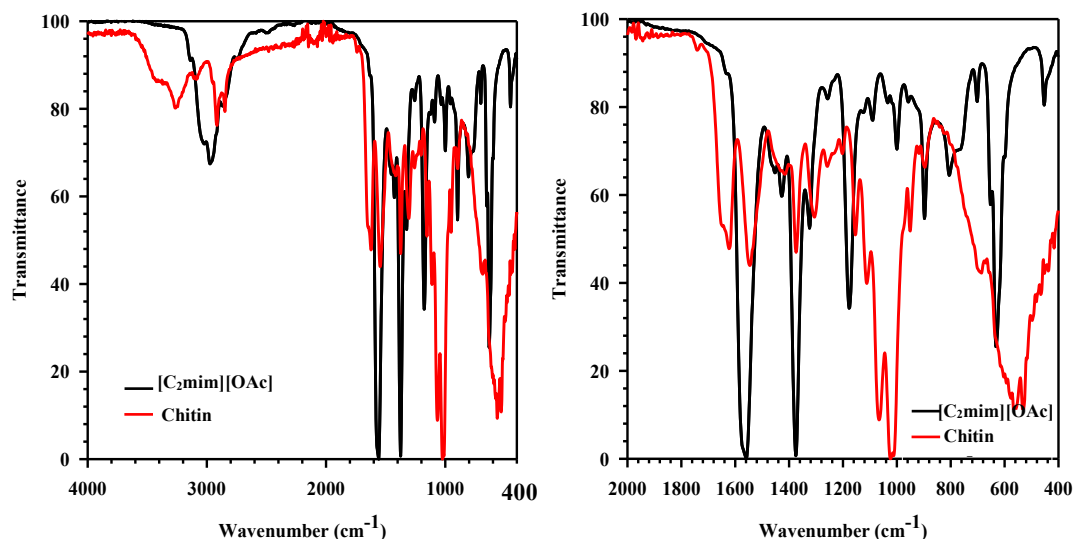


Figure 4.4 FTIR spectra of chitin film (red), and [C₂mim][OAc] (black).

Based on previously published FTIR characterization of the IL,²⁹ five diagnostic peaks were identified, two of which overlap with chitin. Three of the five diagnostic peaks (the sp² C–H stretching peaks at 3100 cm⁻¹, the ring in-plane asymmetric stretching at 1190 cm⁻¹, and the weak asymmetric bending of the HC=CH at 770 cm⁻¹) were not observed in the chitin spectrum. Moreover, overlapping peaks (such as the IL peaks at 1560 cm⁻¹ and 1390 cm⁻¹) have significantly

different intensities. Chitin has been extensively characterized by FTIR spectroscopy,³⁰ and the spectra obtained here are consistent with chitin.

The thermal stability was also recorded. TGA demonstrated the loss of water and the normal chitin decomposition step, with $T_{5\%Dec} = 253.2\text{ }^{\circ}\text{C}$, $T_{50\%Dec} = 343.2\text{ }^{\circ}\text{C}$, and 6.2% ash. The $T_{50\%Dec}$ reported here is 4 $^{\circ}\text{C}$ lower than that reported in our previous publication.¹⁸ No proteins or CaCO_3 were observed in the final film (**Figure 4.5**).

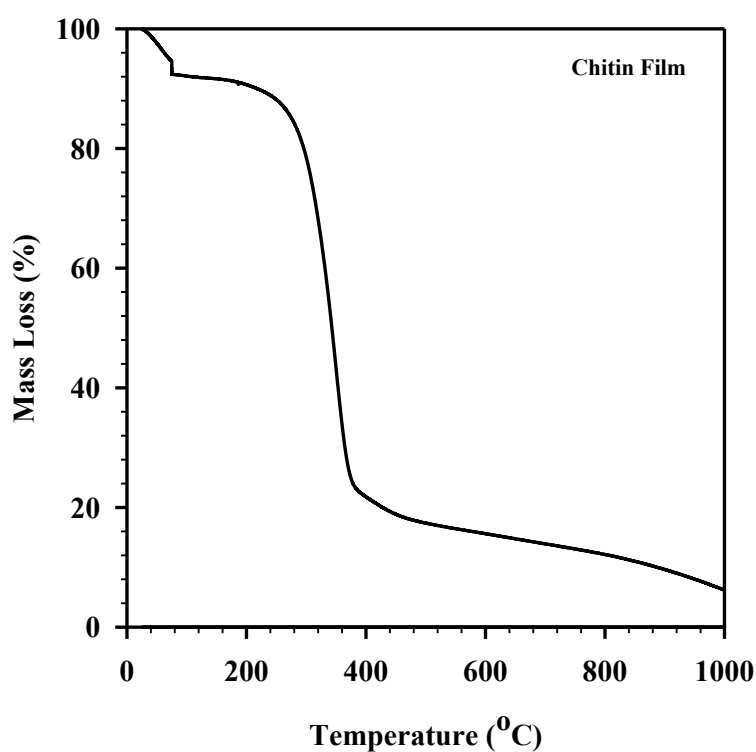


Figure 4.5 TGA data for press dried chitin film.

4.2.4 Film thickness

Once dry, the thickness of the film was measured using microscopic imaging software. Thickness depended not only on the rolling rod used, but also the selected drying method (press or sc- CO_2). As expected, larger wire sizes lead to thicker films, and sc- CO_2 dried films were more

than twice as thick as their press-dried counterparts due to the lack of pore collapse. The thickness for each film is presented in **Table 4.3**.

Table 4.3 Effect of rolling rod on the film thickness of press and sc-CO₂ dried films.

Rolling Rod	Press Film Thickness [μm]	Sc-CO₂ Film Thickness [μm]
RDS 100 (0.26 mm wire)	2.9(8)	6.7(8)
RDS 135 (0.41 mm wire)	5.4(3)	11.0(4)
RDS 150 (0.50 mm wire)	5.7(4)	14.2(8)

4.2.5 Film morphology

To study and compare the surface morphology of press and sc-CO₂ dried films, visual, optical microscopy, and SEM were used. Appearance varied drastically depending on the drying technique used. Films dried by pressing were translucent with a brown hue (**Figure 4.6**, left). The brown hue was likely due to the denser packing of the polymer chains. Press drying flattens the layers together and forces the water out, leading to the removal of pores and a more condensed structure. Films dried by sc-CO₂ drying appeared to have smooth surfaces, were completely white and opaque, and were sticky to the touch (**Figure 4.6**, right). The stickiness was possibly due to the greater presence of free hydroxyl groups available for hydrogen bonding on the surface of the film. Because the sc-CO₂ drying prevents structural collapse, many hydroxyl groups may stay free rather than interacting with one another, yielding a sticky surface. Though initially flat, when a sc-CO₂ dried film was exposed to air for extended time, it gained a slight brown hue and began to curl up, possibly due to the interaction of the film with water molecules present in the atmosphere.

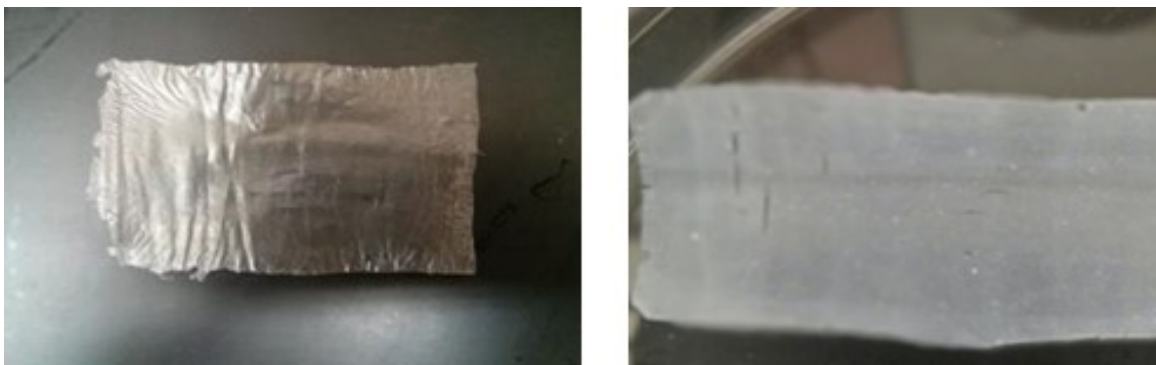


Figure 4.6 Press dried (left) and sc-CO₂ dried (right) films.

Optical microscopy was used to assess the differences in the porosity of the two types of films (**Figure 4.7**). Press dried films were lighter under optical microscopy (thinner, so more light passed through). The press dried film exhibits a nonporous form, as expected due to the pressing of the film, while the sc-CO₂ films exhibited a porous structure and 3D shape (a phenomenon similar to chitin and cellulose materials).³¹⁻³³ The defects seen in the press dried films are surface defects, bumps, and shrinkage, which was confirmed by SEM. It should be noted that the color of the films under the microscope is not an indication of the actual color of the film, but of the thickness of the material; the sc-CO₂ dried film appeared browner in color because it was thicker and less light passed through it.

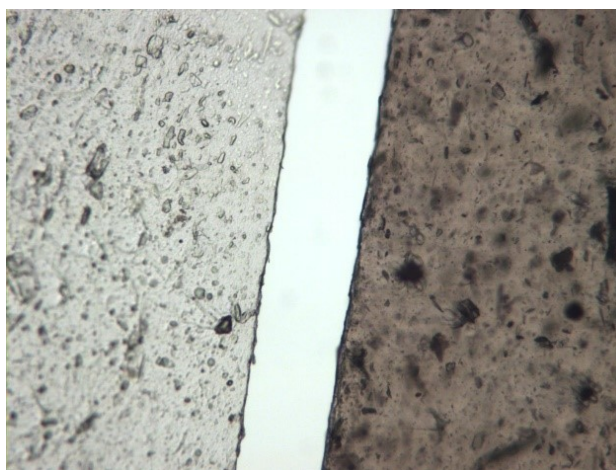


Figure 4.7 Press dried (left) and sc-CO₂ dried (right) films at 100X magnification.

SEM was used to better analyze and compare the surface morphology of the press dried and sc-CO₂ dried films (**Figure 4.8**). The surface of the press dried films had more defects, bumps, and wrinkling. These defects were likely due to the shrinkage that occurs during the drying of the film. The sc-CO₂ dried films had a much smoother surface, but had more foreign objects on the surface. This was likely due to the nature of the drying method, whereby the structure of the film when wet was not lost upon drying, leading to a smoother surface. The foreign objects on the surface are likely broken pieces of chitin that became stuck to the film after drying due to the stickiness of the film. The pores of the sc-CO₂ film could be seen on the backside of one film (**Figure 4.8**).

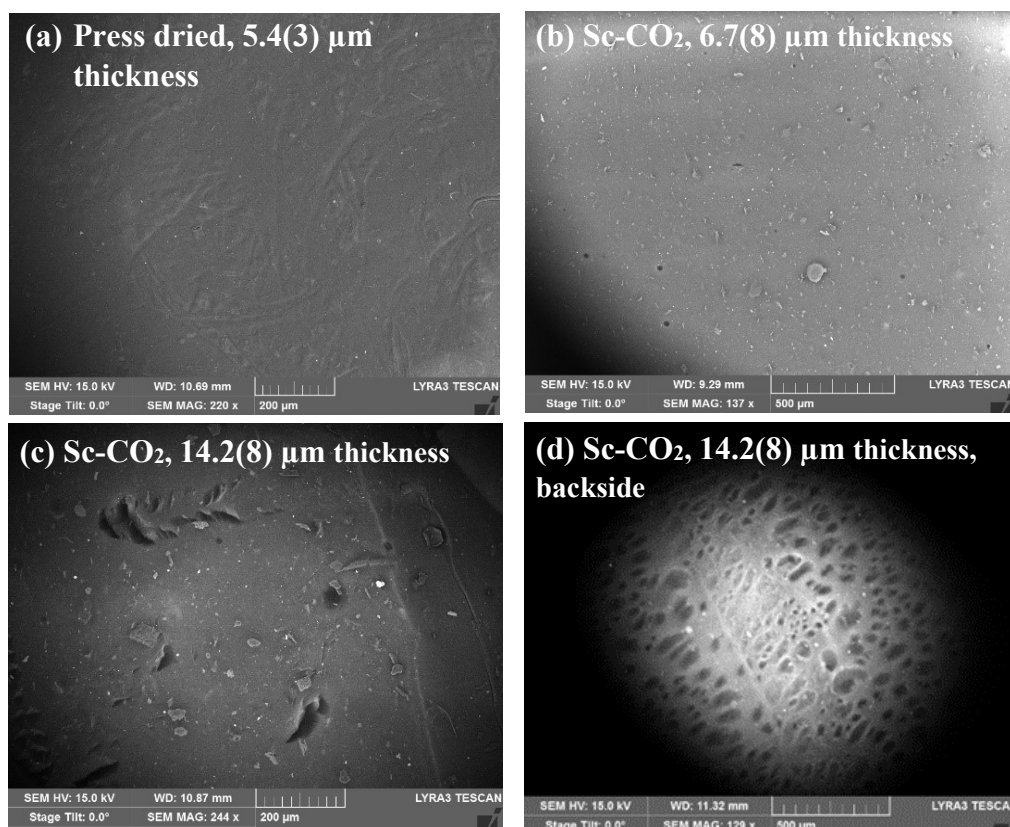


Figure 4.8 (a) press dried film (5.4(3) μm thick), (b) sc-CO₂ dried film. (6.7(8) μm thick), (c) sc-CO₂ film (14.2(8) μm thick), (d) its backside. Image magnifications: 150X-250X. (The magnifications are not the same, as magnification was gradually increased while taking the SEM and the best pictures were selected).

4.2.6 Tensile strength

Tensile strength is also important since it will dictate the material application field (*e.g.*, packaging, biomedical materials, or membranes). Tensile strength was tested for both press dried and sc-CO₂ dried films (**Table 4.4**). The strengths of the press dried films made from RDS 100, RDS 135, and RDS 150 were 19(2) MPa, 17(7) MPa, and 18(1) MPa, respectively. There was no statistical variation in the tensile strength of the different films, the difference in MPa was due to the difference in thickness of the films, but the force in Newtons was the same ($\text{Pa} = \text{N/m}^2$).

Table 4.4 Tensile strength of RDS 100, RDS 135, and RDS 150 for press and sc-CO₂ dried films.

Rolling Rod	Press Film Strength [MPa]	Sc-CO ₂ Film Strength [MPa]
RDS 100 (0.26 mm wire)	19(2)	N/A ^a
RDS 135 (0.41 mm wire)	17(7)	2.6(0.2)
RDS 150 (0.50 mm wire)	18(1)	N/A ^b

^a The films tore very easily resulting in small holes thus the films were unsuitable for the testing.

^b The films curled up/difficult to unroll to be loaded for testing.

The average tensile strength of the RDS 135 sc-CO₂ dried film was much less than that of press dried films, with a tensile strength of 2.6(0.2) MPa. The lower tensile strength can be related to the presence of pores and the lower density of chitin chain packing that results from sc-CO₂ drying. Tensile testing was attempted on sc-CO₂ films made with both the RDS 100 and RDS 150 rod, but it was too difficult to obtain films that could be tested. The RDS 100 films were weak and tore very easily which resulted in films with small holes and were thus unsuitable for testing; the RDS 150 films curled up and became too difficult to unroll enough to load into the tensile testing machine. Though weaker, elongation (how much the film stretched) for sc-CO₂ dried films was greater than that of press dried films (6% *vs.* 1%). Representative tensile curves for press dried

films (from each rolling rod size), and the sc-CO₂ dried film from the RDS 135 rolling rod are shown below in **Figure 4.9**.

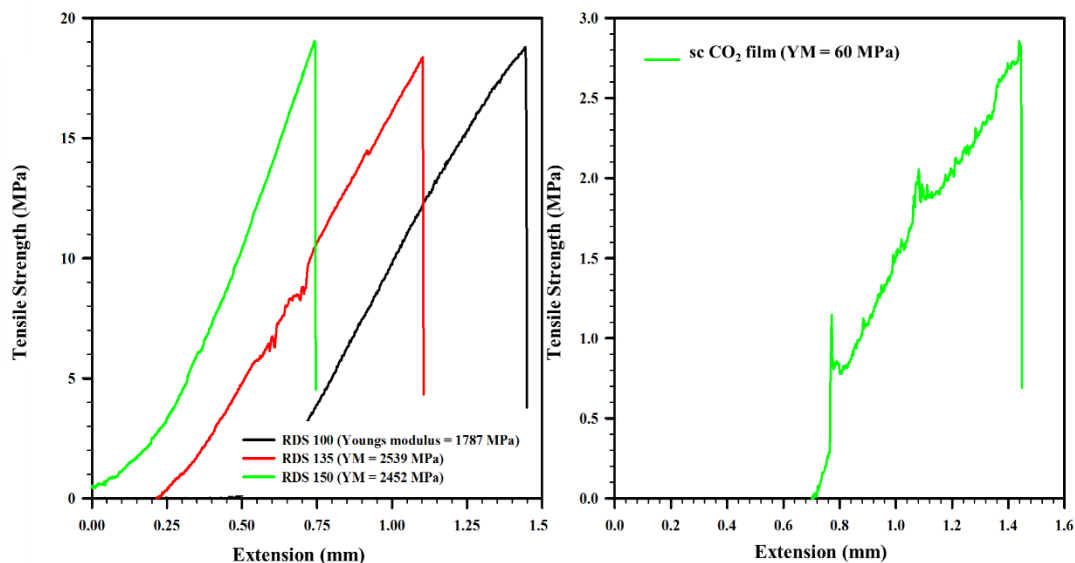


Figure 4.9 Representative tensile strength curves for RDS 100, 135, and 150 press dried films (left), and RDS 135 sc-CO₂ dried film (right).

4.2.7 Water content

Water content was measured gravimetrically for press dried and sc-CO₂ dried films. The percentage of weight lost for all films was less than 0.1 wt%. No significant differences on water content were observed between the two drying methods or film sizes.

4.2.8 Film swelling

The swelling ability of the film was tested by conducting rehydration experiments on both press and sc-CO₂ dried films rolled from RDS 100, RDS 135, and RDS 150. Water uptake was measured by weighing the film dry and after rehydrating in a water bath for 24 h. When placed into water, press dried films would quickly “spread,” due to the immediate absorbance of water, and maintained their color and opacity over 24 h. Sc-CO₂ dried films looked drastically different

when placed into water, immediately losing their white color and gaining the brown hue of the press dried films, likely due to water filling the pores that had been left open from drying.

An inversely proportional relationship between water uptake and film thickness was observed (**Table 4.5**), suggesting limited access to the internal structure of the films once dried. No significant difference was observed on the rehydration percentage of the films made using the same wire rod but different drying method for thinner films. The thicker RDS 150 films had a significant difference in rehydration depending on drying method. For these, films dried by sc-CO₂ absorbed more water than those press dried, suggesting that water can penetrate more easily into the internal structure of the sc-CO₂ dried film due to the increased porosity.

Table 4.5 Rehydration percentage of dry films.

Rolling Rod	Press Dried Film Rehydration [%]^a	Sc-CO₂ Dried Film Rehydration [%]^a
RDS 100 (0.26 mm wire)	777(7)	762(15)
RDS 135 (0.41 mm wire)	682(22)	651(51)
RDS 150 (0.50 mm wire)	504(14)	574(10)

^a Percent rehydrated = Mass rehydrated/mass original*100%

4.2.9 Drug loading and release

Because the films showed the ability swell in water, the ability of chitin to act as a drug eluting membrane was tested. Caffeine was used as a model drug compound to test the capacity of the films for uptake and release of an active substance. Caffeine loading and release was first attempted on press dried films. To load, the coagulated wet film was placed into a saturated aqueous caffeine solution and then dried normally. Once dry, the film was characterized by optical microscopy which revealed crystals of caffeine on the surface of the film, regardless of the concentration of the caffeine bath and the loading time (**Figure 4.10**).



Figure 4.10 Optical microscopy at 40X of caffeine crystals on the surface of a press dried film.

In an attempt to avoid this, the films were quickly rinsed with cold water before drying, but this resulted in no caffeine embedded into the film (determined by quantitative Nuclear Magnetic Resonance, qNMR spectroscopy, **Figure 4.11**).

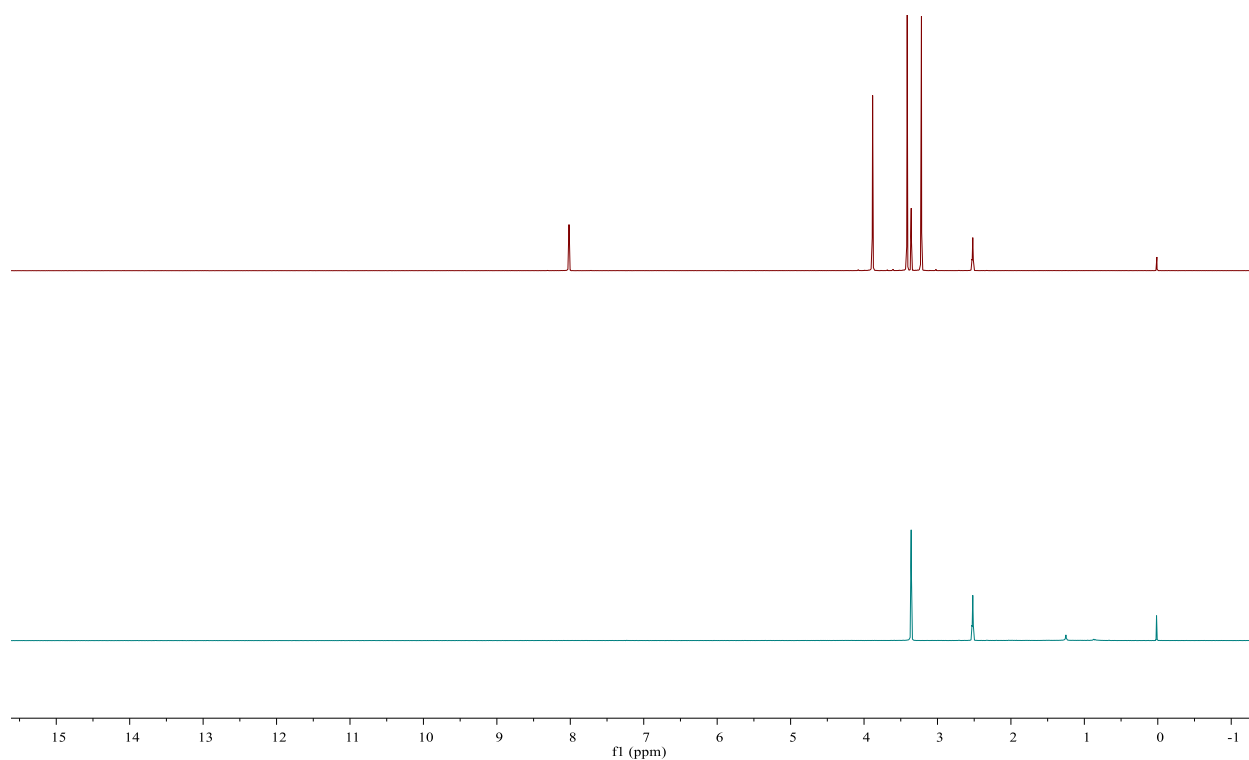


Figure 4.11 ^1H NMR (500 MHz, $\text{DMSO-}d_6$) for caffeine (top), and ^1H NMR (500 MHz, $\text{DMSO-}d_6$) for the solution of the washed film (bottom).

Because the caffeine was only present on the surface rather than inside of press dried films, it washed off immediately upon coming into contact with water and their use for release studies was discarded. Another method, the addition of caffeine to the chitin/IL solution before casting, was attempted. This was done by adding both 10 wt% and 20 wt% caffeine to the prepared chitin/IL solutions, but these also resulted in no caffeine in the film, as it was all washed out in the coagulation step.

For caffeine embedding of sc-CO₂ dried films, drying and loading was done in a single step. Films were prepared, coagulated and washed as previously described. Loading of the film was done prior to drying due to the collapse of structure that occurs when the dry film is wetted. The loading of the caffeine was done before drying, where the films were placed in saturated ethanolic caffeine solution and covered for 72 h, during which time the solution was replaced twice. Films were then sc-CO₂ dried as described in the experimental section. Optical microscopy on the dry film revealed clean surfaces with no crystals, indicating that the remaining caffeine was in the film rather than on the surface (**Figure 4.12**). Although there are dark spots which appear in the optical image which may be interpreted as crystals, this is only an artifact of the image and the film; similar spots appear in the unloaded film (**Figure 4.7**).



Figure 4.12 Optical microscopy image of sc-CO₂ film embedded with caffeine (no visible crystals).

It is also important to note that although this study demonstrated the ability to load caffeine into our film, this method is limited by the solubility of caffeine in ethanol, which is relatively poor (1.5 g/100 mL),³⁴ and due to the solubility of caffeine in supercritical CO₂, it is likely that a portion of the loaded caffeine was removed during the drying process.³⁵ Since sc-CO₂ allows the use of other solvents (*e.g.*, acetone, methanol), the selection of solvent will permit loading of different active pharmaceutical ingredients (APIs) with different solubilities, and allow for control of the concentration of the API in the material.

In order to measure the release of caffeine, the film was placed into PBS solution and caffeine release was recorded over a period of 2100 min (*ca.* 36 h) using UV-vis. Over the 36 h period, 100% of the loaded caffeine was released into the solution. About 80% of the caffeine in the film was released almost immediately (so-called burst release) within the first 20 min, with the remaining 20% of the caffeine released much more slowly over the remaining 20 h (**Figure 4.13**). The experiment was conducted in duplicate; the curves of release perfectly matched. This ability

of the sc-CO₂ dried films for load and release of active substances is promising for the use of these films as drug releasing membranes.

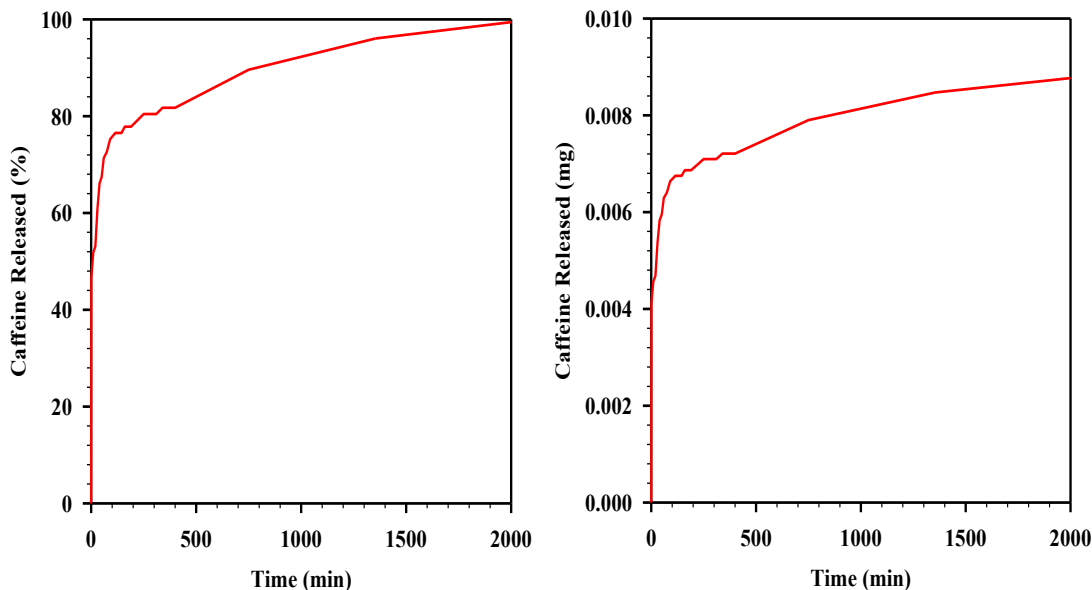


Figure 4.13 Percentage of caffeine released (left) and mg of caffeine released (right).

4.3 Conclusions

We have demonstrated a versatile platform for the preparation of biodegradable chitin films by using an IL process. By controlling the thickness, chitin loading, and drying methods, the resulting morphology and efficacy of the films could also be controlled. For both press dried films and sc-CO₂ films, the morphology, tensile strength, rehydration, and guest loading and release capabilities were studied, and the properties of each of the films compared. Press dried films, when compared to similarly prepared sc-CO₂ dried films, are thinner, less porous, and stronger, yielding films with properties promising for use in packaging applications with further optimization. Sc-CO₂ dried films, on the other hand, are porous, sticky, and capable of loading and release of guests, yielding a material that may have potential as a drug releasing membrane. Further optimization of each type of film could lead to high value, more sustainable chitin-based materials.

4.4 References

- ¹ Gross, R.A.; Kalra, B. *Science*, **2002**, *279*, 803-807.
- ² Dicker, M.; Duckworth, P.; Baker, A.; Francois, G.; Hazzard, M.; Weaver, P. *Composites Part A*, **2014**, *56*, 280-289.
- ³ Thompson, R. C.; Moore, C. J.; vom Saal, F. S.; Swan, S. H. *Phil. Trans. R. Soc. B*, **2009**, *364*, 2153-2166.
- ⁴ Klemm, D.; Heublein, B.; Fink, H. P.; Bohn, A. *Angew. Chem.* **2005**, *44*, 3358-3393.
- ⁵ Prudden, J. F.; Migel P.; Hanson P.; Freidrich, L.; Balassa, L. *Am. J. Surg.* **1970**, *119*, 560-564.
- ⁶ Poirier, M.; Charlet, G. *Carbohydr. Polym.* **2002**, *50*, 363-370.
- ⁷ Hu, X.; Du, Y.; Tang, Y.; Wang, Q.; Feng, T.; Yang, J.; Kennedy, J. F. *Carbohydr. Polym.* **2007**, *70*, 451-458.
- ⁸ Min, B. M.; Lee, S. W.; Lim, J. N.; You, Y.; Lee, T. S.; Kang, P. H.; Park, W. H. *Polymer*, **2004**, *45*, 7137-7142.
- ⁹ Pillai, C. K. S.; Paul, W.; Sharma, C. P. *Prog. Polym. Sci.* **2009**, *34*, 641-678.
- ¹⁰ *Ionic Liquids. Industrial Applications for Green Chemistry*, Rogers, R. D., and Seddon, K. R. Eds.; ACS Symposium Series 818; American Chemical Society: Washington, DC, **2002**.
- ¹¹ Wu, Y.; Sasaki, T.; Irie, S.; Sakurai, K. *Polymer*, **2008**, *49*, 2321-2337.
- ¹² Prasad, K.; Murakami, M.; Kaneko, Y.; Takada, A.; Nakamura, Y.; Kadokawa, J. *Int. J. Biol. Macromolec.* **2009**, *45*, 221-225.
- ¹³ Mundsinger, K.; Muller, A.; Beyer, R.; Hermanutz, F.; Buchmeiser, M. R. *Carbohydr. Polym.* **2015**, *131*, 34-40.
- ¹⁴ Shimo, M.; Abe, M.; Ohno, H. *ACS Sustainable Chem. Eng.* **2016**, *4*, 3722-3727.
- ¹⁵ Swatowski, M. P.; Spear, S. K.; Holbrey, J. D.; Rogers, R. D. *J. Am. Chem. Soc.* **2002**, *124*, 4974-4497.
- ¹⁶ Turner, M. B.; Spear, S. K.; Holbrey, J. D.; Rogers, R. D. *Biomacromolecules*, **2004**, *5*, 1379-1384.
- ¹⁷ Qin, Y.; Lu, X.; Sun, N.; Rogers, R. D. *Green Chem.* **2010**, *12*, 968-971.
- ¹⁸ Shamshina, J. L.; Gurau, G.; Block, L. E.; Hansen, L. K.; Dingee, C.; Walters, A.; Rogers, R. D. *J. Mater. Chem. B*, **2014**, *2*, 3924-3936.
- ¹⁹ Barber, P. S.; Griggs, C. S.; Bonner, J. R.; Rogers, R. D. *Green Chem.* **2013**, *15*, 601-607.
- ²⁰ Shen, X.; Shamshina, J. L.; Berton, P.; Bandomir, J.; Wang, H.; Gurau, G.; Rogers, R. D. *ACS Sustainable Chem. Eng.* **2016**, *4*, 471-480.
- ²¹ Vieira, M.; da Silva, M.; Santos, L.; Beppu, M. *Eur. Polym. J.* **2011**, *47*, 254-263.
- ²² Jayakumar, R.; Menon, D.; Manzoor, K.; Nair, S. V.; Tamura, H. *Carbohydr. Polym.* **2010**, *82*, 227-232.
- ²³ Agrawal, P.; Soni, S.; Mittal, G.; Bhatnagar, A. *Int. J. Low. Extrem. Wounds*, **2014**, *13*, 180-190.
- ²⁴ Ramos, B. Biopolymers Employed in Drug Delivery. In *Biopolymers: Biomedical and Environmental Applications*; Kalia, S.; Averous, L. Eds.; Wiley: Hoboken, NJ, 2011; pp. 559-573.
- ²⁵ Prashanth K. V. H.; Tharanathan, R. N. *Trends Food Sci. Technol.* **2007**, *18*, 117-131.
- ²⁶ Siracusa, V.; Rocculi, P.; Romani, S.; Dalla Rosa, M. *Trends Food Sci. Technol.* **2008**, *19*, 634-643.
- ²⁷ Fetters, L. J.; Lohse, D. J.; Richter, D.; Witten, T. A.; Zirkel, A. *Macromolecules*, **1994**, *27*, 4639-4647.
- ²⁸ Gesser, H. D.; Goswami, P. C. *Chem. Rev.* **1989**, *89*, 765-768.
- ²⁹ Kiefer, J.; Obert, K.; Bosmann, A.; Seeger, T.; Wasserscheid, P.; Leipertz, A. *ChemPhysChem.* **2008**, *9*, 1317-1322.
- ³⁰ Duarte, M. L.; Ferreira, M. C.; Marvao, M. R.; Rocha, J. *Int. J. Biol. Macromol.* **2001**, *28*, 359-363
- ³¹ Ratanajajaroen, P.; Ohshima, M. *J. Supercrit. Fluids*, **2012**, *68*, 31-38.
- ³² Tsiptsias, C.; Stefopoulos, A.; Kokkinomalis, I.; Papadopoulou, L.; Panayiotou, C. *Green Chem.* **2008**, *10*, 965-971.
- ³³ Chili, M.; Rodriguez, C.; Letourneau, J.; Espitalier, F.; Calvet, R. *Supercritical CO₂ Drying of Polysaccharidic Membranes Produced in Ionic Liquid: Application to Cellulose and Chitin*. 9th International Symposium on SuperCritical Fluids; 2009.
- ³⁴ Budavari, S. *The Merck Index*, 12th ed.; Merck & Co., Inc: Whitehouse Station, NJ, 1996; p. 1674.
- ³⁵ Kopcak, U.; Mohamed, R. S. *J. Supercrit. Fluids*, **2005**, *34*, 209-214.

Chapter 5. Graphene/chitin composite films for the assembly of a more sustainable supercapacitor

5.1 Introduction

As the harmful environmental impact of fossil fuel based energy becomes more prevalent, Society's focus has begun to shift towards more sustainable technologies in energy generation and energy storage.^{1,2} However, while energy storage has been touted as an important player in the creation of a more sustainable economy, the materials utilized in the production of energy storage technologies are often dependent on unsustainable components, e.g., synthetic polymers.³ This raises a question about the so-called sustainability of such technologies and poses a need for more sustainable materials in their production.

Supercapacitors are reversible energy storage devices capable of very high energy density and are increasingly being used in applications in electric vehicles and for renewable energy buffering in future energy grids.⁴ The operation of a supercapacitor depends on the physical separation of charges, *via* ion diffusion induced by an electric dipole.^{5,6} Supercapacitors consist of two conductive electrodes, a separator, and an ionic electrolyte. Capacitance is created when ions permeate through the separator, allowing for separation of charge.⁷ While research into the improvement of these devices has been typically focused on advancing conductive materials and electrode assemblies,^{8,9} relatively little work has been performed to enhance the sustainability of such a device. Fluorinated polymers such as polyvinylidene fluoride (PVDF) and polytetrafluoroethylene (PTFE) pervade the assembly of technologies such as batteries and supercapacitors,^{10,11} and are persistent once disposed into the environment.¹² Of further concern is the solvent required in the processing of such polymers for the preparation of films or pastes. Typically, the solvent *N*-methylpyrrolidone (NMP) is used for this process, which is not only toxic, but also a costly part of electrode manufacture.^{13,14}

Biopolymers are sustainable alternatives to synthetic polymers, though they have traditionally been underutilized due to the difficulties associated with their recovery and processing, often requiring chemical modification of the polymer or harsh pulping methods.^{15,16} However, over the past 10 years, it has been found that ILs can be used for the direct dissolution and manipulation of biopolymers such as cellulose and chitin.^{17,18} Some work has been performed for the use of chitin in electrochemical devices, including the preparation of chitin-bound electrode pellets¹⁹ and the use of chitosan-chitin blend films for separators.²⁰ However, as of yet, there has been no construction of a flexible electrochemical device assembled solely from chitinous materials.

In 2010, our group found that high molecular weight chitin can be directly extracted from shrimp shell waste using the IL 1-ethyl-3-methylimidazolium acetate ([C₂mim][OAc]),¹⁸ a method which allows for further solution processing of the biopolymer with a solvent of relatively low toxicity.²¹ Using the IL technology, we developed an IL solution processing platform for the preparation of chitin films, which allows for control of the film size, thickness, and allows for the incorporation of additives.²²

Here, the components of a supercapacitor were prepared from chitinous materials extracted from shrimp shell waste *via* the IL processing of chitin into composite films. As this processing strategy allows for the direct preparation of neat chitin films as well as composites, flexible chitin films without additives were prepared for use as nonconductive separators, and graphene/chitin composite films were prepared as conductive electrodes. For the preparation of composite films, graphene was incorporated into the chitin/IL solution, and films were cast. The preparation and design of such composites were optimized to obtain an electrode material which was both mechanically stable and conductive. The morphology and physical properties of the composite material were studied, and finally the electrode and neat films were assembled into a proof-of-

concept sustainable supercapacitor. Through this work, we ask if chitin can be a sustainable alternative to synthetic polymers for the preparation of more sustainable energy-storage materials.

5.2 Results and Discussion

5.2.1 Preparation of films

Chitin extracted from raw Black Tiger shrimp shells using a modified procedure from our previous work¹⁸ was used for the preparation of films. Films were cast using the processing methods for neat films found in reference,²² however the 2.5 wt% chitin-in-IL loading from our previous work which was based on a different shrimp shell source which had been squeeze dried, and was found to be too high for use in this application, yielding solutions which were too viscous for the dispersion of graphene. Chitin/IL solutions were therefore prepared at lower loadings of both 1.5 wt% and 1.25 wt% for graphene dispersion. An appropriate amount of graphene was added to each solution so that the ratio of graphene to chitin was 60:40, followed by 4 h stirring to disperse the graphene. At the end of this stirring period, a paste had formed in the 1.5 wt% chitin solution due to the higher viscosity of the solution, making it unsuitable for film casting. Upon visual inspection, the 1.25 wt% chitin solution with graphene remained free-flowing, and the graphene dispersion appeared homogeneous; thus, this solution was suitable for film casting. Additional graphene solutions were then prepared, with graphene/chitin ratios of 70/30, 80/20, and 90/10.

All of the resulting solutions were free-flowing and were cast into films followed by coagulation in water. Films were prepared with a casting knife set at 75 μm casting height, though it should be noted that the solution spreads on the plate on which it is cast and the film swells in the coagulation bath, leading to a wet thickness not equal to that set by the casting knife. The wet films were inspected for strength and homogeneity, and the films of 60, 70, and 80 wt% graphene

were homogenous and free of visible defects or tears. However, the 90 wt% graphene film was very fragile, with small pieces of the film coming apart. The films were then removed from the coagulation bath, and press dried between two pieces of parchment paper under weight (*ca.* 2 kg) overnight.

Upon drying, the 60, 70, and 80 wt% films all remained in one piece and were completely black and opaque. These films were flexible and could be manipulated, bent, and cut. The 90 wt% graphene film, however, broke into small pieces upon drying and could not be used. This is likely due to insufficient interactions between polymer chains due to the high loading of graphene and because of this, the 90 wt% films were not further studied.

As a high loading of conductive material is desired for electrochemical applications, only the highest loading film, 80 wt% graphene, was selected for further characterization. All further discussion of the graphene/chitin film will refer explicitly to the 80 wt% graphene/chitin composite films. Neat chitin films were prepared for use as nonconducting separators and a 1.25 wt% chitin loading was maintained for consistency with the graphene/chitin composite films (*i.e.*, all chitin films contained the same amount of chitin). Films were cast, coagulated, press dried, and then cut to diameters of 20 mm and 19 mm for the separator and electrode, respectively, to yield flexible, thin chitin films (**Table 5.1**).

Table 5.1 Observations and properties of neat chitin film and 80 wt% graphene/chitin composite films.

Property		Neat Chitin Film	80 wt% graphene/chitin composite film
Film Image		 100% chitin	 20% chitin
Observations		Film is translucent and flexible. The thin film could be manipulated and bent with ease.	Film is completely black, and appears homogenous. The thin film could be manipulated, but was brittle.
Thickness [mm]		0.026	0.079
Thermal Stability T _{5%dec} [°C]		266	246
Mechanical Properties [MPa]	Tensile Strength	5(1)	1.7(2)
	Young's Modulus	704(46)	257(70)
Swelling in electrolyte based on chitin content [mass %]		230	590

5.2.2 Film thickness

It is desirable for both the electrode material and the separator films used in supercapacitors to be thin, as the construction of such devices often involves their rolling and stacking for compact storage. Thickness of the dry chitin films was measured using a micrometer, and was found to be significantly different between the neat chitin films and the graphene/chitin composite films, with the composite films about 3 times as thick as the neat chitin films (though both were less than 100 μm in thickness). This is understandable, as both films have the same amount of chitin (both prepared from 1.25 wt% chitin in IL). The increased thickness of the composite films suggests that

during coagulation of the films, the graphene has been locked into the separated/colloidal structure (previously observed with graphene and imidazolium ILs).²³

5.2.3 Film morphology

The surface morphology of both neat and composite films and homogeneity of graphene dispersed in the electrode film were inspected using scanning electron microscopy (SEM, **Figure 5.1**). The images revealed the uneven and nonporous surface of the neat chitin film, similar to the neat chitin films previously reported.²² Images of the graphene/chitin composite films revealed a homogeneous distribution of graphene down to the micrometer scale, with no pores, breakage, or cracks observed, demonstrating the successful incorporation of graphene into the chitin film.

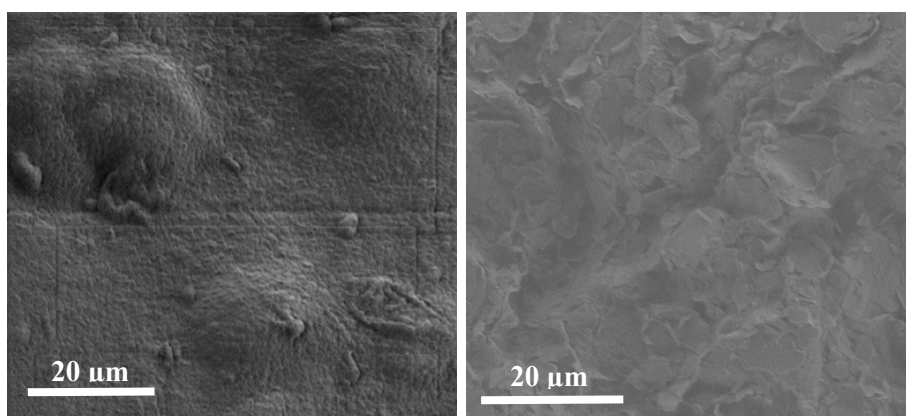


Figure 5.1 SEM images at 2000X magnification for neat chitin film (left) and 80 wt% graphene/chitin composite film (right).

5.2.4 Physical properties of films

For a better understanding of the physical properties of the films and of the interactions between the two components in the composite, thermal and mechanical properties of the film were measured by thermogravimetric analysis (TGA) (**Figure 5.2**) and tensile testing, respectively. Because the graphene does not decompose until very high temperatures, the TGA curve shown for the composite film has been normalized to the mass of chitin in the film in order to better compare to the neat chitin film (**Figure 5.2**, left). The decomposition temperature of 5 wt% of the material

($T_{5\%dec}$) and the overall mass loss profile were found to be similar for the neat chitin film and the graphene/chitin composite films, with values of 266 and 246 °C, respectively (these are similar to the value of 253 °C found for neat chitin films in reference 22). This indicates that the decomposition of the composite material is due to the decomposition of chitin alone, and the preparation of the composite film does not affect the thermal stability of the chitin itself. This also suggests that the interactions between the chitin and graphene are weak, and that the composite is formed through physical interactions rather than chemical interactions between the two film components. It should be noted that the sharp decrease in mass in the composite film normalized TGA after 400 °C is an artifact of the normalization, as the graphene in the material is also losing mass. Full TGA of neat chitin film, both films, and neat chitin is also shown (**Figure 5.2**, right).

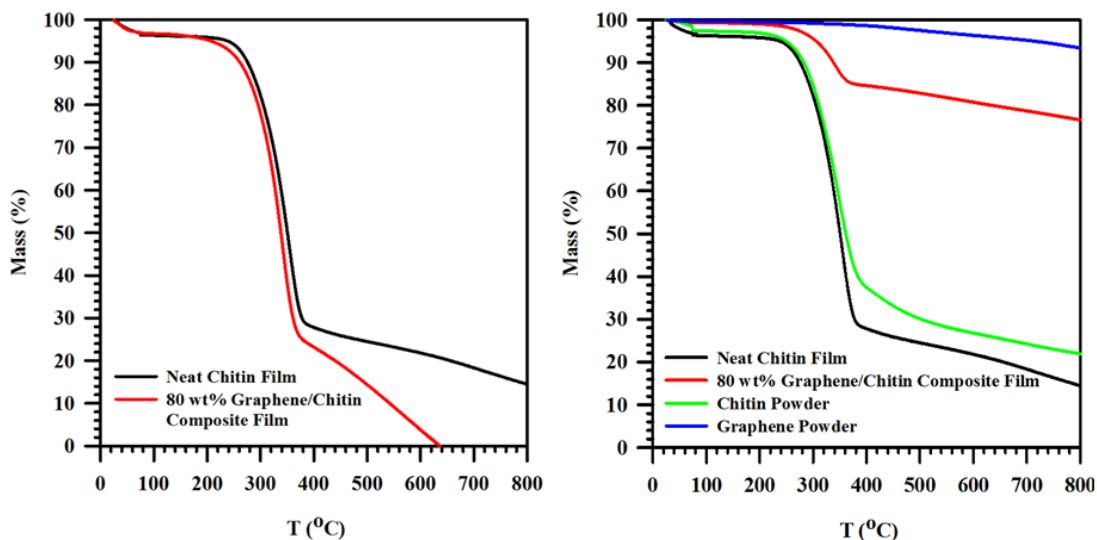


Figure 5.2 TGA of neat chitin and graphene chitin composite films (with the mass of the composite film normalized to mass of chitin) (left), and full TGA for neat chitin film, 80 wt% chitin/graphene composite film, chitin powder, and graphene powder (right).

The thermal stability of chitin in these films demonstrates its ability to function at higher temperatures than PVDF, which melts at 160-170 °C.²⁴ This may make chitin materials more suitable in electrochemical applications which require higher temperatures.

For the targeted application in electrochemical devices, it is necessary for the films to be thin and strong enough to be mechanically stable during their manipulation, so tensile strength and Young's Modulus of the separator and graphene/chitin composite films were also measured (**Figure 5.3**). Films were cut into thin strips (2 x 5 cm) for testing. The tensile strength of neat chitin films (5(1) MPa, with a YM of 704(46) MPa) was much lower when compared to the tensile strength of films previously obtained by the same method²² (where the tensile strength averaged around 17 MPa), however, this could be due to the differences in chitin loading (1.25 vs. 2.5 wt%, respectively) and chitin source.

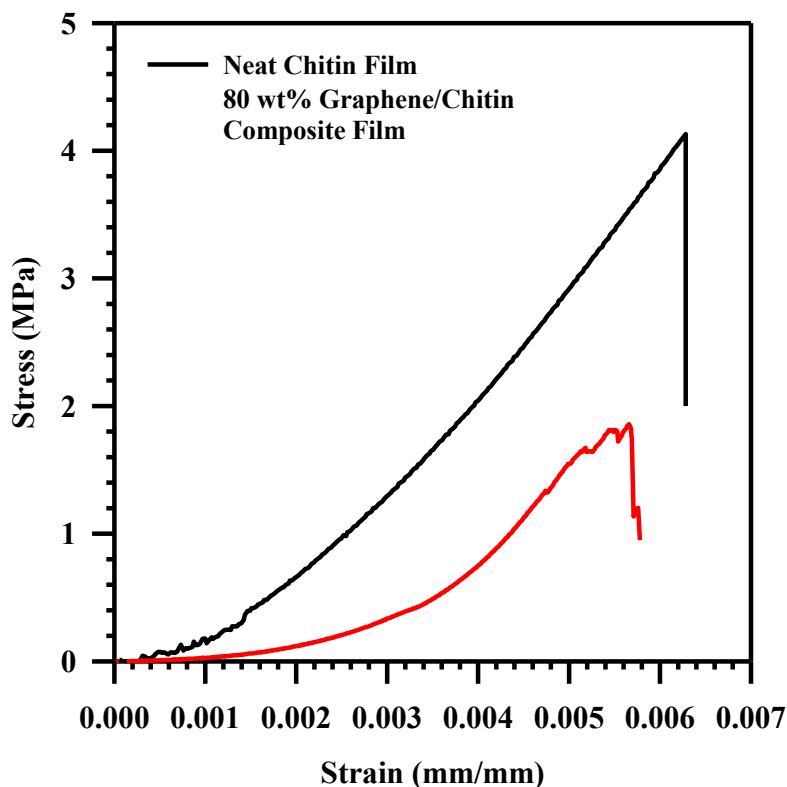


Figure 5.3 Stress/strain curves of neat chitin and 80 wt% graphene/chitin composite film.

The graphene/chitin composite films had even lower tensile strength, 1.7(2) MPa with a YM of 257(70) MPa, much lower than that of the neat chitin films. The lowering of the strength is due to incorporation of the graphene, which does not have good adhesion to the chitin and lessens the interactions between the chains of the biopolymer, lowering the strength of the material. While the materials were mechanically weaker than other chitin films, thinness and porosity are more important to their performance in a supercapacitor, and these properties both come at the cost of mechanical strength.

5.2.5 Swelling of films in aqueous electrolyte

Swelling of both the neat chitin separator and the graphene/chitin electrode was measured in aqueous 2 M $(\text{NH}_4)_2\text{SO}_4$. Pre-weighed films were soaked in electrolyte for 2 h, followed by removal of excess electrolyte and reweighing. Swelling of both the neat and composite films was determined as the mass gained per mass of chitin. The composite film (3.3 mg total with 0.66 mg chitin) gained 3.9 mg after swelling (590% of chitin mass), while the neat film (0.6 mg total chitin) gained 1.4 mg after swelling (230%). This, along with the much lower strength of the composite films, suggests that the presence of the graphene reduces the hydrogen bonding interactions between the chitin chains. This then leads to more hydration sites and greater mass gain when swollen.

5.2.6 Assembly of supercapacitor and electrochemical testing

Finally, the prepared films were used to construct a supercapacitor cell and measure its performance. The electrodes (graphene/chitin composite film) and separator (neat chitin film) were cut into circles of 20 mm and 19 mm diameter, respectively (**Figure 5.4a**). The films were stacked and wetted with electrolyte prior to loading into the electrochemical cell for testing (**Figure 5.4b**). For all tests, aqueous 2 M $(\text{NH}_4)_2\text{SO}_4$ was chosen as it is a common aqueous electrolyte,²⁵ and it

is compatible with the chitin films. Other common aqueous electrolytes such as NaOH, H₂SO₄, or Li₂SO₄ were avoided. Both NaOH and H₂SO₄ could deacetylate or hydrolyze the chitin polymer, respectively, thus rendering them unsuitable for use in an electrochemical device over the long-term. Li₂SO₄ was avoided due to the chelation capacity of chitin for Li⁺ cations, which could inhibit the function of the cell. In addition, the electrolyte (NH₄)₂SO₄ has further advantages such as small, symmetrical hydration spheres when used as an aqueous electrolyte, which have been shown to improve capacitance values in conventional supercapacitors.²⁵

For cell assembly, the films were stacked in a manner so that the graphene/chitin composite films were separated by the neat chitin film, with small amounts (*ca.* two drops by plastic pipette) of 2 M (NH₄)₂SO₄ electrolyte added to each as they were stacked. The film stack was then soaked in a small bath of electrolyte for 2 h, after which time the excess electrolyte was removed by plastic pipette, and the films were loaded into the stainless-steel test cell in a PTFE guide sleeve (**Figure 5.4c-d**). The stainless-steel counter electrode plate was placed onto the top of the stack, and the cell tightened and sealed for setting for 2 h prior to cyclic voltammetry measurements.

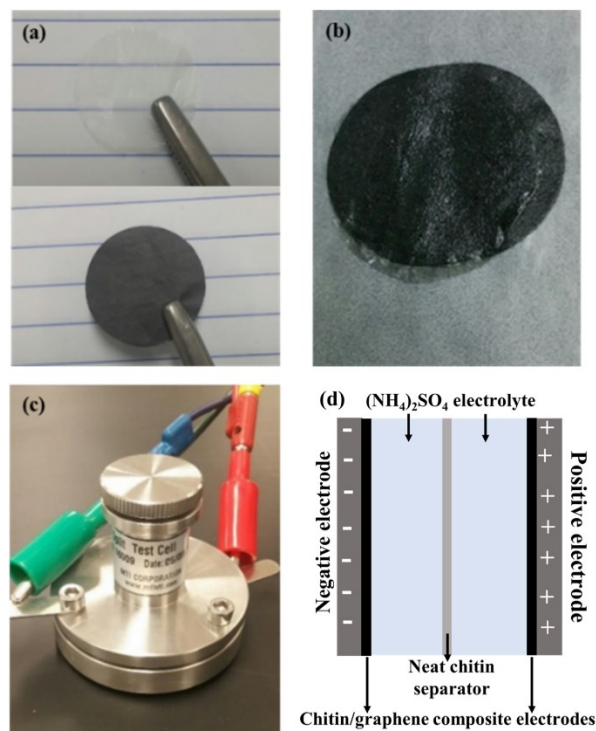


Figure 5.4 (a) Dry films, (b) wetted film assembly, (c) assembled supercapacitor test cell, and (d) schematic showing arrangement of components in test cell.

Cyclic Voltammetry (CV, a controlled potential scan from a start to end voltage at a controlled scan rate) was run on the chitin-based cell to measure the capacitance of the assembled supercapacitor. Capacitance was measured using a voltage window of 0-1 V, at scan rates ranging from 5-50 mV/s to reflect the charge/discharge duration typical of supercapacitor devices.²⁵ The voltammetric response was measured (**Figure 5.5**, left), and from this the capacitance (C_s) was obtained by normalizing the current density to the scan rate and voltage difference (which here was only 1 V) to the composite electrode film mass, using **Eq. 2.1** (**Figure 5.5**, right).

$$C_s = \frac{j}{vd\Delta} \quad \text{Eq 2.1}$$

Visual inspection of the CVs revealed a current response typical of capacitance in an aqueous electrolyte, with a variance from the ‘ideal’ rectangular CV that becomes more obvious with increasing scan rate. Integration of the curves and normalizing the response to electrode mass and scan rate yields capacitance values that range from 655 mF/g at higher scan rates of 50 mV/s to 2450 mF/g at 5 mV/s (**Table 5.2**).

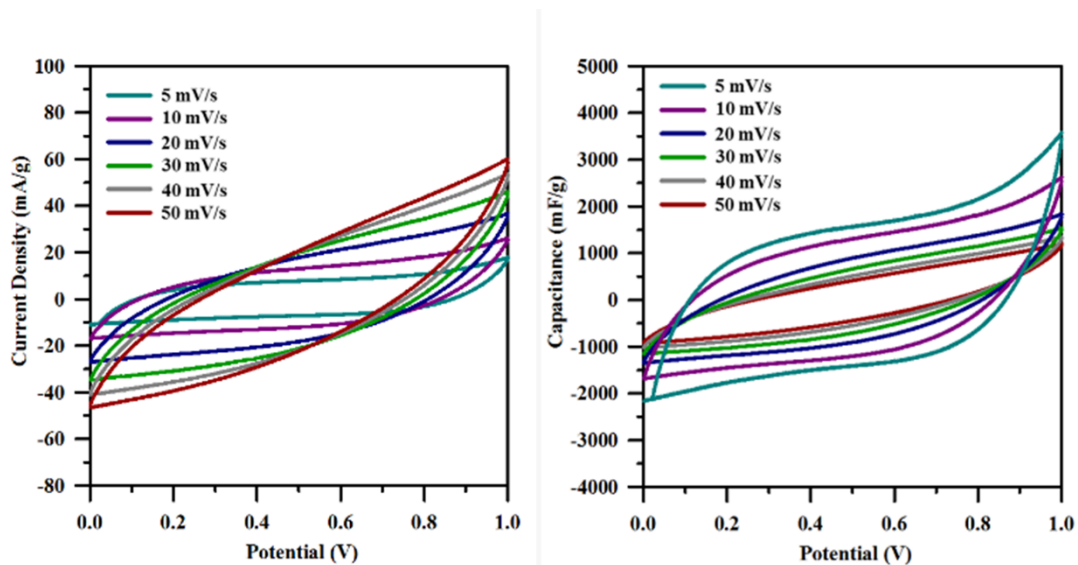


Figure 5.5 Cyclic voltammograms showing current densities (left) and capacitance (right) for the chitin thin film supercapacitor, performed between 0 and 1 V at scan rates ranging from 5-50 mV/s.

Table 5.2 Capacitance values normalized to the mass of the electrode films.

Scan rate [mV/s]	C _s [mF/g]
5	2450
10	1940
20	1332
30	1010
40	794
50	655

Some evidence of a Faradaic process can be observed in the CVs when scanned at slower scan rates, with a current inflection above 0.8 V that is not reversible. While commercial state-of-the-art supercapacitors can yield capacitance values orders of magnitudes higher (on the order of 600 F/g)²⁶ with conventional electrode processing techniques, we demonstrate here that capacitance values on the order of 1 F/g can be achieved with this unoptimized demonstration device assembled from biopolymer-based separator and electrodes.

5.3 Conclusions

In the present work, we have shown that chitin can be used to prepare both composite graphene/chitin films and neat chitin films *via* IL processing of the biopolymer for use as supercapacitor electrodes and separators, respectively. Graphene was homogeneously dispersed in a chitin/IL solution for the preparation of composite films of up to 80 wt% graphene, obtaining a composite film with homogeneous dispersion of graphene, thermal stability, and, although still relatively weak, a film easy to manipulate.

When the films were tested for the assembly of a supercapacitor in a two-electrode setup, the device reached a peak capacitance value of 2.4 F/g, demonstrating the first step towards more sustainable devices. Optimization of the test cell arrangement itself would be expected to greatly increase capacitance values. This includes the use of organic or IL electrolytes, as well as improved test cells. Additionally, porosity, wettability, and thickness of the films are all tied to the function of the capacitor, and optimization, tuning, or functionalization of the chitinous materials could increase the performance of the device.

Furthermore, although chitin was used here due to reproducibility and ease of material preparation, the IL processing method allows for the incorporation and processing of other materials, such as different biopolymers, conductive additives, or stabilizers that could enhance

the conductivity and stability of electrode films. For example, lignins contain many conjugated ring systems, which if used as a binder may enhance conductivity, but the processing of lignin is even more complicated than that of chitin.

This work aims to highlight an oft-forgotten element of sustainable technologies, that the materials and process used in the construction of a sustainable technology should themselves be sustainable. Despite the need for improvements and optimization, we here present flexible, thin films from a renewable feedstock (shrimp shell waste) for the preparation of a functioning electrochemical device, in a first step toward the preparation of more sustainable technologies.

5.4 References

- ¹ Rolison, D. R.; Nazar, L. F. *MRS Bull.* **2011**, *36*, 486-493.
- ² Yang, Z.; Zhang, J.; Kinger-Meyer, M. C. W.; Lu, X.; Choi, D.; Lemmon, J. P.; Liu, J. *Chem. Rev.* **2011**, *111*, 3577-3613.
- ³ Liu, J.; Zhang, J.-G.; Yang, Z.; Lemmon, J. P.; Imhoff, C.; Graff, G. L.; Li, L.; Hu, J.; Wang, C.; Xiao, J.; Xia, G.; Viswanathan, V. V.; Baskaran, S.; Sprenkle, V.; Li, X.; Shao, Y.; Schwenzler, B. *Adv. Funct. Mater.* **2013**, *23*, 929-946.
- ⁴ Koochi-Kamali, S.; Tyagi, V. V.; Rahim, N. A.; Panwar, N. L.; Mokhlis, H. *Renew. Sustainable Energy Rev.* **2013**, *25*, 135-165.
- ⁵ Simon, P.; Taberna, P.-L.; Beguin, F. Electrical Double-Layer Capacitors and Carbons for EDLCs. In *Supercapacitors: Materials, Systems, and Applications*; Béguin, F.; Frackowiak, E., Eds.; Wiley-VCH: Weinheim, Germany, 2013; pp. 131-165.
- ⁶ Wang, Y.; Song, Y.; Xia, Y. *Chem. Soc. Rev.* **2016**, *45*, 5925-5950.
- ⁷ Burke, A. *J. Power Sources*, **2000**, *91*, 37-50.
- ⁸ Zhong, C.; Deng, Y.; Hu, W.; Qiao, J.; Zhang, L.; Zhang, J. *Chem. Soc. Rev.* **2015**, *44*, 7484-7539.
- ⁹ Yu, L.; Chen, G. Z. *J. Power Sources*, **2016**, *326*, 604-612.
- ¹⁰ Li, J.; Daniel, C.; Wood, D. *J. Power Sources*, **2011**, *196*, 2452-2460.
- ¹¹ Talaie, E.; Bonnicksen, P.; Sun, X.; Pang, Q.; Liang, X.; Nazar, L. F. *Chem. Mater.* **2017**, *29*, 90-105.
- ¹² Premraj, R.; Doble, M. *Indian J. Biotechnol.* **2005**, *4*, 186-193.
- ¹³ Figoli, A.; Marino, T.; Simone, S.; Di Nicola, E.; He, X.-M.; Tornaghi, S.; Drioli, E. *Green Chem.* **2014**, *16*, 4034-4059.
- ¹⁴ Wood, D. L.; Li, J.; Daniel, C. *J. Power Sources*, **2015**, *275*, 234-242.
- ¹⁵ Klemm, D.; Heublein, B.; Fink, H.-P.; Bohn, A. *Angew. Chem. Int. Ed.* **2002**, *44*, 3358-3393.
- ¹⁶ Kumar, M. N. V. R. *React. Funct. Polym.* **2000**, *46*, 1-27.
- ¹⁷ Swatloski, R. P.; Spear, S. K.; Holbrey, J. D.; Rogers, R. D. *J. Am. Chem. Soc.* **2002**, *124*, 4974-4975.
- ¹⁸ Qin, Y.; Lu, X.; Sun, N.; Rogers, R. D. *Green Chem.* **2010**, *12*, 968-971.
- ¹⁹ Kolodziej, A.; Fic, K.; Frackowiak, E. *J. Mat. Chem. A*, **2015**, *3*, 22923-22930.
- ²⁰ Stepniak, I.; Galinski, M.; Nowacki, K.; Wysokowski, M.; Jakubowska, P.; Bazhenov, V. V.; Leisegang, T.; Ehrlich, H.; Jesionowski, T. *RSC Adv.* **2016**, *6*, 4007-4013.
- ²¹ BASF <https://wet.kuleuven.be/english/summerschools/archief-summerschools/2010/ionicliquids/lectures/massonne.pdf> (Accessed May 24, 2017).
- ²² King, C.; Shamshina, J. L.; Gurau, G.; Berton, P.; Khan, N. F. A. F.; Rogers, R. D. *Green Chem.* **2017**, *19*, 117-126.

-
- ²³ McCrary, P. D.; Beasley, P. A.; Alaniz, S. A.; Griggs, C. S.; Frazier, R. M.; Rogers, R. D. *Angew. Chem. Int. Ed.* **2012**, *51*, 9784-9787.
- ²⁴ C. L. Beyler and M. M. Hirschler. Thermal decomposition of polymers. In *SFPE Handbook of Fire Protection Engineering*; P. J. DiNenno, Ed.; NFPA: Quincy, MA, 2002; pp 1-113.
- ²⁵ Zhang, X.; Wang, X.; Jiang, L.; Wu, H.; Wu, C.; Su, J. *J. Power Sources*, **2012**, *216*, 290-296.
- ²⁶ Khomenko, V.; Frackowiak, E.; Beguin, F. *Electrochim. Acta*, **2005**, *50*, 2499-2506.

Chapter 6. Conclusions and Future Directions

6.1 Conclusions, contributions to knowledge, and future directions

Petrochemical based polymers have caused major environmental issues worldwide, as plastic debris pervades both land and sea ecosystems, affecting the health of both humans and the environment.¹ The principles of green chemistry can be used to lay the groundwork towards a solution; principles that call for the use of materials which come from renewable feedstocks, which degrade in the environment, and urges the intentional design of more sustainable materials rather than the cleanup of unsustainable ones.² Though synthetic plastics have been obsessively engineered for decades, Nature has meanwhile provided us examples of materials which are not only functional and biodegradable, but which often have more advanced properties. While humans have been using natural materials for thousands of years in simple applications, such as the use of wood for construction and cotton for textiles, Nature offers a versatile collection of highly specialized materials which are extremely efficient and elegant in their design.³ Examples can be seen in Nature's use of chitin in the formation of advanced structures; found as a building block in both the hard, protective exoskeleton of the crab, as well as the delicate, highly ordered structure of the butterfly wing.^{4,5} Nature has shown us that its biopolymers are capable of performing a myriad of functions, which can be mechanically tough, can be flexible, and can even be optically active. With the right tools, we can learn to manipulate these building blocks in ways that allow for the production of more sustainable advanced materials.

Although we have traditionally used Nature's materials for simplistic purposes, advances in materials science and biomimicry has brought us closer to utilizing biopolymers for more elegant applications. Examples can be seen in the recent increase in the use of cellulose microfibrils for the construction of composites and advanced materials.⁶ In this thesis, I have set out to work

towards a greener world by harnessing the capabilities of Nature's biopolymers to design and develop more sustainable functional materials. At the interface of polymer chemistry, green chemistry, and materials science, novel sustainable materials can be designed to not only perform the functions for which petrochemical based polymers are currently used, but also improve upon those functions and bring in new properties and functionalities while reducing the environmental impact. Here, chitin from shrimp shell waste sources was studied and manipulated into new functional forms using ionic liquids, to prepare materials which utilize many of its native properties as well as well as preparing new composite materials which instill other functionalities.

Through the work done here, I have strived to answer some of the basic questions about chitin and its processing *via* IL, from chitin purity from different sources to processing techniques and their applications, taking steps toward the controlled utilization of biopolymers for the design of high value, sustainable materials. Using chitin from shrimp shells, materials which are more sustainable can be developed; materials which are not only sourced from a renewable feedstock but also which degrade innocuously once disposed. Chitin is sourced from a waste product of the fishing industry, and has a huge untapped potential due to its biocompatibility, biodegradability, non-toxicity, and bioactive properties which make it ideal for use in functional materials, from textiles to biomedical technologies to biosensing.⁷⁻⁹ ILs allow for chitin to be manipulated into different architectures¹⁰ (such as fibers,¹⁰ nanomats,¹¹ and hydrogels¹²), and here this IL-processing methodology was used to explore the possibilities of new chitinous materials and composites. IL-processing is a way that this material can be harnessed for the production of advanced neat materials and composites. With a greater understanding of the biopolymer and the IL-processing method which allows for its manipulation, the preparation of more advanced architectures and specialized functionalities which were not possible previously become feasible.

To better understand the sources from which chitin is obtained and to simplify the way in which chitin can be utilized, a method was developed to measure the purity of chitin from chitinous sources quickly and non-destructively.¹³ In this way, the chitin source and resulting material can be better understood for the further development of pure chitinous materials. Chitin purity is extremely important for sensitive applications, especially those which come into contact with humans (such as those biomedical). This method simplifies the way in which chitin content can be measured and therefore can be used to better purify chitin from different sources for material preparation, and leads to a better understanding of purifying chitin for use in more sensitive applications.

With a greater understanding of the source material, the challenge of material preparation could be addressed. The processing of shrimp shell extracted chitin into the film platform was developed and optimized, setting the path for the production of a wide range of materials and applications with a method which allowed for the preparation of neat chitin films for which the properties could be changed depending on the preparation parameters.¹⁴ The production of such a platform allows for growth into new areas, as the preparation of films with different properties was possible, but it also sets a starting point for the development of more advanced methodology which might allow for biomimetic structures and composites.

Porous chitin materials with penetrable networks as well as non-porous materials were prepared through the methodology laid out here. Though the film preparation was optimized and studied primarily to act as a platform for the further preparation of films for more specific applications, preliminary studies demonstrated that the porous chitin films could be used for the loading and release of an active compound. This suggests that the material application may be expanded upon for use in wound care or drug delivery as biodegradable materials in biomedical

applications. For example, lidocaine ibuprofen, which has been shown as capable of simultaneous membrane transport of the two actives,¹⁵ could be loaded into a chitin film for topical wound care with a non-toxic and bioactive patch. The loading, release, and transport properties of the IL in the film and onto a wound could be studied for the development of biocompatible, sustainable wound care materials.

The platform of film preparation itself can be used as a guide in the preparation of more sophisticated architectures such as microspheres or nano-whiskers. New materials prepared through these IL processing techniques each will have their own challenges which can be more deeply understood with the knowledge here gained. It has been shown that processing parameters of the chitin affect the ability to form the material as well as the properties of the final material. Processing parameters such as the chitin source, the solution properties of the chitin in the IL (such as chitin load and viscosity), and the material formation techniques are all critical to the formation and design of viable architectures, and must be tuned and optimized for the preparation of new material forms.

Aside from the preparation of neat chitinous materials, the platform also allows for the preparation of blends and composites *via* the incorporation of additives, and therefore permits a method for the incorporation of additional functionalities into chitinous materials. Polymeric functional materials used currently in technological applications are often used as composites, one example exhibited by the used of commercial conductive electrode materials prepared *via* the incorporation of graphene into PTFE films. The IL-processing based film preparation method was used here for the design of more sustainable chitinous electrode materials (in the preparation of graphene/chitin composite films) for the construction of an electrochemical cell. It was shown that such electrode composite materials could be made in a way which may allow for the replacement

of more traditionally employed environmentally persistent synthetic polymers. The development of such materials and the incorporation of additives came with an entirely new set of challenges for the formation of the material, such as the need for optimization of the viscosity of the chitin solution in order to load the graphene, the loading of the graphene in the solution, and the dispersion of the graphene. Each of these parameters could be optimized for the preparation of conductive chitin-bound graphene films through an understanding of the biopolymer system.

This opens the door to the preparation of other blend and composite materials by the same method. For example, the IL solution processing of biopolymers could be used for the preparation of new, biodegradable packaging materials by incorporating biopolymers with different functionalities, such as the strength of cellulose and chitin, along with the antibacterial properties of chitosan, or the antioxidant activity of lignin. Each of these would of course come with their own challenges, as the dissolution of different biopolymers in IL, the ratio of the components, and the material casting techniques would need to be optimized.

Aside from blends, Nature provides us with examples of composite materials, which with the use of the IL processing method of biopolymers, could be developed in a laboratory setting for the production of sustainable, biomimetic, advanced materials for which the production has hitherto remained a challenge. A specialized example of advanced chitinous materials in Nature can be seen in the teeth of a limpet (an aquatic snail). Limpet teeth are extremely high strength composite materials consisting of iron oxide nanorods within a chitin matrix.¹⁶ Further optimization of the solution processing of chitin, along with an understanding of the interactions between chitin, the composite filler, and the IL can lead to the preparation of high strength, biomimetic composite materials.

ILs allow for the facile processing of chitin for the preparation of sustainable, high value materials. Biopolymers on their own, of course, have their drawbacks, and there are always improvements to be made in the processing and the construction of new materials. Further work on the development of composites and on the functionalization of biopolymeric materials is needed to address specific problems for specific desired applications (for example, strength may be needed for packaging materials, while antibacterial properties may be needed for wound care). By studying and understanding the interactions between the biopolymer, the IL, and additional additives, and by tuning the developed materials to the needs of their applications, novel functional materials can be prepared for more sustainable and technologies.

Biopolymers are a potential solution to the problem of plastic pollution, and here work was done to generate a better understanding of biopolymer manipulation for the development of materials which can be used in place of synthetic ones. This work has strived to set a path towards development of greener materials by utilizing Nature's building blocks and an IL platform in order to controllably manipulate them. ILs can be used to overcome the difficulties traditionally associated with biopolymer processing, and allow for direct manipulation and regeneration of the polymer while avoiding the use toxic solvents. The development of new technologically and economically competitive materials from chitin waste is entirely possible if the research is put into the understanding of the preparation of new materials from chitin.

The IL platform for chitin manipulation opens the door to the possibility of preparing advanced, sustainable materials, but the path to widespread implementation of greener processing techniques will not be an easy one. Aside from the technological barriers present on the lab scale, there are many more barriers to large scale implementation, which would require the cooperation of scientists, engineers, and the market to solve; barriers such as a consistent supply of chitinous

biomass, and a market demand for chitinous materials. However, chitin products have the advantages of their desirable properties, and only need to be utilized on a larger scale to begin to overcome these issues. Such an undertaking could lead to a materials market where the needs of Society are met without disrupting the needs of the environment.

The methodology developed here has hopefully elucidated some ways in which Nature's materials can be harnessed for the preparation of advanced materials, to pave the way for a new generation of biopolymer based materials which can be produced in a facile manner and tuned to advanced applications. As a greater understanding of the polymer processing is gained and more advanced chitinous materials are developed, a path is paved towards a greener world.

6.2 References

- ¹ Thompson, R. C.; Moore, C. J.; vom Saal, F. S.; Swan, S. H. *Phil. Trans. R. Soc. B*, **2009**, *364*, 2153-2166.
- ² Anastas, P. T.; Warner, J. C. *The Twelve Principles of Green Chemistry, Green Chemistry Theory and Practice*; Oxford University Press: New York, 1998; p.30.
- ³ Sanchez, C.; Arribart, H.; Guille, M. M. G. *Nat. Mater.* **2005**, *4*, 277-288.
- ⁴ Raabe, D.; Romano, P.; Sachs, C.; Al-Sawalmih, A.; Brokmeier, H.-G.; Yi, S.-B.; Servos, G.; Hartwig, H. G. *J. Cryst. Growth*, **2005**, *283*, 1-7.
- ⁵ Kinoshita, S.; Yoshioka, S.; Kawagoe, K. *Proc. R. Soc. Lond. B*, **2002**, *269*, 1417-1421.
- ⁶ Siro, I.; Plackett, D. *Cellulose*, **2010**, *17*, 459-494.
- ⁷ Jayakumar, R.; Menon, D.; Manzoor, K.; Nair, S. V.; Tamura, H. *Carbohydr. Polym.* **2010**, *82*, 227-232.
- ⁸ Shahidi, F.; Arachchi, J. K. V.; Jeon, Y.-J. *Trends Food Sci. Technol.* **1999**, *10*, 37-51.
- ⁹ Dutta, P. K.; Dutta, J.; Tripathi, V. S. *J. Sci. Ind. Res.* **2004**, *63*, 20-31.
- ¹⁰ Qin, Y.; Lu, X.; Sun, N.; Rogers, R. D. *Green Chem.* **2010**, *12*, 968-971.
- ¹¹ Barber, P. S.; Griggs, C. S.; Bonner, J. R.; Rogers, R. D. *Green Chem.* **2013**, *15*, 601-607.
- ¹² Shen, X.; Shamshina, J. L.; Berton, P.; Bandomir, J.; Wang, H.; Gurau, G.; Rogers, R. D. *ACS Sustainable Chem. Eng.* **2016**, *4*, 471-480.
- ¹³ King, C.; Stein, R. S.; Shamshina, J. S.; Rogers, R. D. *ACS Sustainable Chem. Eng.* **2017**, *5*, 8011-8016.
- ¹⁴ King, C.; Shamshina, J. L.; Gurau, G.; Berton, P.; Khan, N. F. A. F.; Rogers, R. D. *Green Chem.* **2017**, *19*, 117-126.
- ¹⁵ Wang, H.; Gurau, G.; Shamshina, J.; Cojocar, O. A.; Janikowski, J.; MacFarlane, D. R.; Davis, Jr. J. H.; Rogers, R. D. *Chem. Sci.* **2014**, *5*, 3449-3456.
- ¹⁶ Barber, A. H.; Lu, D.; Pugno, N. M. *J. R. Soc. Interface*, **2015**, *12*, 20141326.